THE MOLECULAR FUNCTION OF mCLCA1, mCLCA2 and mCLCA4 IN MURINE LIFE

A Dissertation

Presented to the Faculty of the Graduate School

of Cornell University

In Partial Fulfillment of the Requirements for the Degree of

Doctor of Philosophy

by

Kai Su Greene

May 2009

THE MOLECULAR FUNCTION OF mCLCA1, mCLCA2 and mCLCA4 IN MURINE LIFE

Kai Su Greene, Ph. D.

Cornell University 2009

Chloride channel, calcium-activated proteins (CLCAs) have been reported to regulate chloride transport and be involved in the pathophysiology of diseases, such as cystic fibrosis, asthma, airway inflammation and cancer. They have been cloned or isolated from multiple species, incluing human, mouse, bovine, equine, rat, porcine and canine. The aim of this research was to understand the function of this group of genes in murine life, focusing on mCLCA4 and its highly homologous family members, mCLCA1 and mCLCA2.

mCLCA4 is one of six members in the murine genome cloned to date, and is highly expressed in smooth muscle. To begin to understand the function of this gene family, I investigated the cellular processing and regulatory sequences of mCLCA4 proteins. The full length mCLCA4 gene product [125 kilo-Dalton (kD)] is made in the endoplasmic reticulum and is cleaved to 90 kD and 40 kD fragments. Both fragments, 90 kD N- terminal and 40 kD C- terminal fragments are secreted out of the cell and associate with the cell membrane. A specific diarginine motif is the retention signal while a dileucine motif is the forward trafficking signal during mCLCA4 secretion. While secretion of mClCA4 excludes this gene product as a channel protein, its association with the membrane may be consistent with a role as a regulator of chloride conductance.

To further understand mCLCA4 gene function, I generated mCLCA4 knock-

out mice. These mice displayed no gross phenotype and bred normally. Specific lung challenge experiments are being undertaken by collaborators to examine the effect of airway challenge on mClCA4 null mice. To further study the function of mCLCA4 *in vivo*, mCLCA1, mCLCA2, mCLCA4 triple knock-out mice were made. A 112 kilo base pair (kb) sequence was deleted from chromosome 3 of the murine genome using bacterial artificial chromosomal (BAC) recombineering techniques. Quantitative PCR was used to screen for positive embryonic stem cell clones that were then injected into blastocysts using standard techniques. Highly chimeric mice were bred to C57Bl/6J mice to produce heterozygous offspring. Currently, the triple gene knock-out mice survive to birth, but further phenotypic evaluation is needed.

BIOGRAPHICAL SKETCH

Kai Su Greene was born and raised in Changchun, China. She went to Jilin University after high school and obtained her B.S with a biochemistry major and chemistry minor. She worked as a researcher, instructor and then promoted to director of the Jilin Province Diagnostic Center where she trained the technicians from hospital diagnostic laboratories in Jilin Province. Kai spent three years at Showa University on a visiting scholar fellowship and Tokyo University as a graduate student in Japan.

Kai came to United States in 1993. She was invited by and worked for Dr. Leslie Pick to study Drosophila genetics at the Mt. Sinai Medical School, New York, NY. After five years of New York City life, she took a job at Wyeth Inc., a pharmaceutical company as a research scientist in Princeton, NJ. She moved to Endicott, New York to join her husband and started to work for Dr. Kotlikoff at Cornell University in year 2000. 2002 was a special year for Kai, she became a US citizen and stared her PhD program. Currently she lives with her husband Dr. Raymond Greene and son Thom Greene in Ithaca, NY.

After completing her degree, she will continue to be a researcher in the field of biology and continue to contribute to scientific discoveries to save human life.

To my parents, Shuzhen Ma and Dongfeng Su, for their love and for reminding me the value of education. I would like to dedicate my dissertation to them

ACKNOWLEDGMENTS

I would like to thank my advisor, Dr. Michael I. Kotlikoff, for his academic guidance and support of my PhD research. Without him I would not even have thought to start my PhD at my age. He invested a great deal of knowledge, resources and encouragement to help me succeed. He gave me the chance to work independently and solve the problems on my own. I am very grateful for this. I am also indebted to all my dissertation committee members for their advice and support in the past six and half years. Every committee member has played an important role in my research and in my graduate student life. They are Dr. Teresa Gunn, Dr. Ellis Loew, Dr. Mark Roberson (in alphabetical order) and former committee member Dr. JunLin Guan. Also I would like to thank all the Kotlikoff lab members (past and present) for their assistance, support and help in many ways. They are Dr. N. Yvonne Tallini for helping with my thesis writing; Dr. Gwendolyn Spizz for helping with my A exam proposal writing; Dr. Michael Craven, Rorbert Doran, Dr. Guangju Ji, Chunlei Huan, Jane Lee, Shaun Reining, Dr. Mark Rishniw, Dr. Bo Shui, Dr. Yongxiao Wang, Dr. Hongbo Xin (in alphabetical order).

I would like to thank Dr. Randolph Elble and Dr. Bendicht Pauli for collaborating with us on CLCA gene family studies. I would also like to thank Mr. Robert Munroe in Dr. John Schementi lab, Cornell University for injecting my mCLCA1,2,4 knock out ES cell clone and Ms. Keyu Deng in Transgenic Facility at Cornell University for mCLCA4 knock-out ES cell clone injecting. There are so many friends and colleagues in Biomedical Sciences Department and Vet school that supported me and helped me, I really appreciate them all.

I would also like to thank The Employee Degree Program of Cornell University. It encouraged me to start my PhD program.

I am indebted to Dr. Isao Niki for his academic guidance, friendship as well as financial support during my Japan years. I am also grateful for Dr. Leslie Pick who invited me to this country and trained me to become an independent researcher.

I am really grateful to and thank my family, without their support I would not have reached this point. My husband, Dr. Raymond Greene, was always fully supportive and encouraged me on my good or bad days. My son, Thom Greene, is my energy source and accompanied me on the weekends while I worked in the lab. My parents, Donfeng Su and Shuzhen Ma, always believe in the importance of education and supported me. My father-in-law, Dr. Thom R. Greene, always supported me and encouraged me. To all my relatives who supported me during these years, my sister-in-law Deborah Greene Modra, my brother Libing Su and his family, my sister Qi Su and her family, thank you.

TABLE OF CONTENTS

Biographical Sketch ……iii

Dedication ……iv

Acknowledgements ……v

Table of contents ……vii

List of figures ……...x

List of Tables ……..xii

Chapter 1 Introduction 1

1.1 CLCA family: mammalian species and expression..……..2

1.2 CLCAs common features……8

1.2.1 Chloride conductance……..8

1.2.2 The structure of CLCA proteins and their cellular location……11

1.3 The relationship between CLCAs and asthma……...14

1.4 The relationship between CLCAs and cystic fibrosis……15

1.5 The function and contribution in cell adhesion, tumor and cell 17

1.6 Summary of CLCAs functions……..19

1.7 References……..20

Chapter 2 The regulation and secretion of mCLCA4 protein 28

2.1 Abstract …… 29

2.2 Introduction ……...29

2.3 Materials and Methods …….31
2.4 Results ……..36
2.5 Discussion ……52
2.6 References ……55

Chapter 3 mCLCA4 knock-out mice and its phenotype 58

3.1 Abstract ……...59
3.2 Introduction ……59
3.3 Materials and Methods ……60
3.4 Results …….67
3.5 Discussion ……...67
3.6 References ……...74

Chapter 4 Generating mCLCA1, 2 and 4 triple knock-out 76

4.1 Abstract ……77
4.2 Introduction ……. 77
4.3 Materials and Methods …….79
4.4 Results ……. 92
4.5 Discussion ……...102
4.6 References ……...107

Chapter 5 Summery and future research direction 108

5.1 Summery ……109

5.2 Future direction and studies..……110

5.3 Reference ……..116

LIST OF FIGURES

Figure 1.1 Orthology summary map of CLCA genes, human and mouse genome loci, knock-out mice, and gene functions ……6

Figure 1.2 Phylogenetic tree of human and mouse CLCA members …….9

Figure 1.3 Human and mouse CLCA protein structure diagram……13

Figure 2.1 Proteolytic processing and cellular localization of mCLCA4……...37

Figure 2.2 The 90 kD N -terminal fragment and C -terminal fragment are secreted into the extracellular space 40

Figure 2.3 Mutation of putative phosphorylation site slows proteolytic cleavage…….42

Figure 2.4 Forward traffic and ER retention signals ……45

Figure 2.5 Glycosylation patterns of mutant proteins ……..48

Figure 2.6 mCLCA4 dileucine sequences are required for forward trafficking of secreted proteins 50

Figure 3.1 Diagram of mCLCA4 knockout mouse and homologous recombination in ES cells 62

Figure 3.2 Genotyping strategy for mCLCA4 ……..66

Figure 3.3 Southern blot and PCR genotyping …….68

Figure 4.1 Diagram of BAC clone RP24-271-G16 …….81

Figure 4.2 Schematic generating BAC-KO124-galk targeting vector ……..83

Figure 4.3 Diagram depicting generation of BAC-KO124-neo/kan targeting vector for ES cells 87

Figure 4.4 Homologous recombination between BAC-KO124-Neo/kan and one chromosome 3 allele in ES cells …….. 94

Figure 4.5 Diagram of the real-time PCR strategy ……...95

Figure 4.6 qPCR using KO124KO4 probe …….97

Figure 4.7 qPCR results …….98

Figure 4.8 PCR strategy and results to genotype mCLCA1,2,4 mice ……100

Figure 4.9 Evaluation of mCLCA1,2,4 eyes ……..104

Figure 5.1 Diagram depicting strategy to make mCLCA1,2,4,6,7,8 knock out mice ……..114

LIST OF TABLES

Table 3.1 Blood chemistry test results from mCLCA4$^{-/-}$ mice and littermate controls ……..71

Table 3.2 Blood CBC test results from mCLCA4$^{-/-}$ mice and littermate controls …….72

Table 4.1 Evaluation of body weight in mCLCA1,2,4 knock out offspring ……..106

CHAPTER 1

INTRODUCTION OF CLCA FAMILY IN ALL SPECIES

Calcium-activated chloride currents play an important role in diverse cellular physiological functions, such as neuronal excitability, regulation of vascular tone, epithelial secretion, fast block to polyspermy and olfactory transduction (24). They have been reported in many cell types such as smooth muscle cells (13-15, 37), cardiac myocytes (35, 78), exocrine glands (7, 22, 62), epithelial cells (5, 16, 49) and endothelial cells (51). The genes involved in these channels have been sought and studied for many years, but the molecular identity of these channels remains unknown. Two candidate gene families contribute to the calcium-activated chloride channel activity, CLCA and Bestrophin (56, 64). Recently, Yang et al. (70) discovered that the transmembrane protein 16A (TMEM16, also called ANO1) may also be a chloride channel protein. This dissertation focuses on the function of the CLCA family in murine life, concentrating on mCLCA4 and two highly homologous family members, mCLCA1 and mCLCA2.

1.1 CLCA family: mammalian species and expression

CLCAs have been reported in the literature for seven mammalian species: human, murine, rat, bovine, equine, porcine and canine. Since the complete sequence of the human genome, CLCA putative orthologs were discovered in more than 30 species as listed on the NCBI Gene database and the Ensemble Gene Tree View (52). The CLCA genomic organization in many species is conserved. The genes cluster together on the same chromosome, but little information is available about the promoters that drive their expression. So far, the following have been cloned and reported: four members from human (hCLCA1, hCLCA2, hCLCA3 and hCLCA4), six plus two predicted members from murine (mCLCA1, mCLCA2, mCLCA3, mCLCA4, mCLCA5 and mCLCA6; ESTs EG622139 and AI747448 are predicted), two members from bovine (bCLCA1, and bCLCA2), one member from porcine

(pCLCA1), one member from equine (eCLCA1), two members from rat (rCLCA1 and rCLCA2) and one from canine (cCLCA1).

The first cDNA of the CLCA family was reported by Cunningham and colleagues (17) using the polyclonal antibody αp38 on a bovine tracheal cDNA library. It was originally named CaCC (calcium-activated chloride channel) and later renamed to bCLCA1 to match the CLCA nomenclature. The full length cDNA of this protein is 3001 base pair (bp) and codes for a 903 amino-acid (aa) protein product that is 140 kDa. The 140 kDa protein product is translated and glycosylated, then cleaved to 90 kDa and 38/32 kDa fragments.

The first CLCA protein was purified from lung endothelial cell matrix extracts using the monoclonal antibody 6D3 by Zhu et al. (76) and was determined to be a 90 kDa fragment of the lung endothelial cell adhesion molecule-1 (Lu-ECAM-1) protein. Later, the gene of this protein was cloned by the same group, from a bovine gene expression library and renamed bCLCA2 (21, 77). bCLCA2 codes for a 130 kDa glycosylated precursor protein and is cleaved into two fragments: 90 and 30 kDa. bCLCA1 and bCLCA2 isoforms share 88% identity, but their tissue distribution is different—bCLCA1 is expressed in epithelial cells while bCLCA2 in endothelial cells. There are two other bovine CLCA genes, bCLCA3 and bCLCA4. All four of these genes are clustered on bovine chromosome 3 (52).

All four human CLCA members are clustered on chromosome 1, 1p31-1p22 (Figure 1.1). hCLCA1 was cloned by Gruber et al. (30) from a human genomic library using bCLCA2 cDNA as the probe. It was also isolated by Angel and colleagues (4) along with the human CLCA family genes, namely hCaCC-1 (the same as hCLCA1), hCaCC-2 (hCLCA4) and hCaCC-3 (hCLCA3). The hCLCA1 gene spans 31 kb and codes for a 914 aa protein. After glycosylation this protein is 125 kDa and is then cleaved into 90 kDa and 38-40 kDa products in the HEK293 cell. hCLCA1 is highly

expressed in small intestine, colon mucosa and appendix, and weakly expressed in uterus, stomach, testis, kidney and fetal spleen. At the cellular level, the expression is detected in basal crypt epithelia and goblet cells by Northern blotting and *in situ* hybridization (30, 47).

hCLCA2 was cloned from a human lung cDNA library with bCLCA2 cDNA as the probe (34). The 2832 bp cDNA is the predicted coding sequence for a 943 aa polypeptide. It is translated to a 120 kDa protein product after glycosylation, and subsequently cleaved into 86 kDa and 34 kDa fragments. Northern blot analysis showed that hCLCA2 is only expressed in trachea and mammary gland tissues. Interestingly, by Northern blot, hCLCA2 expression was not detected in lung, although it was cloned from lung cDNA. This indicates that hCLCA2 has a very low expression level in lung tissue (34, 47).

hCLCA3 was cloned from a human spleen cDNA library using Lu-ECAM-1 (bCLCA2) cDNA as a probe (32). hCLCA3 is expressed in many tissues, such as lung, trachea, spleen, thymus and mammary gland as detected by reverse transcriptase polymerase chain reaction (RT-PCR). Unlike other CLCA members, hCLCA3 cDNA is 3.6 kb with two internal stop codons and encodes 37 kDa and 22 kDa products, respectively. The N-terminal product (37 kDa) is secreted out of cell and the function of this truncated product remains unknown (32).

Using a homology search in the EST database Agnel et al. (4) identified a potentially new human CLCA family member, hCLCA4 (previously referred to as hCaCC2). hCLCA4 was subsequently cloned using the 5' rapid amplification of cDNA ends (RACE) approach. The hCLCA4 cDNA is 3.3 kb and encod a 917 aa protein product. This gene is expressed in multiple areas of the brain such as the amygdala, caudate nucleus, cerebral cortex, frontal lobe, hippocampus, medulla oblongata, occipital lobe, putamen, substantia nigra, temporal lobe, thalamus,

acumbens and spinal cord. The highest level of hCLCA4 expression is in the colon. The weakest expression is in stomach, testis, small intestine, appendix, salivary gland and mammary gland. It also is moderately expressed in the bladder, uterus, prostate and trachea (4, 47).

Only one member has been cloned and expressed from full-length cDNA from ileal gene porcine expression library, pCLCA1 (26, 47). pCLCA1 is a 3.1 kb cDNA and has a 2.7 kb open reading frame (ORF) which encodes a 917 aa protein product cleaved to two polypeptides. The protein product is 78% homologous to hCLCA1. The mRNA of pCLCA1 is expressed in several exocrine epithelial tissues, such as the ileum (crypt and villus epithelia), the trachea and salivary glands.

Base on the rat genome sequence (27, 66) and bioinformatics information (66, 67), there are five CLCA members in rat. Yamazaki and colleagues (69) cloned full length rCLCA1 [Patel et al renamed it rCLCA2 (52)] cDNA from salivary cells. rCLCA1 cDNA is 3.3 kb in length and the predicted ORF encodes a 903 aa protein. A year after, Yoon et al (71) cloned the same gene from rat brain and named it rbCLCA1. The mRNA of rCLCA1 was expressed in the submandibular gland (SMG), ileum and lung. In the SMG, rCLCA1 protein was only detected in the striated duct and not in the acinar cells by immunostaining with anti-rCLCA polyclonal antibody. At the cDNA level, rCLCA1 is highly homologous to mCLCA1and mCLCA2 (87%), mCLCA4 (84%), and hCLCA1 (70%) (69). Jeong et al (38) cloned another rat CLCA gene named rbCLCA2 [Patel et al renamed it rCLCA1 (52)]. The full-length cDNA of rbCLCA2 is 2895 bp and codes for a 902 aa protein.

To date only one CLCA member has been cloned from equine (6). Total mRNA was extracted and purified from horse rectal mucosa, conserved region primers from hCLCA1 and mCLCA3 were used to PCR the isoform from the mRNA pool.

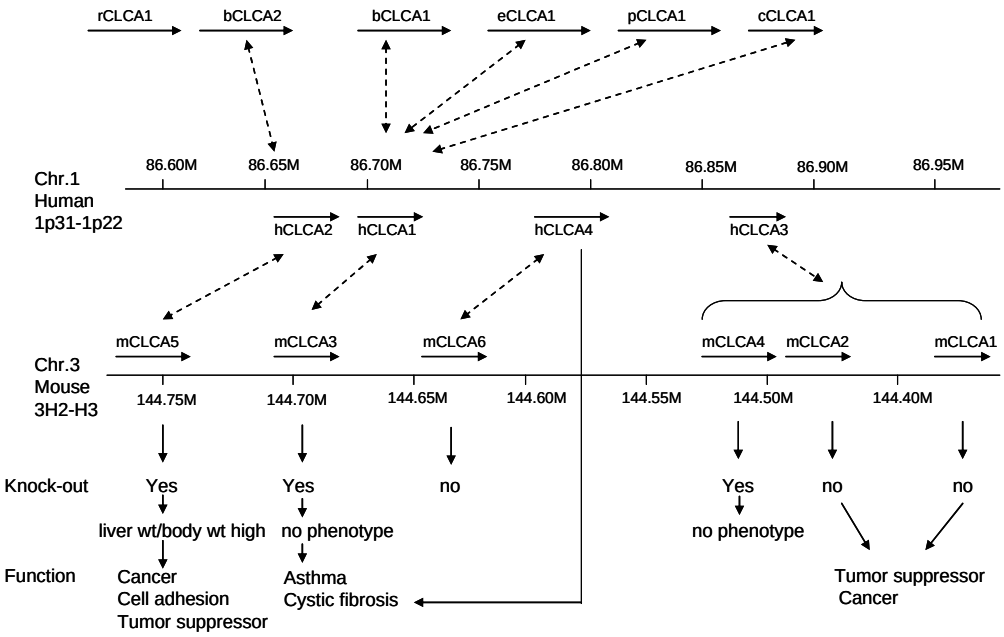

Figure 1.1 Orthology summary map of CLCA genes, human and mouse genome loci, knock-out mice, and gene functions. Double end arrow shows CLCA genes orthology between species. Human and mouse CLCA gene loci based on NCBI Map View. Three single gene knock-out mice have been generated, mCLCA3 (59), mCLCA5 (Deltagen, Inc.) and mCLCA4 (chapter 3). Summary of potential CLCA protein function.

The cDNA of eCLCA1 is 2.9 kb (GenBank accession NO. AY524856) and encodes a 913 aa protein product. *In vitro* translation of eCLCA1 cDNA followed by microsomal membrane experimental methods showed eCLCA protein is a 120 kDa when glycosylated. A 70 kDa and a 80 kDa fragment have been detected from colon mucosa by antibody (a-eCa1) (6). eCLCA1 is highly homologous to hCLCA1 and mCLCA3 (82.4% and 73.5% respectively at the polypeptide level) (6). At the protein level, eCLCA1 is expressed in mucous-producing cells of the respiratory and intestinal tracts, cutaneous sweat glands and renal mucous glands.

Loewen et al. (48) partially cloned cCLCA1 from canine retinal pigment epithelium using pCLCA1 specific primers. The partially predicted aa sequence of cCLCA1 is highly homologous to pCLCA1 and hCLCA1 (48). The mRNA and protein expression pattern of cCLCA1 is unknown.

Six murine members of CLCA (mCLCA1 to mCLCA6) have been cloned and characterized. There are two additional potential members in the murine genome: AI747448 (or mCLCA7) and EG622139 (or mCLCA8), which are on the same chromosome location as the other family members (NCBI database). All the mCLCAs are clustered on chromosome 3 H2-H3 (Figure 1.1). mCLCA1 was cloned from a mouse lung cDNA library using bCLCA2 cDNA as a probe (25). It is a 3.1 kb cDNA and the protein product is 125 kDa after glycosylation. mCLCA2 was cloned from mouse mammary gland mRNA pool using suppression subtractive hybridization method (42). mCLCA4 was cloned by Elble and colleagues (18) using degenerate primers based on bCLCA2. mCLCA1, mCLCA2 and mCLCA4 are not only located next to each other on mouse chromosome 3 but also share 70-80% identity at protein level and are orthologous to hCLCA3 (18, 47, 52) (Figure 1.2). mCLCA3, also named Gob-5, was isolated from mouse intestinal goblet cells (41). The mCLCA3 cDNA is 3 kb long and encodes 913 aa protein that shares homology with hCLCA 1 and pCLCA1

(28, 41) (Figure 1.2). mCLCA 5 and 6 were cloned from mouse eye and intestine RNA extracts, respectively (23). Both ORFs of mCLCA5 and mCLCA6 are approximately 2.8 kb but mCLCA6 may have a splice variant that is 2.6 kb.

In summary, CLCA members exist in at least 30 different species' genomes and 17 members from seven mammalian species have been published to date. All the CLCA members from the same species cluster on the same chromosome and the 17 CLCAs discussed have similar protein structure with a very diverse expression pattern in multiple tissues and organs. All the studied CLCA proteins are cleaved to NH_2-terminus and COOH-terminus fragments after glycosylation.

1.2 CLCAs common features

1.2.1 Chloride conductance

Anionic currents have been detected by either whole cell or single cell patch clamp techniques following transient transfection of the CLCA cDNA into either HEK293T or COS-1 cells. The anionic currents are dependent on intracellular Ca^{2+} concentration and can be blocked by chloride channel blockers, such as 4,4"-diisothiocyanatostilbene-2,2'-disulfonic acid (DIDS), dithiothreitol (DTT) or Niflumic (NAF) (30, 47). CLCA family was considered as a candidate of chloride channel protein based on the finding that bCLCA1 protein appeared to regulate calcium-activated chloride current in tracheal epithelial cells. Thus these data have led investigators to conclude that CLCAs regulate of a family of chloride currents controlled by calcium.

Gruber et al (30) investigated the electrophysiological features of hCLCA1 using whole cell and single cell patch clamp techniques following transient transfection of hCLCA1 cDNA into HEK293T cells. This group demonstrated the

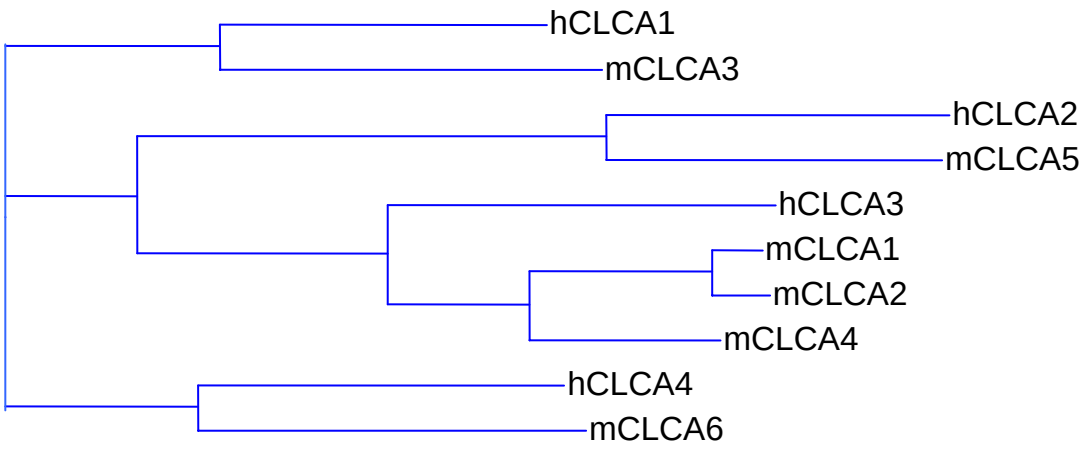

Figure 1.2 Phylogenetic tree of human and mouse CLCA members. The homology tree was generated using mRNA sequences obtained from GeneBank and subsequently aligned with Vector-NTI software (Invitrogen). The bar represents 5% diversity.

whole cell chloride current increased compared to control when intracellular calcium concentration was increased after an application of ionomycin. A similar experiment was performed with hCLCA2 cDNA and after administration of ionomycin the whole cell current as determined by patch clamp increased compared to control. Both of currents were blocked by DIDS, DTT, NAF and tamoxifen. mCLCA1 cDNA was transiently transfected into HEK293 cell and a calcium-activated chloride current was detected by whole cell patch clamp. The current increased with the addition of ionomycin and 2 mM calcium. The mCLCA1 current was inhibited by DTT, DIDS and NAF in 2 mM calcium (25). Romio and colleagues (60) injected mCLCA1 cDNA into Xenopus oocytes and detected a significant current without a calcium ionophore compared to water-injected oocytes. The mCLCA1 current in oocytes, but not the background current, was chloride dependent. Because of the high background current in Xenopus, it was impossible to detect the effect of calcium on the CLCA1 chloride conductance in the presence of ionomycin (60). Greenwood et al. (29) compared the native calcium-activated chloride current in murine portal vein with the mCLCA1 cloned from murine portal vein myocytes. They found that the two channels shared permeability similar to various anions, but the mCLCA1 channel current was not time-dependent while the native one was. Moreover, the mCLCA1 channel showed a lower sensitivity to calcium than the native channel. When they co-expressed mCLCA1 and β-subunit of the big potassium channel (mKCNMB1), the current significantly changed from time-independent to time-dependent and was more sensitive to calcium than without the mKCNB1 subunit. Using the mammalian two-hybrid system they showed that mCLCA1 and mKCNMB1 subunit interacted with each other but it remains unknown whether these two proteins interact in native vascular smooth muscle cells. These results suggested not only that mCLCA1 is a chloride current

regulated by calcium but that mCLCA1 current activity can be modified by other proteins (29, 47).

In summary, many CLCA members from different species produce chloride currents in response to changes in cellular calcium concentration. However, the mechanism of how these proteins contribute to the chloride currents remains unknown.

1.2.2. The structure of CLCA proteins and their cellular location

Epitope insertion in concert position followed by immunohistochemistry and hydropathy techniques resulted in several initial models of the CLCA protein structure. They were predicted to be transmembrane proteins (30-32, 54). Recently, the region including the transmembrane-spanning segments was also predicted using Simple Modular Architecture Research Tool (SMART) and it suggested that CLCA proteins contained von Willebrand factor domain A (VWA), an extracellular soluble domain (47). However, the Markov models for transmembrane segments and protein folding prediction suggested that CLCA proteins are soluble extracellular molecules with VWA domains and are not transmembrane proteins except the hCLCA2 COOH-terminal fragment (20, 52).

It was discovered that all the members of CLCA family are processed similarly using transient transfection of the CLCA cDNA into mammalian cell line such as HEK293T and COS cells (Chapter 2), (9-11, 18, 20, 25). They all code and glycosylate an approximately 130 kDa full-length precursor, then are cleaved to ~ 90 kDa (NH_2-terminus) and ~ 40 kDa (COOH-terminus) fragments. Both fragments, as with hCLCA1, mCLCA3 and mCLCA4, are secreted into the media and associate with the cell membrane. For hCLCA2, the NH_2-terminal fragment was released into the media and the COOH-terminal fragment remained in the membrane. Some CLCA

proteins were cleaved inside the cell such as mCLCA4 (Chapter 2), and some were cleaved outside the cell, such as hCLCA2 (20) (Figure 1.3).

The 90 kDa N-terminus fragment contains a cysteine-rich (also called N-terminal hydrolase) domain in the first 280 aa which is only found in the CLCA family (52, 55). Bioinformatics analysis by Pawlowski et al. (55) suggested the N-terminal hydrolase domain (N-term) contains a zinc metalloprotease domain that potentially functions as a hydrolase and protease. This prediction is supported by hCLCA3 structure—truncated protein with only N-terminal hydrolase domain. The CLCA proteins may possibly self-cleave during their processing (55). However, the mutant protein for this experiment may have misfolded and the cleavage of this protein group is still not certain (52). Moreover, the VWA domain is followed by the N-terminal hydrolase (N-Term) domain in this 90 kDa molecule. The VWA domain is involved in protein-protein interactions and contains a metal ion-dependent adhesion site (MIDAS) motif (68). In human and mice, all CLCA members have an N-Term domain and all members except hCLCA3 and EG622139 (one of the predicted genes) contain a VWA domain in their 90 kDa fragment (52). The 35 kDa COOH-terminal fragment has a conserved fibronectin type III (Fib3) domain that was predicted using JPRED 3 (a secondary structure prediction software), except hCLCA3 and EG622139. The main function of the Fib3 domain is for protein-protein interaction, but no studies have been published to date of how this domain actions in CLCA (52).

In summary, CLCA proteins are ~130 kDa precursors and cleaved to 90 kDa NH_2-terminal and 40 kDa COOH-terminal fragments. The cleavage occurs intracellular in some CLCA family members (mCLCA4, Chapter 2) and extracellular in others (20). CLCA family members contain a hydrolase and a VWA domain in the NH_2-terminal fragment while a Fib3 domain is found in the COOH-terminal fragment.

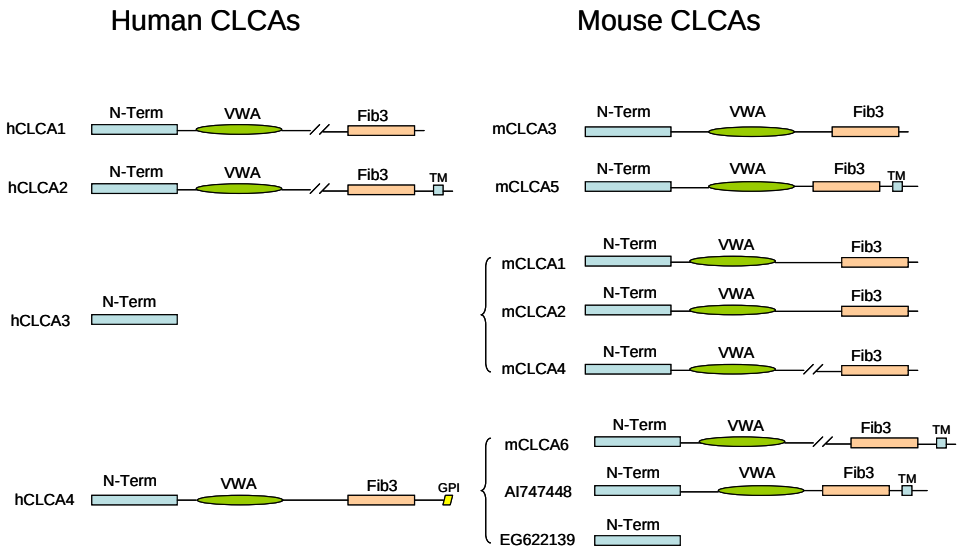

Figure 1.3 Structure of human and mouse CLCA proteins diagram. Each protein contains an N-terminal hydrolase domain (N-Term) (blue) that is cysteine-rich and conserved in all members. Note other common features shared between members. Abbreviations: von Willebrand factor type A, VWA domain; Fibronectin type III, Fib3 (orange); transmembrane, TM (light blue); glycosylphatidylinositol anchor, GPI (yellow). "//" denotes predicted proteolytic cleavage sites.

1.3 The relationship between CLCAs and asthma

Asthma is a chronic inflammatory disorder of the airway. Many cells and elements are involved in the hyperactivity associated with asthma, such as mast cells, eosinophils, T lymphocytes--especially T helper type 1 and 2 (Th1/Th2) subpopulation-cells, neutrophils, cytokines and epithelial cells. As with many other human diseases, asthma is complex disease with multifactorial and/or genetic issues. The main features of asthma are airflow obstruction, bronchial hyper-responsiveness, airway smooth muscle spasm, mucosal edema, airway inflammation and airway remodeling (12, 43).

Evidence suggests that some CLCA gene family members are overexpressed in bronchial allergic asthma and may play a direct role in mucus production and differentiation in goblet cells (36, 63). CLCA overexpression appears to be through cytokine production of T lymphocytes, specifically Th1 and Th2 (72).

hCLCA1 has been found to be upregulated by interleukin-9 (IL-9) and regulates the expression of soluble mucus in airways (63). In IL-9 transgenic mice, mCLCA3 was induced by Th2 cytokines, IL-9, IL-4 and IL-13, but not by interferon-γ (INF-γ) (72). Moreover, hCLCA1 and mCLCA3 were induced in human primary lung culture by Th2 cytokines.

hCLCA1 and its murine homolog mCLCA3 are upregulated in human asthma patients and a murine homolog model of lung tissue disease, respectively (36, 63, 72). Overexpression of hCLCA1 and mCLCA3 resulted in mucus overproduction, goblet cell metaplasia and worsening of the asthma phenotype (50). Reduction in the asthmatic phenotype occurred with an adenoviral mCLCA3 mRNA antisense (mediated repression of mCLCA3 expression). Goblet cell metaplasia and mucin production were inhibited by the functional block of hCLCA1 and mCLCA3 chloride channel activity with chloride channel blocker (such as Niflumic acid) resulting in

reduced airway inflammation in ovalbumin allergen challenged mice (50, 73). In hCLCA1, single nucleotide polymorphisms (SNP) are associated with the susceptibility of human asthma. Kamada et al. (39) identified eight SNPs in hCLCA1 and one was associated with an increased risk of asthma as determined by screening children with and without asthma. Based on the above evidence, mCLCA3 and hCLCA1 are promising therapeutic targets for asthma. Recurrent airway obstruction (RAO) in horses has been used as a model to study human asthma. Range and colleagues (57) observed that eCLCA1 is overexpressed in RAO horse airways as determined by Northern blot, Western blot and real-time PCR techniques. In addition, RAO horses showed goblet cell metaplasia in bronchioles and goblet cell hyperplasia in bronchi and the trachea and eCLCA1 protein as part of airway mucins.

To study the biological role of CLCA proteins, Patel et al. (53) developed an animal model of inflammatory airway disease. Sendai virus, a mouse parainfluenza virus, was used as the infectious agent and resulted in inflammation of small airways. With this model, they found that mCLCA3 gene expression was sufficient for the development of mucous cell metaplasia but did not result in airway hyperreactivity. However, mCLCA3 null mice mucous cell metaplasia was no different when compared to wildtype mice and this may be the result of compensation by other CLCA proteins, namely, mCLCA5 and mCLCA6 (52, 53).

1.4 The relationship between CLCAs and cystic fibrosis

Cystic fibrosis (CF) is a common secretary epithelia disorder that is a fatal multisystem disease due to genetic mutations of the chloride channel protein CF transmembrane conductance regulator (CFTR). Many organs are affected in this disease, such as lung, large and small intestine, sweat glands, pancreas, cutaneous and reproductive organs. The clinical symptoms include heavy airway mucus with poor

hydration and obstruction, bacterial lung infection, pancreatic insufficiency, and obstruction of the small intestine (44, 61, 65). However, the complexity of CF symptoms and clinical phenotype suggest this disease is, in part, regulated by other modulators which remain unknown.

Several laboratories have identified some CLCA family members as potential CF modulators. Ritzka et al. (58) used polymorphic microsatellite markers covering 40 Mbp region of human CLCA locus from chromosome 1p in CF patients to display CFTR-independent residual chloride conductance in gastrointestinal epithelia. The results showed that hCLCA1 and some of hCLCA4 are associated with CFTR-independent, DIDS-sensitive, residual chloride conductance in the rectal mucosa of CF patients. Hoshino and colleagues (36) collected bronchial mucosa endoscopic biopsy from 10 CF patients and six healthy control individuals and found that hCLCA1 overexpression in CF lungs was associated with mucus overproduction. Lastly, Leverkoehne et al. (45) used qPCR to quantify mCLCA1-mCLCA4 expression levels in murine CF small intestines compared to wildtype animals and found that mCLCA3 mRNA copy number was increased threefold in all CF mice and mCLCA2 mRNA copy number was increased due to transcriptional upregulation. Moreover, Brouillard et al. (11) discovered that expression of mCLCA3 proteins was reduced in cystic fibrosis knock-out mice by native/SDS-PAGE analysis. These results suggest that hCLCA1, hCLCA4 and mCLCA3 may play a role in CF disease processes.

In summary, some CLCA family members such as hCLCA1, hCLCA4 and mCLCA3 are thought to play an important role as potential modulators in CF. Thus, the CLCA family may be a pharmaceutical target for patients with CF.

1.5 The function and contribution in cell adhesion, tumor, and cancer

CLCA proteins such as bCLCA2, hCLCA2, mCLCA1, mCLCA2 and mCLCA5 have been reported to play a role in cell adhesion and regulating the development of tumors and cancer.

Over the past decade, research suggests that some members of the CLCA family may be involved in cell adhesion. bCLCA2 was identified as the endothelial adhesion molecule which binds hematogeneous tumor cells and this action leads to vascular arrest before tumor growth and invasion. Studies in mice with melanomas showed that CLCA proteins may promote metastasis to the lung (74-76). 90 kDa bCLCA2 was tightly bound to murine high lung-metastatic B16-F10 melanoma cells compared to low lung-metastatic counterparts B16-L8-F10 and B16-F0. B16 melanoma cell binding to Lu-ECAM-1(90 kDa bCLCA2) was blocked by Lu-ECAM-1 antibody mAb6D3 and was also competitively inhibited by soluble Lu-ECAM-1(74).

hCLCA2 is also expressed in endothelial cells derived from different lung vascular compartments (2, 76) and is critical for colonization in human breast cancer cell lines (2). These results suggested that CLCA binding to endothelia is an important part of hematogeneous metastasis and lung colonization. In addition, it has been shown that hCLCA2 interacted with β4-integrin in MDA-MB-231 breast cancer cell line and that mCLCA1 interacted with focal adhesion kinase; both interactions mediate early metastatic growth (1-3).

Little information is available on the role CLCA proteins play in tumor formation. CLCA gene expression is frequently reduced in tumor cell lines and may contribute to tumor growth (19, 33, 40). Elble et al (19) transfected mCLCA2 into HC11 (mammary epithelial cell line) and found that the rate of apoptosis of serum-starved cells increased significantly compared with control cells. In apoptosis-resistant

tumor cell lines (JC and CSML-0) and in HC11 cells selected for resistance to detachment-induced apoptosis (anoikis), mCLCA1 message was at least thirtyfold less and mCLCA2 function was lost, most likely by disrupted splicing. As a tumor suppresser, the mechanism(s) of CLCA proteins for this purpose is not clear. It has been suggested CLCAs act through the modulation of ion channels in the transformed cell by a proapoptotic signal (19).

Gruber and Pauli (33) used *in situ* hybridization to study the relationship between hCLCA2 and human breast cancer and found that hCLCA2 can be detected in normal breast epithelium tissues such as acini and small ducts but was absent in breast tumor tissue. A similar pattern was also observed in normal and tumor cell lines. hCLCA2 was detected in nontransformed human mammary epithelial cell line such as MCF10A and in the nontumorigenic cell line MDA-MB-453. However, hCLCA2 was not detected in the tumorigenic cell lines such as MDA231, MDA-MB-435, MDA-MB-468 and MCF7. These results were confirmed by Li et al. (46). They confirmed that hCLCA2 was not present in tumorigenic cell lines and that overexpression of hCLCA2 in CLCA2-negative cell lines reduced tumorigenicity and metastasis capacity. The mechanism of hCLCA2 silencing in breast cancer and tumor cell lines may be due to hypermethylation of the hCLCA2 promoter region (46). These results all suggest that hCLCA2 plays a tumor-suppression role in breast cancer. Interestingly, another study showed the hCLCA2 gene is deleted in mantle cell lymphoma specimens (8), again confirming a potential role of CLCA2 in cancer.

The mouse ortholog of hCLCA2, mCLCA5 was expressed in the immortalized cell line HC11 and correlated with either slow or arrested cell growth. Without growth factors or anchorage of the cells, mCLCA5 expression was increased, and the apoptosis effector Bax was increased in parallel. mCLCA5 was down-regulated in

metastatic mammary tumor cell lines (CSML-100 and 4T1). This study indicated that hCLCA2 and mCLCA5 are not only orthologous in sequence but also in function (9).

In conclusion, CLCA members hCLCA2, mCLCA1, mCLCA2 and mCLCA5 play a role in tumor suppression through an apoptotic pathway and in cell adhesion through β-integrin signaling. However, the details of this mechanism(s) remain unknown. bCLCA2 mediates lung metastasis of murine melanomas; again, details of the pathway remain unknown.

1.6 Summary of CLCA function

The CLCA gene family clusters together on the same chromosome and code for protein products with similar structure, but they are functionally diverse. The precursor protein is cleaved into two fragments, both of which are secreted and associate with the cell membrane. They modulate chloride current but do not appear to be the pore-forming structure of chloride channels themselves. Their involvement in the pathophysiology of disease can be divided into two categories. One group, that includes hCLCA1, mCLCA3 and mCLCA5, contributes to asthma, CF and secreted diseases; the other group, such as hCLCA2, mCLCA1, mCLCA2 and mCLCA5, is related to cancer, tumor and cell adhesion functions. However, how CLCAs interact and modulate other protein groups remains largely unknown. This dissertation focuses on the functional role of mCLCA4 and its highly homologous isoforms mCLCA1 and mCLCA2 in murine physiology.

REFERENCE

1. **Abdel-Ghany M, Cheng HC, Elble RC, Lin H, DiBiasio J, and Pauli BU.** The interacting binding domains of the beta(4) integrin and calcium-activated chloride channels (CLCAs) in metastasis. *J Biol Chem* 278: 49406-49416, 2003.

2. **Abdel-Ghany M, Cheng HC, Elble RC, and Pauli BU.** The breast cancer beta 4 integrin and endothelial human CLCA2 mediate lung metastasis. *J Biol Chem* 276: 25438-25446, 2001.

3. **Abdel-Ghany M, Cheng HC, Elble RC, and Pauli BU.** Focal adhesion kinase activated by beta(4) integrin ligation to mCLCA1 mediates early metastatic growth. *J Biol Chem* 277: 34391-34400, 2002.

4. **Agnel M, Vermat T, and Culouscou JM.** Identification of three novel members of the calcium-dependent chloride channel (CaCC) family predominantly expressed in the digestive tract and trachea. *FEBS Lett* 455: 295-301, 1999.

5. **Anderson MP, Sheppard DN, Berger HA, and Welsh MJ.** Chloride channels in the apical membrane of normal and cystic fibrosis airway and intestinal epithelia. *Am J Physiol* 263: L1-14, 1992.

6. **Anton F, Leverkoehne I, Mundhenk L, Thoreson WB, and Gruber AD.** Overexpression of eCLCA1 in small airways of horses with recurrent airway obstruction. *J Histochem Cytochem* 53: 1011-1021, 2005.

7. **Arreola J, Melvin JE, and Begenisich T.** Activation of calcium-dependent chloride channels in rat parotid acinar cells. *J Gen Physiol* 108: 35-47, 1996.

8. **Balakrishnan A, von Neuhoff N, Rudolph C, Kamphues K, Schraders M, Groenen P, van Krieken JH, Callet-Bauchu E, Schlegelberger B, and Steinemann D.** Quantitative microsatellite analysis to delineate the commonly deleted region 1p22.3 in mantle cell lymphomas. *Genes Chromosomes Cancer* 45: 883-892, 2006.

9. **Beckley JR, Pauli BU, and Elble RC.** Re-expression of detachment-inducible chloride channel mCLCA5 suppresses growth of metastatic breast cancer cells. *J Biol Chem* 279: 41634-41641, 2004.

10. **Bothe MK, Braun J, Mundhenk L, and Gruber AD.** Murine mCLCA6 is an integral apical membrane protein of non-goblet cell enterocytes and co-localizes with the cystic fibrosis transmembrane conductance regulator. *J Histochem Cytochem* 56: 495-509, 2008.

11. **Brouillard F, Bensalem N, Hinzpeter A, Tondelier D, Trudel S, Gruber AD, Ollero M, and Edelman A.** Blue native/SDS-PAGE analysis reveals reduced expression of the mClCA3 protein in cystic fibrosis knock-out mice. *Mol Cell Proteomics* 4: 1762-1775, 2005.

12. **Busse WW and Lemanske RF, Jr.** Asthma. *N Engl J Med* 344: 350-362, 2001.

13. **Byrne NG and Large WA.** The action of noradrenaline on single smooth muscle cells freshly dispersed from the guinea-pig pulmonary artery. *Br J Pharmacol* 91: 89-94, 1987.

14. **Byrne NG and Large WA.** Action of noradrenaline on single smooth muscle cells freshly dispersed from the rat anococcygeus muscle. *J Physiol* 389: 513-525, 1987.

15. **Byrne NG and Large WA.** Membrane ionic mechanisms activated by noradrenaline in cells isolated from the rabbit portal vein. *J Physiol* 404: 557-573, 1988.

16. **Clancy JP, McCann JD, Li M, and Welsh MJ.** Calcium-dependent regulation of airway epithelial chloride channels. *Am J Physiol* 258: L25-32, 1990.

17. **Cunningham SA, Awayda MS, Bubien JK, Ismailov, II, Arrate MP, Berdiev BK, Benos DJ, and Fuller CM.** Cloning of an epithelial chloride channel from bovine trachea. *J Biol Chem* 270: 31016-31026, 1995.

18. **Elble RC, Ji G, Nehrke K, DeBiasio J, Kingsley PD, Kotlikoff MI, and Pauli BU.** Molecular and functional characterization of a murine calcium-activated chloride channel expressed in smooth muscle. *J Biol Chem* 277: 18586-18591, 2002.

19. **Elble RC and Pauli BU.** Tumor suppression by a proapoptotic calcium-activated chloride channel in mammary epithelium. *J Biol Chem* 276: 40510-40517, 2001.

20. **Elble RC, Walia V, Cheng HC, Connon CJ, Mundhenk L, Gruber AD, and Pauli BU.** The putative chloride channel hCLCA2 has a single C-terminal transmembrane segment. *J Biol Chem* 281: 29448-29454, 2006.

21. **Elble RC, Widom J, Gruber AD, Abdel-Ghany M, Levine R, Goodwin A, Cheng HC, and Pauli BU.** Cloning and characterization of lung-endothelial cell adhesion molecule-1 suggest it is an endothelial chloride channel. *J Biol Chem* 272: 27853-27861, 1997.

22. **Evans MG and Marty A.** Calcium-dependent chloride currents in isolated cells from rat lacrimal glands. *J Physiol* 378: 437-460, 1986.

23. **Evans SR, Thoreson WB, and Beck CL.** Molecular and functional analyses of two new calcium-activated chloride channel family members from mouse eye and intestine. *J Biol Chem* 279: 41792-41800, 2004.

24. **Fuller CM.** *Calcium-activated Chloride Channels*. San Diego: Academic Press, 2002.

25. **Gandhi R, Elble RC, Gruber AD, Schreur KD, Ji HL, Fuller CM, and Pauli BU.** Molecular and functional characterization of a calcium-sensitive chloride channel from mouse lung. *J Biol Chem* 273: 32096-32101, 1998.

26. **Gaspar KJ, Racette KJ, Gordon JR, Loewen ME, and Forsyth GW.** Cloning a chloride conductance mediator from the apical membrane of porcine ileal enterocytes. *Physiol Genomics* 3: 101-111, 2000.

27. **Gibbs RA, Weinstock GM, Metzker ML, Muzny DM, Sodergren EJ, Scherer S, Scott G, Steffen D, Worley KC, Burch PE, Okwuonu G, Hines S, Lewis L, DeRamo C, Delgado O, Dugan-Rocha S, Miner G, Morgan M, Hawes A, Gill R, Celera, Holt RA, Adams MD, Amanatides PG, Baden-Tillson H, Barnstead M, Chin S, Evans CA, Ferriera S, Fosler C, Glodek A, Gu Z, Jennings D, Kraft CL, Nguyen T, Pfannkoch CM, Sitter C, Sutton GG, Venter JC, Woodage T, Smith D, Lee HM, Gustafson E, Cahill P, Kana A, Doucette-Stamm L, Weinstock K, Fechtel K, Weiss RB, Dunn DM, Green ED, Blakesley RW, Bouffard GG, De Jong PJ, Osoegawa K, Zhu B, Marra M, Schein J, Bosdet I, Fjell C, Jones S, Krzywinski M, Mathewson C, Siddiqui A, Wye N, McPherson J, Zhao S, Fraser CM, Shetty J, Shatsman S, Geer K, Chen Y, Abramzon S, Nierman WC, Havlak PH, Chen R, Durbin KJ, Egan A, Ren Y, Song XZ, Li B, Liu Y, Qin X, Cawley S, Cooney AJ, D'Souza LM, Martin K, Wu JQ, Gonzalez-Garay ML, Jackson AR, Kalafus KJ, McLeod MP, Milosavljevic A, Virk D, Volkov A, Wheeler DA, Zhang Z, Bailey JA, Eichler EE, Tuzun E, et al.** Genome sequence of the Brown Norway rat yields insights into mammalian evolution. *Nature* 428: 493-521, 2004.

28. **Gibson A, Lewis AP, Affleck K, Aitken AJ, Meldrum E, and Thompson N.** hCLCA1 and mCLCA3 are secreted non-integral membrane proteins and therefore are not ion channels. *J Biol Chem* 280: 27205-27212, 2005.

29. **Greenwood IA, Miller LJ, Ohya S, and Horowitz B.** The large conductance potassium channel beta-subunit can interact with and modulate the functional properties of a calcium-activated chloride channel, CLCA1. *J Biol Chem* 277: 22119-22122, 2002.

30. **Gruber AD, Elble RC, Ji HL, Schreur KD, Fuller CM, and Pauli BU.** Genomic cloning, molecular characterization, and functional analysis of human CLCA1, the first human member of the family of Ca2+-activated Cl- channel proteins. *Genomics* 54: 200-214, 1998.

31. **Gruber AD and Pauli BU.** Clustering of the human CLCA gene family on the short arm of chromosome 1 (1p22-31). *Genome* 42: 1030-1032, 1999.

32. **Gruber AD and Pauli BU.** Molecular cloning and biochemical characterization of a truncated, secreted member of the human family of Ca2+-activated Cl- channels. *Biochim Biophys Acta* 1444: 418-423, 1999.

33. **Gruber AD and Pauli BU.** Tumorigenicity of human breast cancer is associated with loss of the Ca2+-activated chloride channel CLCA2. *Cancer Res* 59: 5488-5491, 1999.

34. **Gruber AD, Schreur KD, Ji HL, Fuller CM, and Pauli BU.** Molecular cloning and transmembrane structure of hCLCA2 from human lung, trachea, and mammary gland. *Am J Physiol* 276: C1261-1270, 1999.

35. **Harvey RD and Hume JR.** Autonomic regulation of a chloride current in heart. *Science* 244: 983-985, 1989.

36. **Hoshino M, Morita S, Iwashita H, Sagiya Y, Nagi T, Nakanishi A, Ashida Y, Nishimura O, Fujisawa Y, and Fujino M.** Increased expression of the human Ca2+-activated Cl- channel 1 (CaCC1) gene in the asthmatic airway. *Am J Respir Crit Care Med* 165: 1132-1136, 2002.

37. **Janssen LJ and Sims SM.** Acetylcholine activates non-selective cation and chloride conductances in canine and guinea-pig tracheal myocytes. *J Physiol* 453: 197-218, 1992.

38. **Jeong SM, Park HK, Yoon IS, Lee JH, Kim JH, Jang CG, Lee CJ, and Nah SY.** Cloning and expression of Ca2+-activated chloride channel from rat brain. *Biochem Biophys Res Commun* 334: 569-576, 2005.

39. **Kamada F, Suzuki Y, Shao C, Tamari M, Hasegawa K, Hirota T, Shimizu M, Takahashi N, Mao XQ, Doi S, Fujiwara H, Miyatake A, Fujita K, Chiba Y, Aoki Y, Kure S, Tamura G, Shirakawa T, and Matsubara Y.** Association of the hCLCA1 gene with childhood and adult asthma. *Genes Immun* 5: 540-547, 2004.

40. **Kim JA, Kang YS, and Lee YS.** Role of Ca2+-activated Cl- channels in the mechanism of apoptosis induced by cyclosporin A in a human hepatoma cell line. *Biochem Biophys Res Commun* 309: 291-297, 2003.

41. **Komiya T, Tanigawa Y, and Hirohashi S.** Cloning and identification of the gene gob-5, which is expressed in intestinal goblet cells in mice. *Biochem Biophys Res Commun* 255: 347-351, 1999.

42. **Lee D, Ha S, Kho Y, Kim J, Cho K, Baik M, and Choi Y.** Induction of mouse Ca(2+)-sensitive chloride channel 2 gene during involution of mammary gland. *Biochem Biophys Res Commun* 264: 933-937, 1999.

43. **Lemanske RF, Jr. and Busse WW.** 6. Asthma. *J Allergy Clin Immunol* 111: S502-519, 2003.

44. **Leverkoehne I, Holle H, Anton F, and Gruber AD.** Differential expression of calcium-activated chloride channels (CLCA) gene family members in the small intestine of cystic fibrosis mouse models. *Histochem Cell Biol* 126: 239-250, 2006.

45. **Leverkoehne I, Horstmeier BA, von Samson-Himmelstjerna G, Scholte BJ, and Gruber AD.** Real-time RT-PCR quantitation of mCLCA1 and mCLCA2 reveals differentially regulated expression in pre- and postnatal murine tissues. *Histochem Cell Biol* 118: 11-17, 2002.

46. **Li X, Cowell JK, and Sossey-Alaoui K.** CLCA2 tumour suppressor gene in 1p31 is epigenetically regulated in breast cancer. *Oncogene* 23: 1474-1480, 2004.

47. **Loewen ME and Forsyth GW.** Structure and function of CLCA proteins. *Physiol Rev* 85: 1061-1092, 2005.

48. **Loewen ME, Smith NK, Hamilton DL, Grahn BH, and Forsyth GW.** CLCA protein and chloride transport in canine retinal pigment epithelium. *Am J Physiol Cell Physiol* 285: C1314-1321, 2003.

49. **Morris AP and Frizzell RA.** Ca(2+)-dependent Cl- channels in undifferentiated human colonic cells (HT-29). II. Regulation and rundown. *Am J Physiol* 264: C977-985, 1993.

50. **Nakanishi A, Morita S, Iwashita H, Sagiya Y, Ashida Y, Shirafuji H, Fujisawa Y, Nishimura O, and Fujino M.** Role of gob-5 in mucus overproduction and airway hyperresponsiveness in asthma. *Proc Natl Acad Sci U S A* 98: 5175-5180, 2001.

51. **Nilius B, Prenen J, Szucs G, Wei L, Tanzi F, Voets T, and Droogmans G.** Calcium-activated chloride channels in bovine pulmonary artery endothelial cells. *J Physiol* 498 (Pt 2): 381-396, 1997.

52. **Patel AC, Brett TJ, and Holtzman MJ.** The Role of CLCA Proteins in Inflammatory Airway Disease. *Annu Rev Physiol*, 2008.

53. **Patel AC, Morton JD, Kim EY, Alevy Y, Swanson S, Tucker J, Huang G, Agapov E, Phillips TE, Fuentes ME, Iglesias A, Aud D, Allard JD, Dabbagh K, Peltz G, and Holtzman MJ.** Genetic segregation of airway disease traits despite redundancy of calcium-activated chloride channel family members. *Physiol Genomics* 25: 502-513, 2006.

54. **Pauli BU, Abdel-Ghany M, Cheng HC, Gruber AD, Archibald HA, and Elble RC.** Molecular characteristics and functional diversity of CLCA family members. *Clin Exp Pharmacol Physiol* 27: 901-905, 2000.

55. **Pawlowski K, Lepisto M, Meinander N, Sivars U, Varga M, and Wieslander E.** Novel conserved hydrolase domain in the CLCA family of alleged calcium-activated chloride channels. *Proteins* 63: 424-439, 2006.

56. **Qu Z, Wei RW, Mann W, and Hartzell HC.** Two bestrophins cloned from Xenopus laevis oocytes express Ca(2+)-activated Cl(-) currents. *J Biol Chem* 278: 49563-49572, 2003.

57. **Range F, Mundhenk L, and Gruber AD.** A soluble secreted glycoprotein (eCLCA1) is overexpressed due to goblet cell hyperplasia and metaplasia in horses with recurrent airway obstruction. *Vet Pathol* 44: 901-911, 2007.

58. **Ritzka M, Stanke F, Jansen S, Gruber AD, Pusch L, Woelfl S, Veeze HJ, Halley DJ, and Tummler B.** The CLCA gene locus as a modulator of the gastrointestinal basic defect in cystic fibrosis. *Hum Genet* 115: 483-491, 2004.

59. **Robichaud A, Tuck SA, Kargman S, Tam J, Wong E, Abramovitz M, Mortimer JR, Burston HE, Masson P, Hirota J, Slipetz D, Kennedy B, O'Neill G, and Xanthoudakis S.** Gob-5 is not essential for mucus overproduction in preclinical murine models of allergic asthma. *Am J Respir Cell Mol Biol* 33: 303-314, 2005.

60. **Romio L, Musante L, Cinti R, Seri M, Moran O, Zegarra-Moran O, and Galietta LJ.** Characterization of a murine gene homologous to the bovine CaCC chloride channel. *Gene* 228: 181-188, 1999.

61. **Schwiebert EM, Morales MM, Devidas S, Egan ME, and Guggino WB.** Chloride channel and chloride conductance regulator domains of CFTR, the cystic fibrosis transmembrane conductance regulator. *Proc Natl Acad Sci U S A* 95: 2674-2679, 1998.

62. **Smith PM and Gallacher DV.** Acetylcholine- and caffeine-evoked repetitive transient Ca(2+)-activated K+ and C1- currents in mouse submandibular cells. *J Physiol* 449: 109-120, 1992.

63. **Toda M, Tulic MK, Levitt RC, and Hamid Q.** A calcium-activated chloride channel (HCLCA1) is strongly related to IL-9 expression and mucus production in bronchial epithelium of patients with asthma. *J Allergy Clin Immunol* 109: 246-250, 2002.

64. **Tsunenari T, Sun H, Williams J, Cahill H, Smallwood P, Yau KW, and Nathans J.** Structure-function analysis of the bestrophin family of anion channels. *J Biol Chem* 278: 41114-41125, 2003.

65. **Turcios NL.** Cystic fibrosis: an overview. *J Clin Gastroenterol* 39: 307-317, 2005.

66. **Twigger SN, Pruitt KD, Fernandez-Suarez XM, Karolchik D, Worley KC, Maglott DR, Brown G, Weinstock G, Gibbs RA, Kent J, Birney E, and Jacob HJ.** What everybody should know about the rat genome and its online resources. *Nat Genet* 40: 523-527, 2008.

67. **Wheeler DL, Barrett T, Benson DA, Bryant SH, Canese K, Chetvernin V, Church DM, Dicuccio M, Edgar R, Federhen S, Feolo M, Geer LY, Helmberg W, Kapustin Y, Khovayko O, Landsman D, Lipman DJ, Madden TL, Maglott DR, Miller V, Ostell J, Pruitt KD, Schuler GD, Shumway M, Sequeira E, Sherry ST, Sirotkin K, Souvorov A, Starchenko G, Tatusov RL, Tatusova TA, Wagner L, and Yaschenko E.** Database resources of the National Center for Biotechnology Information. *Nucleic Acids Res* 36: D13-21, 2008.

68. **Whittaker CA and Hynes RO.** Distribution and evolution of von Willebrand/integrin A domains: widely dispersed domains with roles in cell adhesion and elsewhere. *Mol Biol Cell* 13: 3369-3387, 2002.

69. **Yamazaki J, Okamura K, Ishibashi K, and Kitamura K.** Characterization of CLCA protein expressed in ductal cells of rat salivary glands. *Biochim Biophys Acta* 1715: 132-144, 2005.

70. **Yang YD, Cho H, Koo JY, Tak MH, Cho Y, Shim WS, Park SP, Lee J, Lee B, Kim BM, Raouf R, Shin YK, and Oh U.** TMEM16A confers receptor-activated calcium-dependent chloride conductance. *Nature* 455: 1210-1215, 2008.

71. **Yoon IS, Jeong SM, Lee SN, Lee JH, Kim JH, Pyo MK, Lee BH, Choi SH, Rhim H, Choe H, and Nah SY.** Cloning and heterologous expression of a Ca2+-activated chloride channel isoform from rat brain. *Biol Pharm Bull* 29: 2168-2173, 2006.

72. **Zhou Y, Dong Q, Louahed J, Dragwa C, Savio D, Huang M, Weiss C, Tomer Y, McLane MP, Nicolaides NC, and Levitt RC.** Characterization of a

calcium-activated chloride channel as a shared target of Th2 cytokine pathways and its potential involvement in asthma. *Am J Respir Cell Mol Biol* 25: 486-491, 2001.

73. **Zhou Y, Shapiro M, Dong Q, Louahed J, Weiss C, Wan S, Chen Q, Dragwa C, Savio D, Huang M, Fuller C, Tomer Y, Nicolaides NC, McLane M, and Levitt RC.** A calcium-activated chloride channel blocker inhibits goblet cell metaplasia and mucus overproduction. *Novartis Found Symp* 248: 150-165; discussion 165-170, 277-182, 2002.

74. **Zhu D, Cheng CF, and Pauli BU.** Blocking of lung endothelial cell adhesion molecule-1 (Lu-ECAM-1) inhibits murine melanoma lung metastasis. *J Clin Invest* 89: 1718-1724, 1992.

75. **Zhu D and Pauli BU.** Correlation between the lung distribution patterns of Lu-ECAM-1 and melanoma experimental metastases. *Int J Cancer* 53: 628-633, 1993.

76. **Zhu DZ, Cheng CF, and Pauli BU.** Mediation of lung metastasis of murine melanomas by a lung-specific endothelial cell adhesion molecule. *Proc Natl Acad Sci U S A* 88: 9568-9572, 1991.

77. **Zhu DZ and Pauli BU.** Generation of monoclonal antibodies directed against organ-specific endothelial cell surface determinants. *J Histochem Cytochem* 39: 1137-1142, 1991.

78. **Zygmunt AC and Gibbons WR.** Calcium-activated chloride current in rabbit ventricular myocytes. *Circ Res* 68: 424-437, 1991.

CHAPTER 2

MCLCA4 ER PROCESSING AND SECRETION REQUIRES LUMINAL SORTING MOTIFS*

----The regulation and secretion of mCLCA4 protein

* This article was published in *Am J Physiol Cell Physiol* 295: C279-C287, 2008
First published May 21, 2008; doi: 10.1152/ajpcell.00060.2008

Chunlei Huan**, Kai Su Greene**, Bo Shui, Gwendolyn Spizz, Haitao Sun, Robert M. Doran, Partricia J. Fisher, Mark S. Roberson, Randolph C. Elble, and Michael I. Kotlikoff

** Chunlei Huan and Kai Su Greene contributed equally to this study.

2.1 Abstract

Ca^{2+}-activated Cl^- channel (CLCA) proteins are encoded by a family of highly related and clustered genes in mammals that are markedly upregulated in inflammation and have been shown to affect chloride transport. Here we describe the cellular processing and regulatory sequences underlying murine (m) CLCA4 proteins. The 125-kDa mCLCA4 gene product is cleaved to 90 kDa and 40 kDa fragments and the NH_2- and COOH-terminal fragments are secreted, where they are found in cell media and associated with the plasma membrane. The 125-kDa full-length protein is only found in the endoplasmic reticulum (ER), and specific luminal diarginine retention and dileucine forward trafficking signals contained within the CLCA4 sequence regulate export from the ER and proteolytic processing. Mutation of the dileucine luminal sequences resulted in ER trapping of the immaturely glycosylated 125-kDa peptide, indicating that proteolytic cleavage occurs following recognition of the trafficking motifs. Moreover, the mutated dileucine and diarginine signal sequences directed processing of a secreted form of enhanced green fluorescent protein in a manner consistent with the effects on mCLCA4.

2.2 Introduction

Ca^{2+}-activated Cl^- channel (CLCA) proteins are highly upregulated in human asthma and animal models of mucosal inflammation (15, 17, 23). Since their initial cloning in bovine epithelium (1) and endothelium (4), numerous mammalian CLCA genes have been described with distinct, tissue-specific expression patterns (2, 13, 18). Originally described as integral membrane proteins that may be chloride channels, CLCAs have recently been shown to undergo extensive processing, including proteolytic cleavage and secretion (3, 6, 14), suggesting a more complex role than the regulation of chloride permeability and mucous secretion. In the mouse, the highly

homologous mCLCA genes are tightly clustered on Chromosome 3 (H3) in a manner that may enable coordinated transcriptional regulation, and the marked alteration in expression of CLCA genes in several disease states has provoked further interest in their function (12, 20, 23). mCLCA4, which is most closely related to mCLCA2 and mCLCA1 (the orthologs of hCLCA3), is expressed in epithelial and smooth muscle cells (2) and contains conserved family features including predicted proteolytic cleavage and serine phosphorylation sites, although neither the processing nor phosphorylation of mCLCA4 have been experimentally demonstrated.

Post-translational processing in the endoplasmic reticulum (ER) is critical for the proper trafficking of proteins to their cellular targets, including the plasma membrane, secretory vesicles, and other organelles (21). Proper assembly and processing occurs through the folding and glycosylation of the native peptide and the recognition of specific motifs by chaperone proteins (5). With respect to proteins that traverse the secretory pathway, specific glycosylations occur that are recognized by carbohydrate binding proteins that serve to sort and direct the peptides to the appropriate destination (10). Specific motifs regulating ER retention and forward trafficking have recently been demonstrated in the integral membrane, sodium-dependent glutamate subtype glial transporter (GLT-1), consisting of dileucine (LL) pairs N-terminal to a diarginine (RxR) sequence (11). In the GLT-1 transporter, 3 dileucine pairs occur as part of a pattern of heptad leucines closely followed by a highly conserved diarginine sequence that is conserved in glutamate transporters and found in several channel or receptor proteins (11). The former sequences regulate the forward transport of the full–length GLT-1 translation product in monomeric and multimeric forms for endosomal transport to the plasma membrane and the latter RxR sequence serves as an ER retention motif (11).

We have utilized heterologous expression of tagged mCLCA4 proteins to determine the intracellular processing and cellular localization of the full length and processed peptides. Tagged mCLCA4 proteins specific for the N and C –terminal fragments were created that were processed in the same way as native proteins. We report that the full length mCLCA4 proteins are cleaved into 90 and 40 kDa fragments within the ER compartment, that both peptides are secreted and associate with the plasma membrane, and that internal dileucine and diarginine sequences serve as ER trafficking signals in mCLCA4 proteins.

2.3 Materials and Methods

2.3.1 Cell Culture and Heterologous Expression

HEK293T and CHO cells were grown in DMEM (Invitrogen, Carlsbad, CA) supplemented with 10% fetal bovine serum, 1% penicillin/streptomycin (Invitrogen, Carlsbad, CA) and 1% L-glutamine (Invitrogen, Carlsbad, CA). Cells were transfected with mCLCA4 constructs cloned into the mammalian expression vector pIRES2-EGFP (Clontech Laboratories, Mountain View, CA), using Lipofectamine 2000 (Invitrogen, Carlsbad, CA) and the manufacturer's protocol (for transient transfection of adherent cells using a half dosage of Lipofectamine 2000). For immunocytochemistry experiments, cells were initially transfected with myc-tagged and other constructs. Twenty-four hours later, transfected cells were plated onto slide chambers coated with 17 μg/ml poly-D-lysine in the same growth medium. Twenty-four hours following plating, transfected cells were washed 3 times with phosphate buffered saline (PBS), then fixed with 2% paraformaldehyde. After fixation, cells were washed with PBS, blocked with 10% nonfat dried milk in Tris-buffered saline (TBS), and permeabilized with 0.05% Triton X-100. For Myc-tagged mCLCA4 constructs, mCLCA4 expression was determined by sequential incubation with 4A6

anti-Myc antibody (1:100, Upstate, Lake Placid, NY), and Texas Red conjugated (or FITC conjugated) horse anti-mouse IgG secondary antibody (1:80, Vector Laboratories, Burlingame, CA). Slides were visualized with an Olympus Fluoview (FV5-PSU) confocal microscope. The hCLCA2ss-EGFP-4L/4A construct was made by fusing EGFP with the putative trafficking sequences. Expression was detected using an EGFP polyclonal antibody (1:8, Chemican, Temecula, CA), followed by a FITC conjugated goat anti-rabbit IgG secondary antibody (1:80, Vector, Burlingame, CA). Cells were imaged using a Zeiss Meta confocal microscope.

2.3.2 mCLCA4 Expression

All insertions were performed by PCR-based, site-directed mutagenesis (ExSite, Strategene, La Jolla, CA). Myc insertions were expressed and proteins separated by gel electrophoresis to insure proper processing of mCLCA4 to 90 and 40 kDa fragments. NH_2-terminal specific tagged mutants were produced by insertion of the Myc tag between Ser^{21} and Ser^{22} (mCLCA4-21myc). COOH-terminal specific mutants were produced by inserting a Myc tag between Asn^{713} and Asp^{714} (mCLCA4-713myc). Both N and COOH-terminal Myc insertion mutants were found to be processed normally. Amino acid substitutions were produced by site-directed mutagenesis of mClCA4 as previously described (16). All mutants were confirmed by DNA sequencing. To test the activity of mCLCA4 trafficking sequences, 120 bp sequences containing the putative dileucine and diarginine trafficking signals (amino acids 565-605), or the respective mutants (2R/2A or 4L/4A), were inserted into the C-terminus of EGFP cDNA containing the N-terminal hCLCA2 (secretion) signal sequence (hCLCA2ss), by PCR amplification of the pcDNA3.1Zeo vector (3) using a primer containing the putative trafficking sequences. The three DNA constructs (hCLCA2ss-EGFP-WT or 2R/2A or 4L/4A-pcDNA3.1Zeo) were transfected into

HEK293T cells as above. EGFP fluorescence was detected at 24 and 48 h and cells imaged using a confocal (Zeiss Meta) or widefield epifluorescence (Nikon TE300) microscopes. Cell lysates were collected using the same amount of RIPA buffer and 15ug protein was used for immunoblot in each condition. Seventy-two hours after transfection, the media was collected for immunopricipetation and immunoblot as described below.

2.3.3 Protein Preparation and Immunoblotting

After 48 h transfection, cells were washed with ice-cold PBS and lysed in (150 µl) RIPA buffer (20 mM Tris buffer at pH 7.5 containing 10% glycerol, 150 mM NaCl, 1 mM EDTA, 1 mM EGTA, 1% Triton 100-X, 5 mM sodium β-glycerophosphate, 50 mM sodium fluoride, 5 mM sodium pyrophosphate, 1 mM sodium vanadate, 0.1% SDS, 0.5% sodium deoxycholate, 1.46 µM pepstatin A, 10.5 µM leupeptin, 960 µM benzamidine, 1.53 µM aprotinin, and 570 µM phenylmethylsulfonylfloride). Samples were centrifuged (34,000 rpm for 30 min at 4ºC) to remove insoluble cellular debris and the supernatants were boiled in denaturing sample buffer (200 mM Tris buffer at pH 6.8 containing 8% SDS, 40% sucrose, 0.4% bromophenol blue, and 100 mM DTT) and proteins resolved by SDS-PAGE on a 10% gradient gel. Gels were electroblotted to PVDF membranes and the membranes were blocked in TBS containing 0.1% Triton X-100 and 5% non-fat dried milk. Subsequently, the membranes were immunostained with the anti-Myc antibody 4A6 (1:1000, Upstate, Lake Placid, NY), or anti-EGFP antibody (1:1000, Chemicon, Temecula, CA), or anti-α-tubulin antibody (1:10,000, Sigma, Saint Louis, MO), washed extensively then exposed to a horseradish peroxidase-conjugated goat anti-mouse secondary antibody (1:3000; Bio-Rad, Hercules, CA). Immunoblots were visualized by enhanced chemiluminescence (Pierce Biotechnology, Rockford, IL) on a

Kodak Image Station 440 (NEN Life Science Products, Boston, MA). For immunoprecipitation (IP), culture media was collected 48 h and 72 h after transfection and pre-cleared with protein A/G-agarose beads (Santa Cruz Biotechnology, Santa Cruz, CA) at 4°C for 30 min. Precleared media was then incubated overnight with an anti-Myc antibody (4A6) (1:100), followed by incubation with protein A/G-agarose beads. Protein A/G-agarose beads were washed extensively in RIPA buffer and boiled in an equal volume of 2X SDS loading buffer, followed by Western blotting as described above.

2.3.4 ER-Golgi transport inhibition

Twenty-four hours post transfection of mCLCA4-21-Myc HEK293T cells were washed and treated with 2 μg/ml Brefeldin A (BFA; 0.02% Ethanol in DMEM); control wells were washed and exposed to the same medium without BFA. BFA – treated cells were either exposed to the drug for 24 h (BFA condition), or the inhibition reversed by wash after 4 h and exposure to 0.02% Ethanol in DMEM for an additional 20 h (Wash). After 24 h, the medium was collected for immunoprecipitation; cells were lysed for protein extraction and equal concentrations of protein/sample were used for Western blotting. All experiments were performed in triplicate.

2.3.5 Subcellular Fractionation

Forty-eight hours after transfection cells were washed with cold PBS and scraped into 1 ml of homogenization buffer containing 250 mM sucrose, 10 mM Tris at pH 8.0, 50 mM NaF, 1.9 mM benzamidine, 1.1 mM phenylmethylsulfonylfluoride, and 1 mM EDTA, with 2.92 μM pepstatin A, 21 μM leupeptin, and 3 μM aprotinin. Cells were homogenized and centrifuged at 600 g for 10 minutes to remove nuclei and

the supernatants transferred to a new tube and subsequently centrifuged at 100,000 g for 60 minutes to pellet membrane fractions. Supernatants were adjusted to 100 mM NaCl and 1% Triton X-100; this fraction was designated S2 and was immunoblotted as described above. The pellets were washed in homogenization buffer, centrifuged at 100,000 g for 30 minutes and the pellets were solubilized in 150 µl of homogenization buffer containing 100 mM NaCl and 1% Triton X-100; this fraction was designated P2 and was immunoblotted as described above.

2.3.6 In Vitro Deglycosylation

Deglycosylation assays were carried out with peptide-N-glycosidase F (PNGase) and endoglycosidase H (Endo H) using proprietary buffers provided (New England Biolabs, Ipswich, MA). Briefly, cells were lysed as described above and centrifuged at 13,000 rpm for 25 min, and the supernatants were mixed with denaturation buffer (2 µl to 60 µl cell lysate). Samples were boiled for 10 min, divided into thirds, and treated with either G7/NP-40 buffer and PNGase, G5 buffer and endo H, or with no enzymes. After incubation, all samples were boiled for 5 min, subjected to SDS-PAGE and immunoblotted, as described above.

2.3.7 Statistical Analysis

The density of proteins in images of Western blots was quantitated using ImageJ. Statistical comparisons were made by student's T test or one-way ANOVA (student-neuman-keuls) using SigmaStat, with between group p values < 0.05 considered statistically significant.

2.4. Results

2.4.1. mCLCA4 proteins undergo proteolytic cleavage and membrane association.

To determine the degree to which the 909 amino acid, full length mCLCA4 translation product undergoes intracellular processing and the fate of the processed peptides, NH_2- and COOH-terminal Myc insertion mutants were created, expressed in HEK293T, and analyzed by Western blotting and immunocytochemistry. Expression of the NH_2-terminal Myc construct (mCLCA4-21Myc) and analysis of cell lysates demonstrated immunoreactive bands of approximately 125 and 90 kDa (Figure 2.1A), whereas expression of the C -terminal insertion clone (mCLCA4-713) resulted in immunoreactive bands of 125 and 40 kDa, and NH_2 and COOH-fragment Myc insertion clones (mCLCA4-21,713Myc) produced all 3 bands (Figure 2.1A). In time course experiments in which the proportion of 90 kDa relative to 125 kDa protein (90 kDa/125 kDa ratio) was examined 24 and 48 h following transfection, the proportion of 90 kDa protein increased progressively with time (Figure 2.1B; see also Figure 2.3A). These results are consistent with the endocytic cleavage of the 125 kDa full length peptide to 90 kDa and 40 kDa NH_2 and COOH-terminal peptides, respectively.

The cellular localization of the Myc-tagged mCLCA4 proteins was examined by immunocytochemistry in cells transfected with bicistronic constructs that included EGFP. As shown in Figure 2.1C, both NH_2 and COOH-terminal fragments are associated with the plasma membrane. This pattern of localization cannot be explained by immunodetection of the parent 125-kDa fragment, as the full length peptide is only found in the ER. As shown in Figure 2.1D, prominent nuclear rim staining was observed along with plasma membrane localization, consistent with ER localization of the full length fragment and similar to findings for hCLCA1 and hCLCA2 (3, 7).

Figure 2.1. **Proteolytic processing and cellular localization of mCLCA4**. **A**. Western blot of lysates from HEK293T cells expressing amino and carboxy terminal Myc-tagged mCLCA4 cDNA. mCLCA4 proteins migrate as a 125 kDa full length protein that is cleaved to a 90 kDa NH_2-terminal and a 40 kDa COOH-terminal fragment. Note that the apparent ratio of 125 and 90 kDa proteins in the blot at right is distorted by the double labeling of the full length peptide only. **B**. The ratio of 90 kDa to 125 kDa proteins (mClCA4-21Myc) in 3 separate western blot experiments as in A after 24 and 48 h. The relative amount of proteolytic product was significantly increased at 48 h compared to 24 h ($p<0.05$; see also Figure 2.3A) **C**. HEK293T Cells were transfected with a mCLCA4-IRES-EGFP plasmid and immunostained, revealing a prominent plasma membrane expression pattern for both NH_2 and COOH-terminal specific Myc-tagged proteins. **D**. HEK293T cells were transfected with mCLCA4-21Myc-IRES-EGFP plasmid, followed by anti-myc immunostaining. Nuclear rim staining (arrows) is consistent with ER localization of the full length protein.

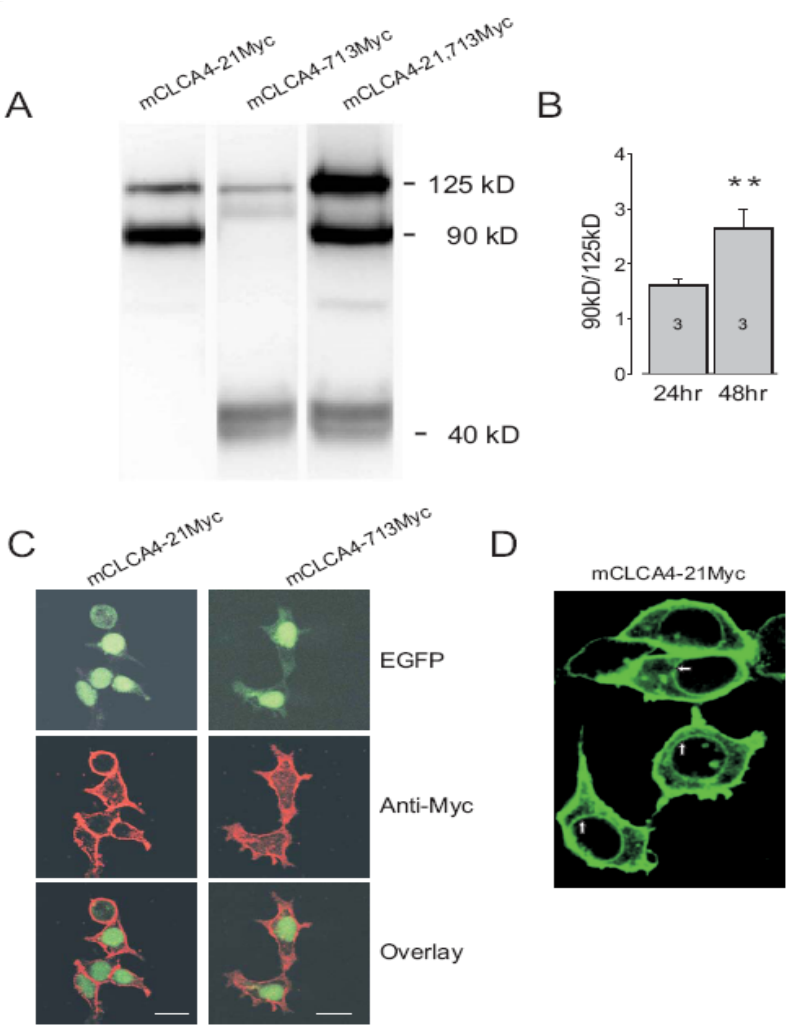
A
mCLCA4-21Myc
mCLCA4-713Myc
mCLCA4-21,713Myc
125 kD
90 kD
40 kD
B
90kD/125kD
**
3
3
24hr
48hr
C
mCLCA4-21Myc
mCLCA4-713Myc
EGFP
Anti-Myc
Overlay
D
mCLCA4-21Myc

2.4.2. Secretion of the 90 kDa NH_2 and 40 kDa COOH–terminal mCLCA4 peptides.

As previous reports indicated that NH_2 and COOH-terminal fragments from some CLCAs are secreted (3, 6, 8), we attempted to immunoprecipitate Myc-tagged mCLCA proteins from media surrounding transfected cells. As shown in Figure 2.2A, Western blots of the immunoprecipitates revealed the presence of the 90 kDa NH_2 and 40kDa COOH-terminal peptides in the cell media. Moreover, exposure of cells to the ER-Golgi transport inhibitor Brefeldin A (BFA, 2 μg/ml for 24 h), markedly reduced the amount of protein present in the media, whereas washout of BFA (4 h) reversed this effect (Figure 2.2B). Thus mCLCA4 is processed into two peptides, both of which are secreted and associate with the plasma membrane.

2.4.3 mCLCA4 is not phosphorylated at RARSPT but mutation alters proteolytic cleavage

mCLCA1, mCLCA2, mCLCA4, bCLCA1, and bCLCA2 proteins contain a predicted phosphorylation hotspot ($R^{592}ARSPT^{597}$) near the COOH terminus of the NH_2-terminal peptide (2). To further understand the significance of this motif, we mutated S^{595} and T^{597} residues to A (mCLCA4-21MycAA) or D (mCLCA4-21MycDD). Our original goal was to determine whether these residues undergo phosphorylation by serine/threonine kinases. Transfection of cells with these constructs and Western blotting of proteins failed to demonstrate a shift in electrophoretic mobility of the 90 kDa fragment; these studies included extensive serum deprivation alone or additional exposure to forskolin, phorbol ester, methacholine, ionomycin, or several protein kinase inhibitors (data not shown), and were paired with control experiments in which phosphorylation produced the expected

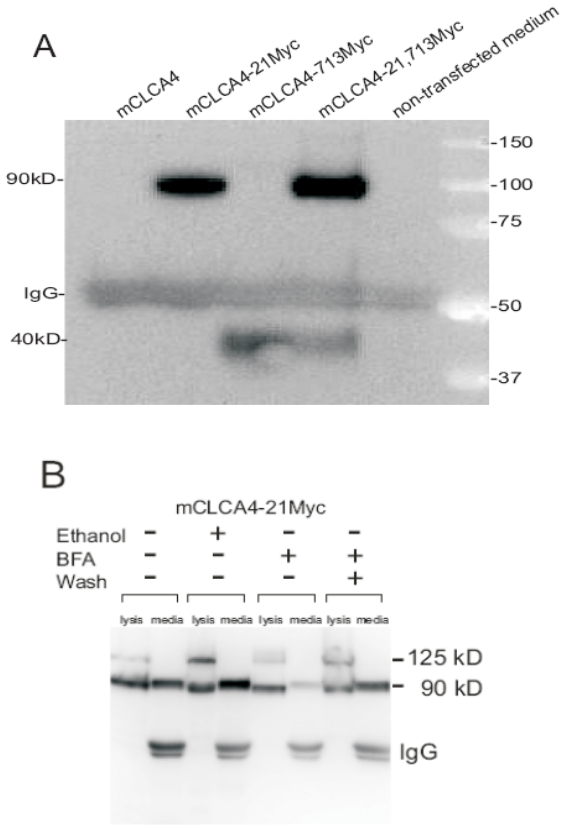

Figure 2.2. **The 90 kDa NH_2-terminal fragment and COOH-terminal fragment are secreted into the extracellular space**. **A**. Media from HEK293T cells transfected with Myc–tagged cDNAs was immunoprecipitated with a Myc antibody and immunoblotted with the same antibody. Note detection of both the 90 kDa NH_2- and 40 kDa COOH-terminal peptides in the cell media. **B**. Experiments were performed as in Panel A. Continuous exposure to 2 µg/ml Brefeldin A (BFA) for 24 h markedly inhibited secretion of the 90 kDa fragment, whereas replacement of BFA after 4 h with DMEM and further incubation for 20 h (wash) reversed the inhibition. Lysates are shown next to immunoprecipitates for identification of the proteins.

mobility shift in similar size proteins (data not shown). In the experiments mCLCA4-21MycAA mutant clones displayed a consistent proteolytic phenotype, however. Western blotting indicated that the mCLCA4- 21MycAA mutant underwent less proteolytic cleavage than either wildtype or mCLCA4-21MycDD proteins, resulting in a significant shift in the ratio of the 90 to 125 kDa proteins (Figure 2.3A, B). This finding was observed over a time course of 12 – 72 hours (data not shown) and in both HEK293T and CHO cells (Figure 2.3C). The apparent shift in the degree of proteolytic cleavage of the parent 125 kDa translation product was not due to a shift in the localization of the fragments. Subcellular fractionation of cellular lysate indicated that both proteins were almost exclusively associated with cellular membranes, and that a relative decrease in production of the 90 kDa fragment was observed within this membrane pellet (Figure 2.3D). Similarly, immunoprecipitation of the 90 kDa fragment from media of transfected cells demonstrated that the 90 kDa fragment of the mCLCA4-21MycAA mutant was secreted into the media (Figure 2.3E), indicating that a marked change in distribution or folding did not occur.

2.4.3. Dileucine and diarginine sequences regulate ER retention and export of mCLCA4.

The alteration in proteolytic processing observed in the mCLCA4-21MycAA mutant suggested the possibility that the RARSPT sequence might be involved in the regulation of ER export, resulting in less efficient export of the parent 125 kDa full–length protein and an attendant decrease in processing to the 90 kDa NH_2-terminal fragment. Examination of the neighboring sequence indicated the presence of two upstream dileucines that have been shown to regulate ER retention and export in combination with an RxR motif (11), which is contained within the targeted RARSPT sequence. The RAR sequence is shared between mCLCA1, mCLCA2, and mCLCA4,

Figure 2.3. **Mutation of putative phosphorylation site slows proteolytic cleavage**. **A**. Mutant mCLCA4 cDNAs in which the S and T residues in the $R^{592}ARSPT^{597}$ sequence (residues 592-596) were mutated to AA or DD were expressed and lysates blotted. The immunoblot shows the consistent finding in all experiments of a decrease in the amount of proteolytic cleavage in the AA mutant (8 experiments). **B**. Proteins were obtained and processed as in Panel A. Mean ratios of the density of the 90 and 125 kDa bands in 8 experiments. The relative amount of 90 kDa proteolytic product decreased significantly in the AA mutant ($p<.005$). All other comparisons were not significant. **C**. Decreased processing of the native peptide was observed in both HEK293T and CHO cell lines. **D**. Subcellular fractionation revealed that most mCLCA4 protein was membrane associated, but the AA mutant resulted in an increase in the amount of 125 kDa protein. S, supernatant; P, pellet. E. Immunoprecipitation indicated that both mutants are secreted into the extracellular space.

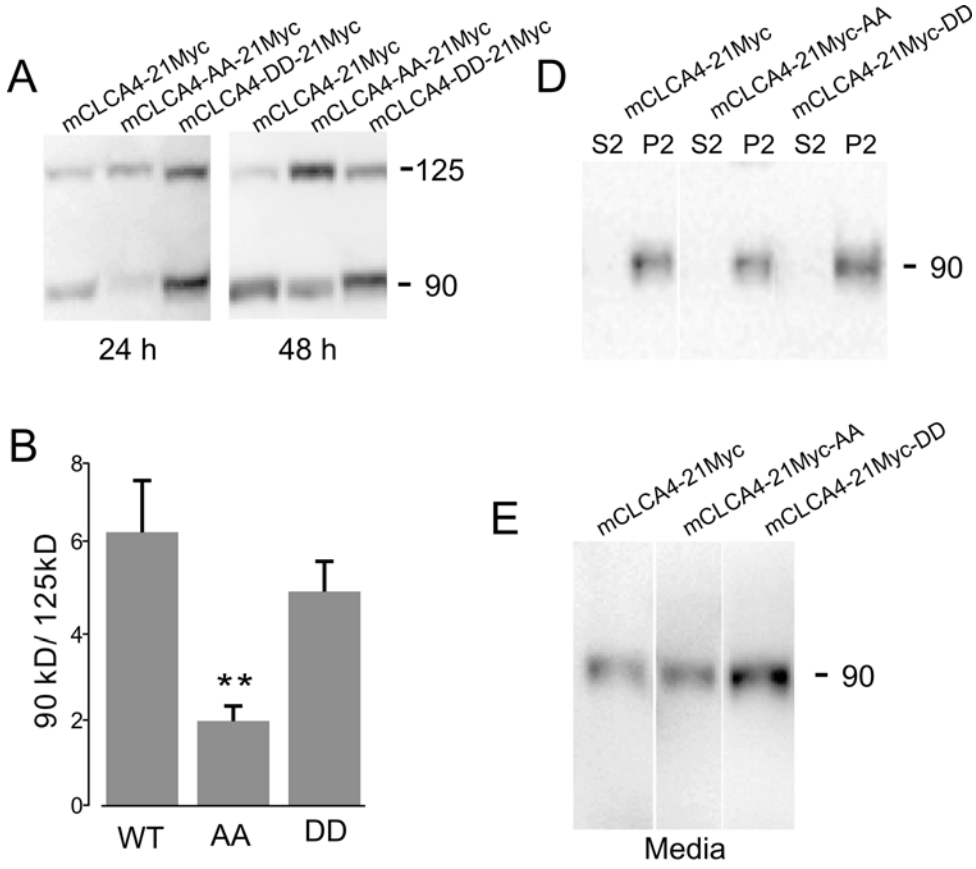
A
mCLCA4-21Myc
mCLCA4-AA-21Myc
mCLCA4-DD-21Myc
mCLCA4-21Myc
mCLCA4-AA-21Myc
mCLCA4-DD-21Myc
125
90
24 h
48 h
D
mCLCA4-21Myc
mCLCA4-21Myc-AA
mCLCA4-21Myc-DD
S2 P2 S2 P2 S2 P2
90
B
90 kD/ 125kD
8
6
4
2
0
**
WT
AA
DD
E
mCLCA4-21Myc
mCLCA4-21Myc-AA
mCLCA4-21Myc-DD
90
Media
C
mCLCA4-21Myc
mCLCA4-AA-21Myc
mCLCA4-21Myc
mCLCA4-AA-21Myc
HEK CHO HEK CHO
125
90

but is not preserved in other mCLCAs, whereas the dileucine sequences are unique to mCLCA4. LI sequences are found in mCLCA1 and mCLCA2 (Figure 2.4A), however, and may play a similar role. In other proteins, cytoplasmic dileucines appear to serve as an ER export or forward trafficking signal through the binding of chaperones, whereas the RxR is an ER retention signal (11). To determine the relevance of these sequences we created additional mutants that eliminated the more COOH-terminal dileucine (2L/2A), both dileucine sequences (4L/4A), the RxR sequence (2R/2A), or both the dileucine and RxR sequences (4L2R/6A) (Figure 2.4B). Mutation of either the C -terminal dileucine or both dileucine pairs prevented forward trafficking of mCLCA4 proteins to the cell membrane (Figure 2.4C), indicating a potent role of these sequences in forward trafficking. However mutation of the putative RxR retention sequence also resulted in perinuclear localization of mCLCA4 (Figure 2.4C).

To further understand the role of these motifs we examined the glycosylation pattern of putatively ER–trapped proteins in lysates from transfected cells. In vitro deglycosylation of tagged proteins from mCLCA4 –expressing cells demonstrated that the 125 kDa protein was sensitive to both PNGase F and Endo H (Figure 2.5A), indicating that the full length mClCA4 protein is immaturely glycosylated and resides within the ER compartment, as PNGase F cleaves both mature and immature N -linked glycans, whereas Endo H digests high-mannose carbohydrates found in the ER or medial Golgi. Conversely, the 90 kDa and 40 kDa cleaved fragments were sensitive to PNGase F, but markedly less sensitive to Endo H, suggesting that a minor component of these proteins are immaturely glycosylated (Figure 2.5A), consistent with export from the ER and mature glycosylation. The 125 kDa full length protein displayed a deglycosylation pattern consistent with ER trapping (Figure 2.5B) and the

Figure 2.4. **Forward traffic and ER retention signals. A**. Alignments of the amino acid sequence of the highly related mCLCAs identifies the dileucine signals in mCLCA4 and the diarginine signals that are unique to these three genes. Similar signals in GLT-1 are shown for comparison. Regions of identity are shown in grey; sequence numbering is shown for mCLCA4. **B**. Alanine mutations of the transport and retention signals are shown in red. **C**. Immunolocalization of the dileucine and diarginine mutants. Note the perinuclear localization of all mutants and an absence of immunoreactive protein at the membrane.

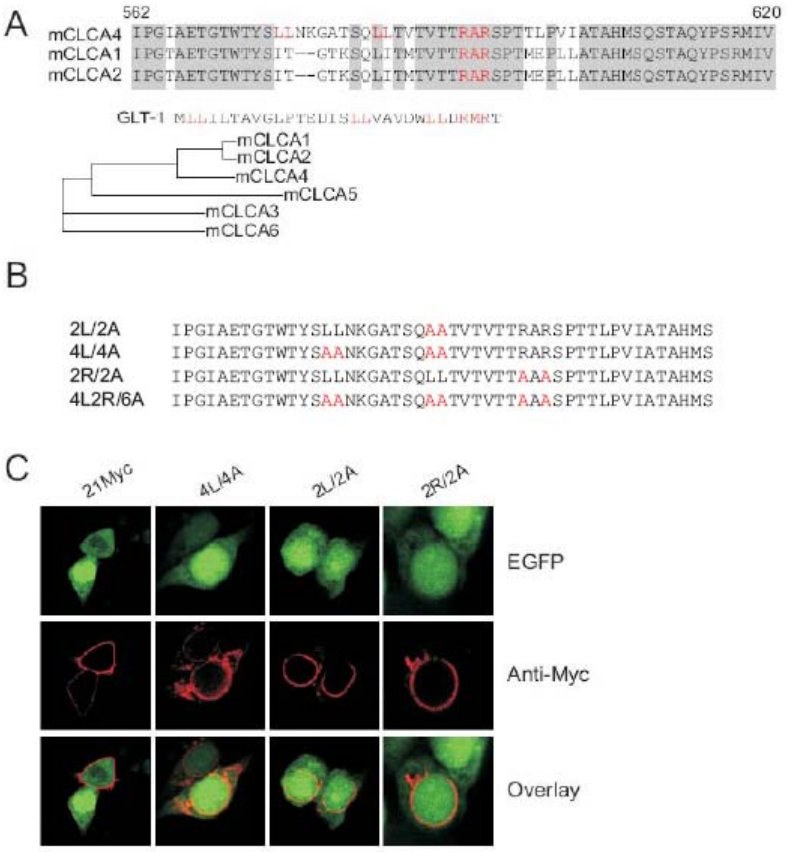
A
562
620
mCLCA4 IPGIAETGTWTYSLLNKGATSQLLTVTVTTRARSPTTLPVIATAHMSQSTAQYPSRMIV
mCLCA1 IPGTAETGTWTYSIT--GTKSQLITMTVTTRARSPTMEPLLATAHMSQSTAQYPSRMIV
mCLCA2 IPGTAETGTWTYSIT--GTKSQLITMTVTTRARSPTMEPLLATAHMSQSTAQYPSRMIV
GLT-1 MLLILTAVGLPTEDTSLLVAVDWLLDRMRT
mCLCA1
mCLCA2
mCLCA4
mCLCA5
mCLCA3
mCLCA6
B
2L/2A IPGIAETGTWTYSLLNKGATSQAATVTVTTRARSPTTLPVIATAHMS
4L/4A IPGIAETGTWTYSAANKGATSQAATVTVTTRARSPTTLPVIATAHMS
2R/2A IPGIAETGTWTYSLLNKGATSQLLTVTVTTAAASPTTLPVIATAHMS
4L2R/6A IPGIAETGTWTYSAANKGATSQAATVTVTTAAASPTTLPVIATAHMS
C
21Myc
4L/4A
2L/2A
2R/2A
EGFP
Anti-Myc
Overlay

90 kDa NH_2–terminal fragment was not present in the lysate of 2L/2A and 4L/4A dileucine mutants. Similarly, mutation of the RxR sequence (2R/2A) resulted in the apparent loss of the 90 kDa fragment in the lysate. To further test whether ER trapping of the export mutants was complete, we immunoprecipitated proteins from the cell media of tagged (NH_2-terminal fragment specific) wildtype and ER mutant transfectants. These experiments demonstrated that the ER export mutants (2L/2A and 4L/4A) did not produce the 90 kDa secreted protein, whereas the 90 kDa cleavage produce was abundant in the 2R/2A ER retention mutant (Figure 2.5C). Our failure to detect the 90 kDa peptide of 2R/2A in cell lysates (Figure 2.5B), despite its presence in the media, is likely due to the augmented forward trafficking effected by mutation of the retention signal. Unlike GLT-1, the combined mutant (4L2R/6A) did not rescue forward trafficking, as the 90 kDa fragment was not observed in the lysate or in the media (data not shown). Moveover, the mCLCA4-21MycAA and mCLCA4-21MycDD mutants were deglycosylated in a manner consistent with predominately mature glycosylation of the 90 and 40 kDa fragments. The ratio of 90 kDa to 125 kDa protein in the cell lysate and medium for the WT, AA mutant and DD mutant was 81%, 60% and 79%, respectively, consistent with less complete processing of the AA mutant. This was not a result of block of secretion of the mutants, as WT, AA, and DD proteins were found in the medium (Figure 2.5D).

To more definitively test the function of putative mCLCA4 trafficking signal sequences, we created chimeric proteins in which a 40 amino acid mCLCA4 peptide containing the wildtype, LL, or R-R mutants was placed immediately COOH-terminal to a secreted EGFP construct (3) (Figure 2.6A). Consistent with the mCLCA4 mutational results, 48 h after transfection chimeric EGFP proteins containing the 4L/4A mutation markedly accumulated within the cell, whereas WT and 2R/2A mutant proteins were poorly retained in cells and in those cases were diffusely

Figure 2.5. **Glycosylation pattern of mutant proteins**. **A**. PNGaseF or Endo H deglycosylation of N and C -terminal fragment tagged mCLCA4 proteins indicated that the 125 kDa full length protein is immaturely glycosylated (sensitive to both enzymes), whereas the 90 and 40 kDa fragments were only partially sensitive to Endo H, indicating more mature glycosylation. **B**. The dileucine and diarginine mutants demonstrate marked ER or early Golgi trapping as there is no observable 90 kDa fragment and the 125 kDa protein displays an immature glycosylation pattern. **C**. Mutation of the diarginine (RxR) motif does not result in ER trapping, as the 90 kDa fragment is detected in the media by immunoprecipitation, indicating highly efficient forward trafficking. Conversely, mutation of the dileucine signals results in complete loss of forward trafficking. **D**. The AA R^{592}ARAPA^{597} mutant displays a glycosylation pattern consistent with delayed processing, but not ER trapping, as the 90 kDa proteolytic fragment from this mutant, as well as the DD mutant, is resistant to Endo H. Media lanes were by IP.

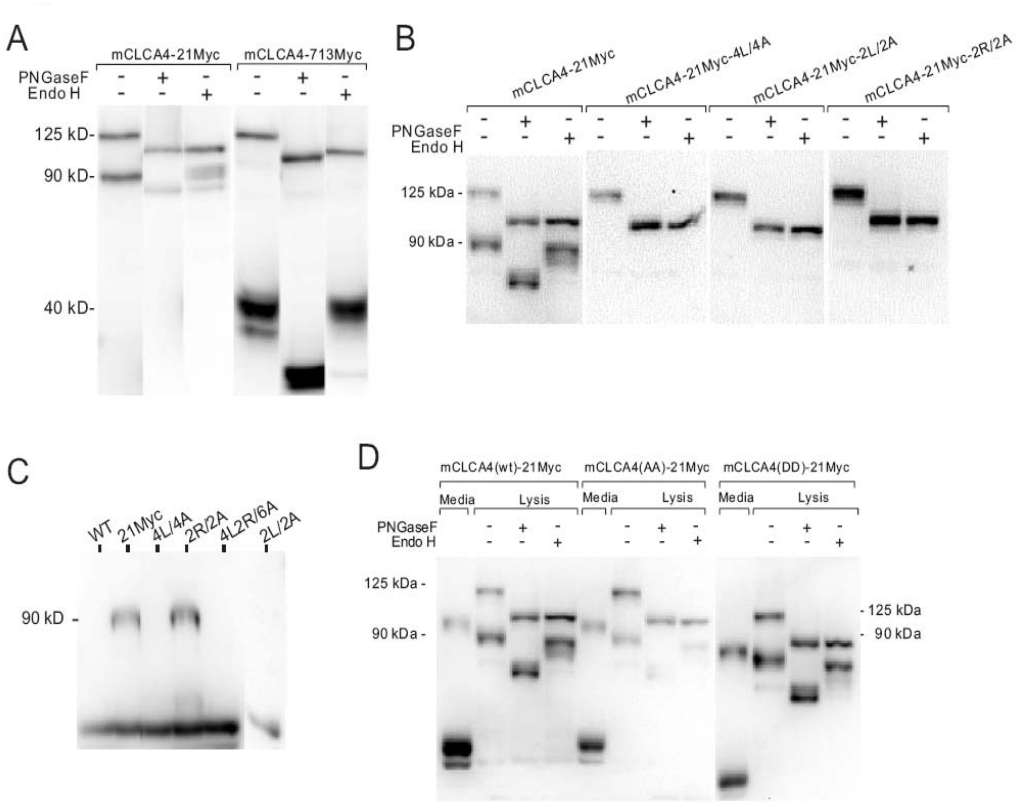
A
mCLCA4-21Myc
mCLCA4-713Myc
PNGaseF
Endo H
125 kD-
90 kD-
40 kD-
B
mCLCA4-21Myc
mCLCA4-21Myc-4L/4A
mCLCA4-21Myc-2L/2A
mCLCA4-21Myc-2R/2A
PNGaseF
Endo H
125 kDa -
90 kDa -
C
WT
21Myc
4L/4A
2R/2A
4L2R/6A
2L/2A
90 kD -
D
mCLCA4(wt)-21Myc
mCLCA4(AA)-21Myc
mCLCA4(DD)-21Myc
Media
Lysis
PNGaseF
Endo H
125 kDa -
90 kDa -
125 kDa
90 kDa

Figure 2.6. **mCLCA4 dileucine sequences are required for forward trafficking of secreted proteins**. **A**. Schematic of construct used to examine mCLCA4 dileucine and diarginine sequences. The N -terminal signal sequence (SS) from hCLCA2 was used to direct EGFP to secretory compartments. A 40 amino acid fragment of mCLCA4 was positioned C -terminal to EGFP, similar to its location with respect to the N -terminal mCLCA4 fragment. Dileucine (LL) and diarginine (RxR) sequences are shown. **B**. Widefield (above, 10X) and confocal (below, 40X) images of HEK293T cells 48 h after transfection (scaled to equivalent fluorescence intensity). The expression pattern indicates EGFP trapping in the 4L/4A mutant (approximately 70% of the cells showed EGFP localized to the cytosol and 30% exhibited a more vesicular staining pattern) and are consistent with rapid secretion of EGFP by WT and RxR mutant cells. Below, confocal images show a predominate cytosolic pattern in EGFP –retaining WT and 2R/2A cells, and a vesicular pattern in cells transfected with the 4L/4A mutant. Fluorescence of WT and 2R/2A images was substantially lower and is scaled to show roughly equivalent maximum intensity as 4L/4A. **C**. Immunoprecipitation of GFP from medium 72 h after transfection; quantification of the EGFP band is shown below (representative of 3 experiments). Little or no 4L/4A protein was detected in the media in these experiments, further supporting vesicle trapping, whereas slightly more 2R/2A protein was detected, consistent with rapid secretion of the EGFP constructs in which the retention signal has been mutated. The "C" lane indicates non –transfected control.

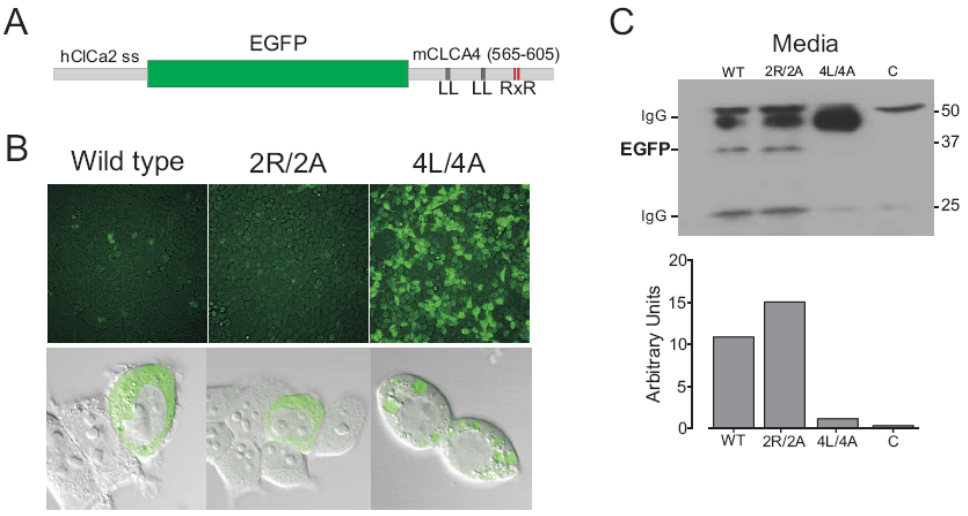
A
hClCa2 ss
EGFP
mCLCA4 (565-605)
LL LL RxR
B
Wild type
2R/2A
4L/4A
C
Media
WT 2R/2A 4L/4A C
IgG
EGFP
IgG
50
37
25
Arbitrary Units
20
15
10
5
0
WT 2R/2A 4L/4A C

present within the cytosol (Figure 2.6B). Moreover, immunoprecipitation and immunoblotting indicated substantial WT and 2R/2A protein in the cell media, indicating efficient forward trafficking and secretion, but accumulation in the media of 4L/4A mCLCA4 mutant protein was markedly reduced (Figure 2.6C).

These results confirm the function of dileucine and RxR ER regulatory sequences in mClCA4. No secreted protein was detected in dileucine mutants, indicating a complete block of forward trafficking, whereas secreted protein was detected in RxR mutants, indicating that the motif functions as an ER retention signal. These observations are consistent with the role of the RxR motif in GLT-1 (11). Moreover, the decrease in processing efficiency observed in the RARSPT mutant mCLCA4-21MycAA likely results from conformational effects on the RxR retention sequence imposed by mutation of the neighboring S^{595} and/or T^{597} residues.

2.5. Discussion

We have used epitope insertion and immunodetection to examine the processing and fate of mCLCA proteins. Our results indicate that mCLCA4 cDNA encodes a full length protein of approximately 125 kDa that is proteolytically cleaved into large NH_2-terminal (90 kDa) and smaller COOH-terminal (40 kDa) fragments. The data are consistent with cleavage within the ER or early in the trans Golgi network, as the full length mClCA4 protein displays an ER –like immunoreactive pattern, does not traffic to the plasma membrane, and is immaturely glycosylated (Figure 2.5D). Both the N and C -terminal cleavage products are secreted and found in the media, where they rapidly associate with the plasma membrane, and protein isolated from cell lysates displays a mature glycosylation pattern (Figures 2.1B, 2.5A), further suggesting that only the proteolytic products are forward trafficked beyond the ER.

The topology and cellular fate of CLCA proteins has undergone substantial refinement since the initial modeling indicating multiple transmembrane segments (1, 7, 9). More recent structural analysis indicates a single COOH-terminal transmembrane segment (22) and a conserved NH_2-terminal hydrolase domain (19). This prediction has been supported by experimental data indicating the secretion of a CLCA fragment into the extracellular space (3, 6, 14), although differences exist as to whether the NH_2-terminal fragment (6) or both the NH_2- and COOH-terminal fragments (3) are secreted extracellularly, with the latter data inconsistent with a single transmembrane domain. For mCLCA3, the two proteins are reported to remain physically associated and secreted into the extracellular space (14), whereas the COOH-terminal fragment of the highly related human homologue hCLCA1 does not appear to be associated with the secreted NH_2-terminal cleaved peptide, and is not found in the extracellular media (6).

Based on results from hCLCA2, Elble et al (3) have suggested a general model of CLCA processing in which the full–length precursor is transported to the cell surface where it undergoes cleavage by an endopeptidase, resulting in release of the NH_2-terminal fragment, while the COOH-terminal fragment with its transmembrane segment remains as an integral membrane protein. Our data are in general consistent with this model, although it appears that both proteins remain associated with the plasma membrane and that the full–length precursor of mCLCA4 does not traffic to the plasma membrane, since the 125 kDa fragment is sensitive to EndoH digestion (Figure 2.5A,B,D). Also, unlike hCLCA2, we were unable to demonstrate tight association between the two fragments by co-immunoprecipitation (data not shown).

We have also extended these observations by determining the luminal motifs that regulate trafficking of mCLCA4. Kalandze et al (11) described cytosolic diarginine retention and dileucine forward trafficking signals regulating the trafficking

of GLT-1, an intrinsic membrane protein. Interestingly, mutation of all of the dileucine motifs in GLT-1 was required to abolish forward trafficking, as 2L/2A and 4L/4A proteins were still maturely glycosylated and inserted in the plasma membrane. The 6L/6A GLT-1 mutation resulted in ER trapping, but also resulted in markedly less full length protein in the lysate, suggesting misfolding and degradation. By contrast, secretion of the 90 kDa NH_2-terminal peptide was completely inhibited in 2L/2A and 4L/4A mutants of the luminal protein mCLCA4, and high amounts of ER trapped 125 kDa protein were observed (Figure 2.5B). Mutation of the diarginines also produced an apparent loss of 90 kDa product in the protein lysate, however protein was readily detected in the cell medium, suggesting augmented forward trafficking associated with loss of the RxR retention signal. The apparent absence of the 90 kDa peptide from the plasma membrane suggests that the RxR motif may also be required for surface association. Chimeric constructs clearly demonstrated the role of the dileucine sequences in forward trafficking (Figure 2.6B, C) and the prominent vesicular pattern of EGFP expression in 4L/4A mutants confirms the importance of these sequences as retention signals. As CLCA proteins appear to undergo distinct processing (3, 6, 14), these motifs may underlie significant functional differences in these family members. Studies designed to determine the function of the separate membrane–associated fragments should provide more clarity with respect to the role of CLCAs in ion transport and secretion.

REFERENCE

1. **Cunningham SA, Awayda MS, Bubien JK, Ismailov, II, Arrate MP, Berdiev BK, Benos DJ, and Fuller CM.** Cloning of an epithelial chloride channel from bovine trachea. *J Biol Chem* 270: 31016-31026, 1995.

2. **Elble RC, Ji G, Nehrke K, DeBiasio J, Kingsley PD, Kotlikoff MI, and Pauli BU.** Molecular and functional characterization of a murine calcium-activated chloride channel expressed in smooth muscle. *J Biol Chem* 277: 18586-18591, 2002.

3. **Elble RC, Walia V, Cheng HC, Connon CJ, Mundhenk L, Gruber AD, and Pauli BU.** The putative chloride channel hCLCA2 has a single C-terminal transmembrane segment. *J Biol Chem* 281: 29448-29454, 2006.

4. **Elble RC, Widom J, Gruber AD, Abdel-Ghany M, Levine R, Goodwin A, Cheng HC, and Pauli BU.** Cloning and characterization of lung-endothelial cell adhesion molecule-1 suggest it is an endothelial chloride channel. *J Biol Chem* 272: 27853-27861, 1997.

5. **Ellgaard L and Helenius A.** Quality control in the endoplasmic reticulum. *Nat Rev Mol Cell Biol* 4: 181-191, 2003.

6. **Gibson A, Lewis AP, Affleck K, Aitken AJ, Meldrum E, and Thompson N.** hCLCA1 and mCLCA3 are secreted non-integral membrane proteins and therefore are not ion channels. *J Biol Chem* 280: 27205-27212, 2005.

7. **Gruber AD, Elble RC, Ji HL, Schreur KD, Fuller CM, and Pauli BU.** Genomic cloning, molecular characterization, and functional analysis of human CLCA1, the first human member of the family of Ca2+-activated Cl- channel proteins. *Genomics* 54: 200-214, 1998.

8. **Gruber AD and Pauli BU.** Molecular cloning and biochemical characterization of a truncated, secreted member of the human family of Ca2+-activated Cl- channels. *Biochim Biophys Acta* 1444: 418-423, 1999.

9. **Gruber AD, Schreur KD, Ji HL, Fuller CM, and Pauli BU.** Molecular cloning and transmembrane structure of hCLCA2 from human lung, trachea, and mammary gland. *Am J Physiol* 276: C1261-1270, 1999.

10. **Hebert DN, Garman SC, and Molinari M.** The glycan code of the endoplasmic reticulum: asparagine-linked carbohydrates as protein maturation and quality-control tags. *Trends Cell Biol* 15: 364-370, 2005.

11. **Kalandadze A, Wu Y, Fournier K, and Robinson MB.** Identification of motifs involved in endoplasmic reticulum retention-forward trafficking of the GLT-1 subtype of glutamate transporter. *J Neurosci* 24: 5183-5192, 2004.

12. **Leverkoehne I, Holle H, Anton F, and Gruber AD.** Differential expression of calcium-activated chloride channels (CLCA) gene family members in the small intestine of cystic fibrosis mouse models. *Histochem Cell Biol* 126: 239-250, 2006.

13. **Loewen ME and Forsyth GW.** Structure and function of CLCA proteins. *Physiol Rev* 85: 1061-1092, 2005.

14. **Mundhenk L, Alfalah M, Elble RC, Pauli BU, Naim HY, and Gruber AD.** Both cleavage products of the mCLCA3 protein are secreted soluble proteins. *J Biol Chem* 281: 30072-30080, 2006.

15. **Nakanishi A, Morita S, Iwashita H, Sagiya Y, Ashida Y, Shirafuji H, Fujisawa Y, Nishimura O, and Fujino M.** Role of gob-5 in mucus overproduction and airway hyperresponsiveness in asthma. *Proc Natl Acad Sci U S A* 98: 5175-5180, 2001.

16. **Nara M, Dhulipala PD, Wang YX, and Kotlikoff MI.** Reconstitution of beta-adrenergic modulation of large conductance, calcium-activated potassium (maxi-K) channels in Xenopus oocytes. Identification of the camp-dependent protein kinase phosphorylation site. *J Biol Chem* 273: 14920-14924, 1998.

17. **Patel AC, Morton JD, Kim EY, Alevy Y, Swanson S, Tucker J, Huang G, Agapov E, Phillips TE, Fuentes ME, Iglesias A, Aud D, Allard JD, Dabbagh K, Peltz G, and Holtzman MJ.** Genetic segregation of airway disease traits despite redundancy of calcium-activated chloride channel family members. *Physiol Genomics* 25: 502-513, 2006.

18. **Pauli BU, Abdel-Ghany M, Cheng HC, Gruber AD, Archibald HA, and Elble RC.** Molecular characteristics and functional diversity of CLCA family members. *Clin Exp Pharmacol Physiol* 27: 901-905, 2000.

19. **Pawlowski K, Lepisto M, Meinander N, Sivars U, Varga M, and Wieslander E.** Novel conserved hydrolase domain in the CLCA family of alleged calcium-activated chloride channels. *Proteins* 63: 424-439, 2006.

20. **Ritzka M, Stanke F, Jansen S, Gruber AD, Pusch L, Woelfl S, Veeze HJ, Halley DJ, and Tummler B.** The CLCA gene locus as a modulator of the gastrointestinal basic defect in cystic fibrosis. *Hum Genet* 115: 483-491, 2004.

21. **Teasdale RD and Jackson MR.** Signal-mediated sorting of membrane proteins between the endoplasmic reticulum and the golgi apparatus. *Annu Rev Cell Dev Biol* 12: 27-54, 1996.

22. **Whittaker CA and Hynes RO.** Distribution and evolution of von Willebrand/integrin A domains: widely dispersed domains with roles in cell adhesion and elsewhere. *Mol Biol Cell* 13: 3369-3387, 2002.

23. **Zhou Y, Dong Q, Louahed J, Dragwa C, Savio D, Huang M, Weiss C, Tomer Y, McLane MP, Nicolaides NC, and Levitt RC.** Characterization of a calcium-activated chloride channel as a shared target of Th2 cytokine pathways and its potential involvement in asthma. *Am J Respir Cell Mol Biol* 25: 486-491, 2001.

CHAPTER 3

THE FUNCTIONAL STUDY OF MCLCA4 IN MURINE LIFE

-----mCLCA4 knock-out

3.1 Abstract

mCLCA4 is highly expressed in smooth muscle and other cells, and following transient transfection of mCLCA4 cDNA into HEK293T cells a chloride current is detected. This suggests that mCLCA4 plays a role in regulating of chloride currents. To better understand the function of mCLCA4 in murine life, I generated mice lacking CLCA4 expression via gene targeting of the mCLCA4 gene locus. A 4.8 kb genomic sequence, that included exons 1 to 3, was deleted from the mouse genome and resulted in no mCLCA4 gene expression and no protein production. There was no obvious gross phenotype in the mCLCA4 homozygous knock-out mice and they appeared to breed normally.

3.2 Introduction

As candidate calcium-activated chloride channel proteins, the CLCA family has drawn the attention of our smooth muscle electrophysiological research laboratory, especially mCLCA4, one of the murine members that is highly expressed in smooth muscle cells. To understand mCLCA4 function, *in vitro* protein processing and trafficking were studied (See Chapter 2). To determine the function of mCLCA4 *in vivo* I generated mice lacking the mCLCA4 gene.

The calcium-activated chloride channel protein family was originally described as an integral membrane protein that may act as a chloride channel (5, 7, 15). Recent studies showed that these family members are soluble secreted proteins associated with the plasma membrane (see Chapter 2)(3, 4, 12), suggesting this group of proteins plays a more complex role than just regulating chloride currents. The most convincing study recently showed that some members (such as hCLCA1, mCLCA3 and eCLCA1) play a role in the pathophysiology observed in asthma and cystic fibrosis (8, 11, 13, 14, 16). The other CLCA proteins are involved in tumor suppression (such as hCLC2,

mCLCA1 and mCLCA2) (2, 6). To date, there are no functional studies on the involvement of the mCLCA4 protein in any disease processes.

As one of the six cloned mouse CLCA members that cluster on mouse chromosome 3, mCLCA4 is highly and preferentially expressed in organs that contain a high percentage of smooth muscle cells, such as aorta, stomach, uterus, bladder and intestine (1). It was cloned from RNA isolated from mouse bladder and stomach smooth muscle layers that were dissected free from the mucosa followed by reverse transcription PCR based on bCLCA2 cDNA as primers. Transient transfection studies of mCLCA4 cDNA in HEK293T cells demonstrated the presence of an anionic current when cells were exposed to increased intracellular calcium by administration of ionomycin or methacholine. The current characteristics were similar to the smooth muscle chloride current found in many tissues (1, 9, 18). The full-length mCLCA4 cDNA is 2.7 kb and codes for a 909 aa protein precursor. It yields ~125 kDa product after glycosylation in HEK293T cells that is cleaved into 90 kDa NH_2-terminal and 40 kDa COOH-terminal fragments. Both protein fragments of mCLCA4 are secreted out of the cell and associate with the plasma membrane (see Chapter 2).

To understand the function of mCLCA4 in murine life, mice lacking mCLCA4 gene expression were generated. Gross phenotypic characterization of mCLCA4 null mice was completed by a pathologist at Cornell University's Veterinary School of Medicine and no gross phenotype was observed.

3.3 Materials and Methods

3.3.1 Generation of mCLCA4 null mice

3.3.1.1 Generating the targeting vector

A 17.3 kb mCLCA4 genomic DNA fragment with partial restriction enzyme digestion information was provided by Keith Nehrke at the Aab Institute for

Biomedical Research, University of Rochester. It contained a 7 kb 5' flanking sequence including exons 1 to 6 that was verified by restriction enzyme mapping and partial sequence analysis. The deletion sequence was designed to eliminate a 4.8 kb fragment that included exons 1 to 3 of the mCLCA4 gene. Two homologous arms, upstream of the deletion fragment, were designed and generated from the 17.3 kb genomic DNA fragment. A 2.5 kb Short-arm fragment was released by EcoRV and XbaI enzyme sites and a 6 kb Long-arm fragment was removed by EcoRV and KpnI sites (Figure 3.1A). The pKO-Neo/loxp targeting vector contained Neomycin/Kanamycin (Neo/kan) positive and thymidine kinase (TK) negative selection genes. Homologous arms were subcloned into pKO-Neo/loxp vector through XhoI* (* blunted end of XhoI site to match EcoRV site) and XbaI sites for the short arm (located before Neomycin gene) and SalI* (* blunted end of SalI site to match EcoRV site) and KpnI sites for the Long-arm (after Neomycin gene). The targeting vector-PKO-Neo/loxp containing two homologous arms was verified by sequencing (Figure 3.1B).

3.3.1.2 ES Cell Targeting

The feeder dependent R1 mouse embryonic stem (ES) cell line [129X1/SvJX129S1.Sv-+p+Tyr-cMgfs1-J/+(129)C129] was obtained from the Nagy Laboratory (http://www.mshri.on.ca/nagy/). The neomycin resistant feeder cells were generated in our lab. The ES cells were grown in DMEM media supplemented with 15% ES qualified fetal calf serum (Hyclone), 1x L-glutamine (Gibco/Invitrogen), 1x nonessential amino acids (Gibco/Invitrogen), 1x sodium pyruvate (Gibco/Invitrogen), 1x β-mercaptoethanol (Gibco/Invitrogen), 1x Penicillin/Streptomycin (Gibco/Invitrogen) and 1000 U/ml leukemia inhibitory factor (LIF) (ESGRO, Millipore). After the targeting fragment was electroporated into the ES cells, 48 hours

Figure 3.1 Diagram of mCLCA4 knock-out mouse and homologous recombination in ES cells. A. Diagram of 17.3 kb mCLCA4 genomic DNA fragment used to make mCLCA4 knock-out mice. A 4.8 kb fragment including exon 1 to 3 was deleted; the homologous arms were 2.5 kb with EcoRV/XbaI digestion sites and 6 kb with EcoRV/KpnI digestion sites, respectively. B. Diagram of homologous recombination between targeting vector and mouse genomic DNA mCLCA4 gene locus in ES cells. A 4.8 kb of mCLCA4 sequence was replaced by the loxP-neo-loxP fragment after the homologous recombination occurred between the two arms. Note: XhoI* or SalI* indicated that the PGK-Neo vector was digested by XhoI or SalI following by filling in with dNTPs to make blunted end to match EcoRV site during construction of the targeting vector.

A. 17.3 kb mCLCA4 genomic DNA fragment

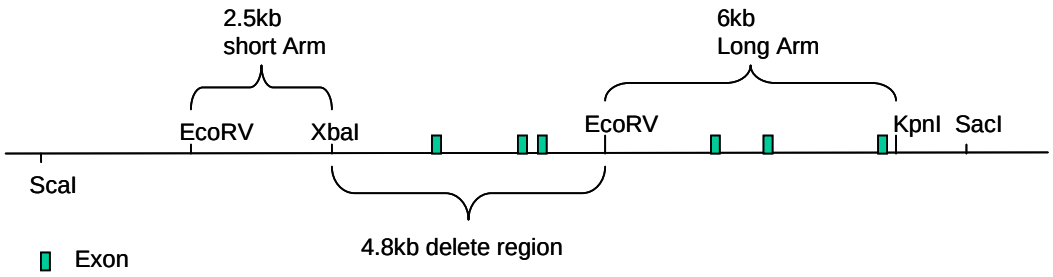

B. Homologous recombination between Genomic allele and Targetting vector

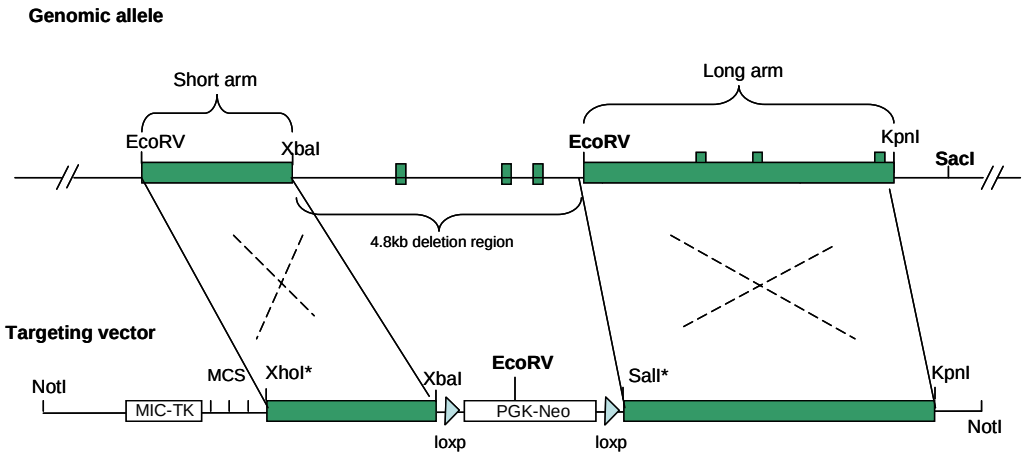

later 150 ng/ml G418 sulfate (selection drug for Neomycin gene, Gibco/Invitrogen) and 2 μM gancyclovir (selection drug for TK gene, Roche) were added to the media (150 ng/ml and 2 μM). The plates were coated with 0.1% gelatin (Chemicon) for 30 minutes at room temperature and liquid removed. The feeder cells were plated at a density of 10^6 cells per 100 mm gelatin coated plates and cultured in a 37^0 C 5% CO_2 incubator for at least two hours before use. The ES cells were plated on feeder cells and cultured in a 37^0C, 5% CO^2 incubator. ES cell media was changed daily and cells split when plates reached confluence.

The targeting vector was linearized with NotI in order to increase the homologous recombination efficiency in ES cells. 25 μg linearized targeting vector DNA (15 kb) was added to $8x10^6$ ES cells in 0.8 ml phosphate buffered saline (PBS) and transferred to an electroporation cuvette with a 0.4 cm gap. The ES cell-DNA mixture was electroporated using the following conditions: 240 V, 500 μF using a BioRad Gene Pulser with Capacitance Extender. The ES cells in the cuvette were placed on ice for 20 minutes then plated on four 100 mm neomycin resistant feeder (NRF) plates with 10 ml DMEM media plus supplements. Forty eight hours after electroporation, the ES cells were selected with G418 (200 μg/ml) and gancyclovir (2 μM) in DMEM media for 10 days. The individual ES cell colonies were picked and were grown in 96 well plates with feeder cells. The colony plates were split and two plates were frozen in liquid nitrogen with 2x ES Freezing Media (Chemicon International) and one plate used for DNA.

3.3.1.3 Positive ES cell clones screening

Standard Southern blot techniques were used to screen the ES cell for positive clones. ES cell DNA was extracted based on the protocol in Gene Targeting (10) and digested with EcoRV and SacI restriction enzymes. The DNA mixes were run on 0.8%

agarose gels and transferred from the gels to blotting membranes. A 500 bp DNA fragment in the genomic region (out of long-arm region) was used as the probe (probe 5) to distinguish the wildtype allele (7.5 kb band) and the knock-out allele (9.2 kb band) (Figure 3.2). Neomycin gene fragment (Neo-probe, 600bp) was used as a second probe to confirm the positive clones by only detecting the knock-out allele band (9.2 kb) on the same Southern blot.

3.3.1.4 ES cell clone injection and breeding strategy.

One positive ES cell clone (1H8) was injected into 3.5 days blastocysts of C57Bl/6J at the Cornell Transgenic Core Facility using standard microinjection techniques (10). Two highly chimeric founders (one approximately 90% and the other approximately 80%) were obtained and mated to C57BL/6J to obtain heterozygous mice. Heterozygous mice were identified using PCR with the following primers sets "a" (GGCCAGGTGTGCACACCTGTAA) and "b" (GCTGGGGATGCGGTGGGCTCTA) with a resultant 410 bp product from the targeted allele on "a" and "c" (CCCACGCCATTTTCAACTGGATTTG) to amplify a 370 bp product from the wildtype allele. This result was also confirmed by Southern blot with probe5 and Neo-probe. Heterozygous mice were mated to produce homozygous null allele mCLCA4 mice, identified by PCR with the same primer sets above and verified by Southern blot with probe 5.

3.3.2 Phenotypic evaluation.

Evaluation of six mCLCA4 mice (two wildtype, two heterozygotes, two homozygotes) at six weeks of age was performed by Dr. Ana Alcaraz at Cornell University's Department of Anatomical Pathology at the Veterinary School of Medicine. Multiple organs (such as heart, liver, brain, stomach, thymus, lung, large

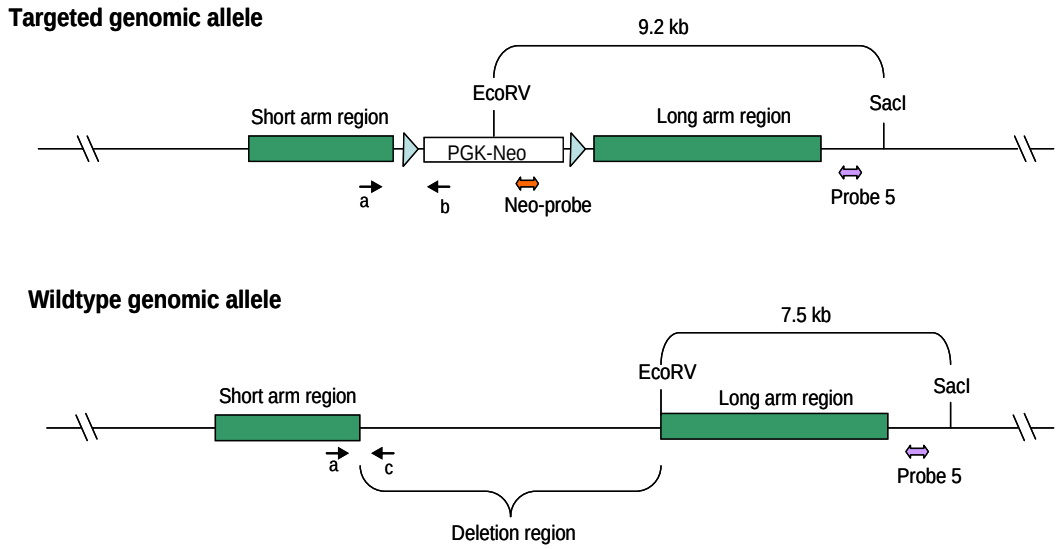

Figure 3.2 Diagram of mCLCA4 homozygous, heterozygous and wildtype genotyping scheme. The targeted allele and wildtype allele of mCLCA4 gene region are shown. Southern blot screening yielded a 9.2 kb band in the targeted genomic allele while a 7.5 kb band would be detected for the wildtype allele. PCR using primers "a" and "b" produced a 410 bp product from mice carrying the targeted genomic allele while PCR using primers "c" and "d" only detected a 370 bp product from the wildtype allele. Heterozygous mice have both 410 bp and 370 bp PCR products.

and small intestines, bladder, and ovary) were weighed for comparison to total body weight. Blood chemistry and complete blood count (CBC) were tested in the Diagnostic Laboratory at Cornell University's Veterinary School of Medicine.

3.4 Results

3.4.1 Generation and Gross Phenotypic Evaluation of mCLCA4 null mice

Two chimeric mCLCA4 founder lines were generated by replacing a 4.8 kb fragment including a portion of the mCLCA4 5' region and exons 1 to 3, resulting in a gene that can not be expressed (Figure 3.3). Homozygous, heterozygous and wildtype mice were identified by PCR (420 bp, 370 bp plus 410 bp, or 370 bp, products respectively) using specific primers (Figure 3.3). Mice were systemically evaluated, comparing wildtype littermate controls to heterozygous and homozygous null mice. Body weight, body size and behavior were not different between the three genotypes. Even after aging to 14 months, no gross differences could be detected. Next, organ weights such as liver, spleen, stomach, large and small intestine, and lung tissues, were evaluated, but no apparent differences were observed. Table 1 shows the blood chemistry profiles obtained from wildtype and null mCLCA4 mice; no obvious differences were observed. Table 2 shows the complete blood count (CBC) result. The homozygous mCLCA4 null mice appeared in normal Mendelian ratios, indicating no reduction in viability.

3.5 Discussion

3.5.1 Rationale for Generation of mCLCA4$^{-/-}$ mice

mCLCA4 was cloned from a mouse smooth muscle RNA pool and characterized by Elbe et al (1). It is highly expressed in organs that contain a significant amount of smooth muscle cells (1). HEK293T cells transiently transfected

Figure 3.3 Southern blot and PCR genotyping. A. Southern blot screening results from ES cells using probe 5 and confirmed with Neo-probe. With probe 5, two ES cell clones (1H8 and 1G10) were identified by a 9.2 kb band (targeted genomic allele) and 7.5 kb band (wildtype genomic allele band). Note other ES cells only showed 7.5 kb wildtype band. With Neo-probe, only the targeted genomic allele 9.2 kb band was detected in these two clones. B. Mouse tail DNA PCR genotyping results. Homozygous mice only yield a 410 bp band, wildtype mice 370 bp band and heterozygous littermates 410 bp and 370 bp bands.

A.

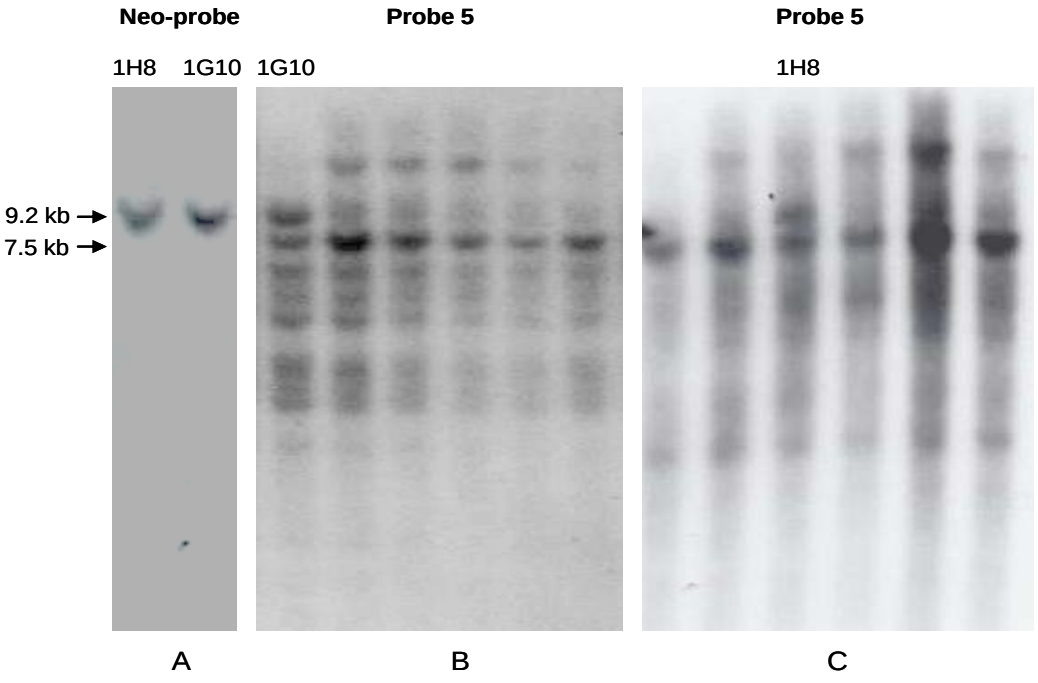
Neo-probe
Probe 5
Probe 5
1H8
1G10
1G10
1H8
9.2 kb
7.5 kb
A
B
C

B.

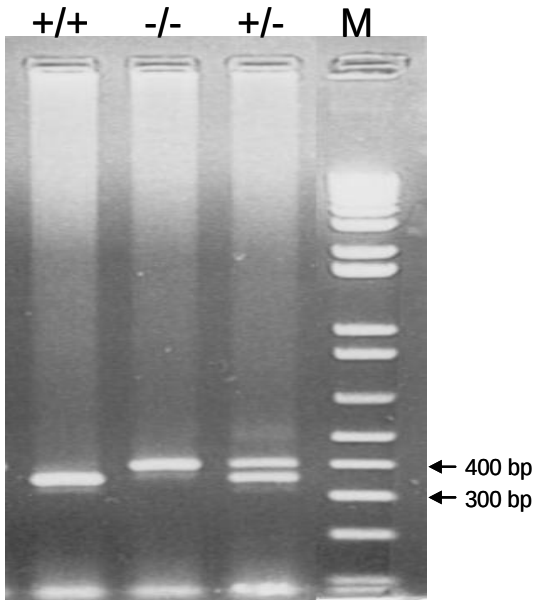
+/+
-/-
+/-
M
400 bp
300 bp

Table 3.1 Blood chemistry test results from mCLCA4 null mice and their littermates

Blood Chemistry Test Result for mCLCA4				
	WT male	mCLCA4 (-/-) male	WT female	mCLCA4(-/-) female
SODIUM (mEq/L)	149	152	156	154
POTASSIUM (mEq/L)	8.5	7.3	6.9	7.4
CHLORIDE (mEq/L)	112	109	116	113
BICARB (mEq/L)	21	23	16	32
ANION GAP (mEq/L)	25	27	31	16
Na/K	18	21	23	21
UREA (mg/dL)	33	28	18	37
CREAT-rb (mg/dL)	0.2	0.2	0.2	0.2
CALCIUM (mg/dL)	10.3	10.3	8.9	10.5
PHOSPHATE (mg/dL)	8.9	8	9	5.7
MAGNES-xb (mEq/L)	1.9	1.9	1.6	1.9
gTOT Prot (g/dL)	5.3	6.1	4.5	4.4
ALB-blk (g/dL)	3.2	3.3	2.8	3
GLOBULIN (g/dL)	2.1	2.8	1.7	1.4
A/G	1.52	1.18	1.65	2.14
GLUCOSE (mg?dL)	234	253	213	177
ALT/P5P (U/L)	52	55	18	40
AST/P5P (U/L)	256	129	142	76
ALK PHOS (U/L)	89	60	57	39
GGT (U/L)	< 3	< 3	< 3	< 3
TOT BILI (mg/dL)	0.2	0.2	2.4	0.1
DIR BILI (mg/dL)	0	0	0	0
IND BILI (mg/dL)	0.2	0.2	2.4	0.1
AMYLASE (U/L)	2762	3309	2089	3915
CHOLESTER (mg/dL)	115	186	87	110
hCK (U/L)	1521	449	765	457
IRON (ug/dL)	195	207	142	323
TIBC (ug/dL)	325	413	250	471
%SAT	60	50	57	69
LIPEMIA	13	21	20	25
HEMOLYSIS	379	786	153	123
ICTERUS	0	0	0	0

Table 3.2 Blood CBC test results from mCLCA4 null mice and their littermates.

Blood CBC Test Result for mCLCA4				
	WT male	mCLCA4 (-/-) male	WT female	mCLCA4 (-/-) female
HCT (%)	49	52	47	52
HB (g/dL)	15.5	15.8	14.5	16
RBC (mill/uL)	10.2	10.7	9.1	10.2
MCV (fL)	48	49	52	51
MCH (pg)	15	15	16	16
MCHC (g/dL)	32	30	31	31
RDW (%)	11.8	14.8	13.6	12.4
WBC (thou/uL)	4.3	4.6	7.7	4.9
SEGMENT N (thou/uL)	1.4	0.3	0.6	0.6
BAND N (thou/uL)	0	0	0	0
LYMPH (thou/uL)	2.5	3.9	6.9	3.7
MONO (thou/uL)	0.3	0.3	0.2	0.4
EOSIN (thou/uL)	0.1	0.1	0	0.2
BASO (thou/L)	0	0	0	0
PLAT SMEAR	adeq	adeq	Low	adeq
PLAT (thou/uL)	1555	660	737	410
MPV (fL)	7.3	6.9	7.3	6.3
TP-REF (g/dL)	6.8	6.7	5.1	5.9
RBC morpholology	polychromasia-moderate	Howell-jolly bodies-few, poly	polychromasia-moderate	polychromasia-moderate
Parasites	none seen	none seen	none seen	none seen
WBC Exam	no significant abnormalities	no significant abnormalities	no significant abnormalities	no significant abnormalities
Plasma Appearance	normal	normal	normal	normal

with mCLCA4 cDNA display a significant chloride current (1). This protein is made in the ER and cleaved inside the cell, and then both fragments are secreted out of the cell and associated with the plasma membrane (See Chapter 2). Taken together, these results suggest that mCLCA4 may be a regulator of a chloride current. To better understand the function of mCLCA4, mCLCA4 knock-out mice were created by deleting the first three exons and a portion of the 5' region of the mCLCA4 gene from the mouse genome resulting in gene disruption at the genomic level (Figure 3.1).

3.5.2 Lack of mCLCA4 does not result in a gross phenotype

mCLCA4$^{-/-}$ mice did not show any abnormal phenotype from birth to 14 months of age as evidenced by the lack of statistical differences in the ratios obtained from multiple organs compared to body weight. This suggests these mice do not have gross cardiac, lung, liver or kidney dysfunction. Even though only two littermate wildtype controls and null animals were taken for the blood chemistry and CBC panels, the mCLCA4 null values were similar to the wildtype mice and published mouse values for normal mouse strains (17). The chemistry profiles suggested that mCLCA4 mice have normal renal and liver function while the CBC values indicated mCLCA4 null mice do not suffer from anemia, infection or leukemia. Just to note, the blood samples were hemolyzed which artificially raised the potassium value due to the release of cellular contents into the serum and may explain the high potassium values observed across all the samples. Possible reasons a mCLCA4 null phenotype was not observed include: 1) loss of mCLCA4 was compensated for by other highly homologous family members, such as mCLCA1 and/or mCLCA2; 2) a subtle phenotype is present but may only be observed under certain conditions of stress; and/or 3) mCLCA4 is not necessary to sustain murine life.

3.5.3 Further study plan

I am convinced that this group of genes plays critical and diverse roles in murine life. Studies are being undertaken by collaborators (Michael Holtzman et al. at Washington University, School of Medicine, St. Louis, MO) to examine the effect of airway challenge on mCLCA4 null mice. In addition, if the CLCAs are critical genes, a loss of function in family member may be compensated for by the other family members. For example, Patel et al. (14) showed that mCLCA5, mCLCA6 and mCLCA7 (AI747448) may compensate for loss of mCLCA3. This may be the case in mCLCA4$^{-/-}$ mice, where I would predict the most highly related family members mCLCA1 and/or mCLCA2, could compensate for loss of mCLCA4. These three genes, which cluster on mouse chromosome 3, share 80% identity at the protein level. Since there are no antibodies available for mCLCA1, mCLCA2 or mCLCA4, further experiments to evaluate functional compensation are limited. To test my hypothesis that mCLCA1 and mCLCA2 genes compensate for mCLCA4's function, I generated mCLCA1,2,4 triple knock-out mice, which will be discussed in Chapter 4.

In summary, I generated mCLCA4 gene knock-out mice but no gross phenotype was observed. To further understand the mCLCA4 gene and other family member functions, I generated triple gene knock-out (mCLCA1, mCLCA2 and mCLCA4) mice, discussed in Chapter 4.

REFERENCE

1. **Elble RC, Ji G, Nehrke K, DeBiasio J, Kingsley PD, Kotlikoff MI, and Pauli BU.** Molecular and functional characterization of a murine calcium-activated chloride channel expressed in smooth muscle. *J Biol Chem* 277: 18586-18591, 2002.

2. **Elble RC and Pauli BU.** Tumor suppression by a proapoptotic calcium-activated chloride channel in mammary epithelium. *J Biol Chem* 276: 40510-40517, 2001.

3. **Elble RC, Walia V, Cheng HC, Connon CJ, Mundhenk L, Gruber AD, and Pauli BU.** The putative chloride channel hCLCA2 has a single C-terminal transmembrane segment. *J Biol Chem* 281: 29448-29454, 2006.

4. **Gibson A, Lewis AP, Affleck K, Aitken AJ, Meldrum E, and Thompson N.** hCLCA1 and mCLCA3 are secreted non-integral membrane proteins and therefore are not ion channels. *J Biol Chem* 280: 27205-27212, 2005.

5. **Gruber AD, Elble RC, Ji HL, Schreur KD, Fuller CM, and Pauli BU.** Genomic cloning, molecular characterization, and functional analysis of human CLCA1, the first human member of the family of Ca2+-activated Cl- channel proteins. *Genomics* 54: 200-214, 1998.

6. **Gruber AD and Pauli BU.** Tumorigenicity of human breast cancer is associated with loss of the Ca2+-activated chloride channel CLCA2. *Cancer Res* 59: 5488-5491, 1999.

7. **Gruber AD, Schreur KD, Ji HL, Fuller CM, and Pauli BU.** Molecular cloning and transmembrane structure of hCLCA2 from human lung, trachea, and mammary gland. *Am J Physiol* 276: C1261-1270, 1999.

8. **Hauber HP, Tsicopoulos A, Wallaert B, Griffin S, McElvaney NG, Daigneault P, Mueller Z, Olivenstein R, Holroyd KJ, Levitt RC, and Hamid Q.** Expression of HCLCA1 in cystic fibrosis lungs is associated with mucus overproduction. *Eur Respir J* 23: 846-850, 2004.

9. **Janssen LJ and Sims SM.** Spontaneous transient inward currents and rhythmicity in canine and guinea-pig tracheal smooth muscle cells. *Pflugers Arch* 427: 473-480, 1994.

10. **Joyner A.** *Gene Targeting*, 2000.

11. **Kamada F, Suzuki Y, Shao C, Tamari M, Hasegawa K, Hirota T, Shimizu M, Takahashi N, Mao XQ, Doi S, Fujiwara H, Miyatake A, Fujita K, Chiba Y,**

Aoki Y, Kure S, Tamura G, Shirakawa T, and Matsubara Y. Association of the hCLCA1 gene with childhood and adult asthma. *Genes Immun* 5: 540-547, 2004.

12. **Mundhenk L, Alfalah M, Elble RC, Pauli BU, Naim HY, and Gruber AD.** Both cleavage products of the mCLCA3 protein are secreted soluble proteins. *J Biol Chem* 281: 30072-30080, 2006.

13. **Nakanishi A, Morita S, Iwashita H, Sagiya Y, Ashida Y, Shirafuji H, Fujisawa Y, Nishimura O, and Fujino M.** Role of gob-5 in mucus overproduction and airway hyperresponsiveness in asthma. *Proc Natl Acad Sci U S A* 98: 5175-5180, 2001.

14. **Patel AC, Brett TJ, and Holtzman MJ.** The Role of CLCA Proteins in Inflammatory Airway Disease. *Annu Rev Physiol*, 2008.

15. **Pauli BU, Abdel-Ghany M, Cheng HC, Gruber AD, Archibald HA, and Elble RC.** Molecular characteristics and functional diversity of CLCA family members. *Clin Exp Pharmacol Physiol* 27: 901-905, 2000.

16. **Range F, Mundhenk L, and Gruber AD.** A soluble secreted glycoprotein (eCLCA1) is overexpressed due to goblet cell hyperplasia and metaplasia in horses with recurrent airway obstruction. *Vet Pathol* 44: 901-911, 2007.

17. **Schnell MA, Hardy C, Hawley M, Propert KJ, and Wilson JM.** Effect of blood collection technique in mice on clinical pathology parameters. *Hum Gene Ther* 13: 155-161, 2002.

18. **Wang Q, Hogg RC, and Large WA.** Properties of spontaneous inward currents recorded in smooth muscle cells isolated from the rabbit portal vein. *J Physiol* 451: 525-537, 1992.

CHAPTER 4

A FUNCTIONAL STUDY OF MCLCA1, MCLCA2 AND MCLCA4 IN MURINE LIFE

------ mCLCA1, mCLCA2 and mCLCA4 genes triple knock-out

4.1 Abstract

mCLCA1, mCLCA2 and mCLCA4 share high identity at the gene level, mRNA level and the protein level. The three of them are clustered next to each other on mouse chromosome 3 (H2-H3). mCLCA4 null mice did not show any obvious phenotype from one day old to >1 year of age. Potentially, the loss of function of mCLCA4 protein in mCLCA4$^{-/-}$ mice was compensated for by other family members, namely mCLCA1 and/or mCLCA2 proteins. To test this hypothesis, I created mCLCA1, mCLCA2, mCLCA4 triple knock-out mice; as these highly homologous genes are contiguous on chromosome 3, the generation of these mice required the development of a bacterial artificial chromosome (BAC) deletion strategy. Using BAC recombineering methods, I deleted a 112 kb specific region of chromosome 3 from a BAC containing all 3 genes, and then targeted the modified BAC to the appropriate location in ES cells by homologous recombination. Using polymerase chain reaction (PCR) and real-time quantitative PCR (qPCR), I developed a method to screen the ES cell positive clones. Three os seven chimeric male founders obtained and mated to C57Bl/6J females. To date three gene triple knock-out mice have been born and initial characterizations started.

4.2. Introduction

The CLCA family of proteins is encoded by a group of genes clustered together on the same chromosome. Human CLCAs are on chromosome 1, 1p22-1p31 region, while mouse CLCAs are on chromosome 3 (H2-H3) (NCBI-MGI data base). mCLCA1 and mCLCA2 share 95% homology at the protein level. mCLCA4 shares 80% at the protein level with either mCLCA1 or mCLCA2. mCLCA1, mCLCA2 and mCLCA4 are orthologous to hCLCA3, which is truncated at the protein level because of a stop codon in the mRNA.

Three single gene knock-out mice have been generated for the mCLCA family, mCLCA3 knock-out mice were generated by Robichaud et al. (2), mCLCA5 knock-out mice were generated by Deltagen, Inc. (San Carlos, CA) and mCLCA4 knock-out mice were generated by me. Evaluation of the mCLCA5 mice showed liver weight versus body weight ratio was higher in knock-out mice compared to wildtype littermates (MGI data base). There was no obvious phenotype observed in mCLCA3 [MGI data base, (2)] nor mCLCA4 knock-out mice (See Chapter 3). The observed normal phenotype may due to: 1) the function of these genes being compensated for by other family members; 2) the presence of subtle phenotypes, not yet detected; 3) the function of these genes being compensated for by some other unknown genes; 4) the genes are not essential for normal physiology. It seems unlikely that these genes are not necessary for murine life based on the exsitance of orthologous members existing in more than 30 species. My hypothesis is that these genes play an important role with variable functions in the mouse and that loss of function in knock-out mice is compensated for by other CLCA members.

I examined this hypothesis by generating mCLCA1, mCLCA2, mCLCA4 triple gene knock-out mice. Due to the large region needed to be deleted and the long homologous arms involved, the traditional knock-out method was not suitable for this purpose. The strategy I developed utilized the BAC recombineering (recombination-mediated genetic engineering) technique for the 3 gene deletion in bacteria (http://recombineering.ncifcrf.gov).

SW102 bacterial strain created by Warming et al. (7) at NCI (http://recombineering.ncifcrf.gov/) was used for this work. It contains 3 λ prophage genes, gem, bet and exo, that are driven by a λPL promoter and a galk selection system. The λPL promoter is controlled by a temperature-sensitive repressor c*I*857 and it is activated at 42˚C and inactivated at 32˚C. Exonuclease (exo) creates single-

stranded overhangs on the 5' to 3' on the linearized DNA. Bet proteins protect the overhangs and help the recombination process. Gem products inhibit *E.Coli* RecRCD protein to prevent linear DNA degradation. The SW102 bacterial strain is kept in 32˚C normally and the three recombination genes will be expressed sufficiently when the strain is heat-shocked at 42˚C making this bacterial stain ideal for recombineering.

In the galk selection system, the galactokinase (galk) gene is deleted and the galactose operon is modified but remains functional in SW102 cells. Therefore the galk gene can be added with the targeting construct to the cells and thereby the ability to grow on the plates with only galactose as carbon source. In this case, the galk selection has the advantage over kanamycin selection due to the high background issue. The disadvantage of the galk selection system is that there is no galk selection system in ES cells and it has to be replaced by a neomycin/kanamycin cassette.

Regular PCR and Relative Quantification (RQ) real-time PCR method were used for screening ES cell positive clones after ES cell targeting. Seven, nearly 100% chimera (base on the coat color) male founder mice were obtained and mated to produce homozygous null mCLCA1, mCLCA2 and mCLCA4 mice. Further analysis will be required to determine if a phenotype is present.

4.3. Materials and Methods

4.3.1 BAC clone handling and confirmation

BAC clone RP24-271-G16 (Children's Hospital Oakland Research Institute) was chosen based on its size (192.6 kb) and it containing the mCLCA1, mCLCA2, mCLCA4 and EG622139 genes. The DH10B bacterial strain containing RP24-271-G16 was streaked onto chloramphenicol (CM)(Chemicon) (12.5µl/ml) /Luria-Bertani (LB) (selection for BAC Bone) plates and incubated at 37°C overnight. Six colonies were picked and grown in 5 ml CM/LB(12.5µl/ml) liquid overnight. Each bacterial

culture (0.2-0.5 ml) was frozen in 20% glycerol and stored in a -80°C freezer. The remaining culture media was used for mini-prep DNA using the standard mini-prep DNA protocol (http://recombineering.ncifcrf.gov/). The BAC sequence was confirmed by: 1) digesting the BAC DNA with SpeI restriction enzyme and showing the same bands pattern as the BAC sequence in Vector-NTI program; 2) obtaining two end PCR products from BAC vector to BAC end region (PCR-C and PCR-D) and sequencing them [primers: RP24-T7 (TAATACGACTCACTATAGGGAGA) and G16R1 (GCTGTGTCCCCAAGACCAGCTA)], 699 bp); Sp6-BAC-end [RP24-Sp6 (ATTTAGGTGACACTATAG) and G16-F1 (GTACTTCATAGCCTCAGTAATA), 453bp]; 3) generating ans sequencing two PCR products from the BAC middle region [primers: PCR-A (GGTCTACTATGTGACAGAATAG and GCTAATCAGACGAATCTGCCTG, 544 bp) and PCR-B (TGCTGTCCATGCTCAGGCAAAG and ACAGTATCAGCACCTTTATAATG, 531 bp)] (Figure 4.1.)

4.3.2 SW102-RP24-271-G16 BAC strain generation

The bacterial recombineering strain SW102 and galactokinase (galk) selection vector were obtained from National Institute of Cancer (NIC) (Frederick, VA National Institute of Health). BAC mini prep DNA and SW102 bacterial competent cells without drug selection were made according to the NIC BAC recombineering web site protocol (http://recombineering.ncifcrf.gov/). The BAC DNA (3µl of 50µl mini prep) was electroporated into 40 µl SW102 competent cells (1.75kV, 25µF, 200 Ω), then 1 ml of LB was added into the DNA-cell mix immediately and transferred into 15 ml culture tube. The tube was shaken at 32˚C for 1 hour. The cells were placed on CM/LB (12.5µg/ml) plates then incubated at 32˚C for 2-3 days until the BAC colonies

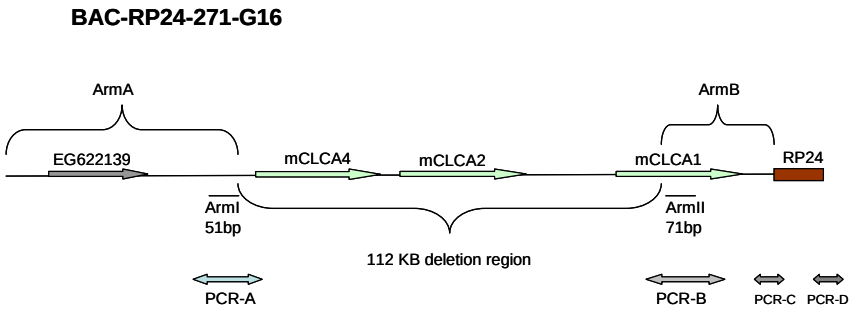

Figure 4.1 Diagram of BAC clone RP24-271-G16. Two homologous arms (ArmI and ArmII) for BAC recombineering in SW102 bacterial cell; two homologous arms (ArmA and ArmB) for genomic homologous recombination in ES cells. Deletion region was 112 kb. RP24 is the BAC vector (BAC bone). PCR-A, PCR-B, PCR-C and PCR-D were the PCR products and locations for BAC clone confirmation.

appeared. BAC mini prep DNA was made from the BAC colonies and sequence confirmed by sequencing four PCR products, two BAC ends and two products around the arms with the same primers as described (Figure 4.1).

4.3.3 ArmI-galk-ArmII targeting fragment construction

The total 112 kb fragment that included the partial mCLCA4 5' region, mCLCA4 gene, mCLCA2 gene and the beginning 22.5 kb of mCLCA1 gene was deleted from BAC RP24-271-G16. Two homologous arms were designed and used to construct the targeting fragment, ArmI (51 base pair) located just before 112 kb deletion region and ArmII (71 base pair) located just after 112 kb deletion region (Figure 4.1). Two specific long oligos were made by IDT (Integrated DNA Technologies). Oligo1: ArmI (51bp) plus 20 bp of beginning em7 promoter for galk gene (CTTCACAAAACTCCTTTTACAGGTATTATTGTTCTTACTTTACAGGTAAGA-GATATCGAATTCCTGTTGAC); Oligo2: ArmII (71bp) plus the last 20 bp of galk gene from galk vector (CCGAGCAGCACCTGGATAGCTAGGGTGCTCAGTCGTCTGACTATCGCCAG CTACCCACAACACCCACCAA-TCAGCACTGTCCTGCTCCTT).1.3 kb of PCR product (named ArmI-galk-ArmII) was generated by PCR primers (Oligo1 and Oligo2) with galk vector as the template. PCR cycling conditions were: 94˚C 2 min, 94˚C 30sec, 58˚C 30 sec, 72˚C 1.5 min, repeat 5 cycles from second step, 94˚C 30 sec and 72˚C 1.5 min for 35 cycles. The PCR product was purified from a 0.8% agarose (Invitrogen) gel following the Qiagen Kit Gel Extraction Protocol and sequenced (Figure 4.2 A).

Figure 4.2 Schematic generating BAC-KO124-galk targeting vector.

A. Generating ArmI-galk-ArmII targeting fragment by PCR. B. Homologous recombination occurs between BAC-RP24-271-G16 and ArmI-galk-ArmII in SW102 cells and results in a BAC-KO124-galk vector with 112 kb sequence deletion. PCR product crossing the arms, PCR(i) and PCR(ii) are shown (double end arrows).

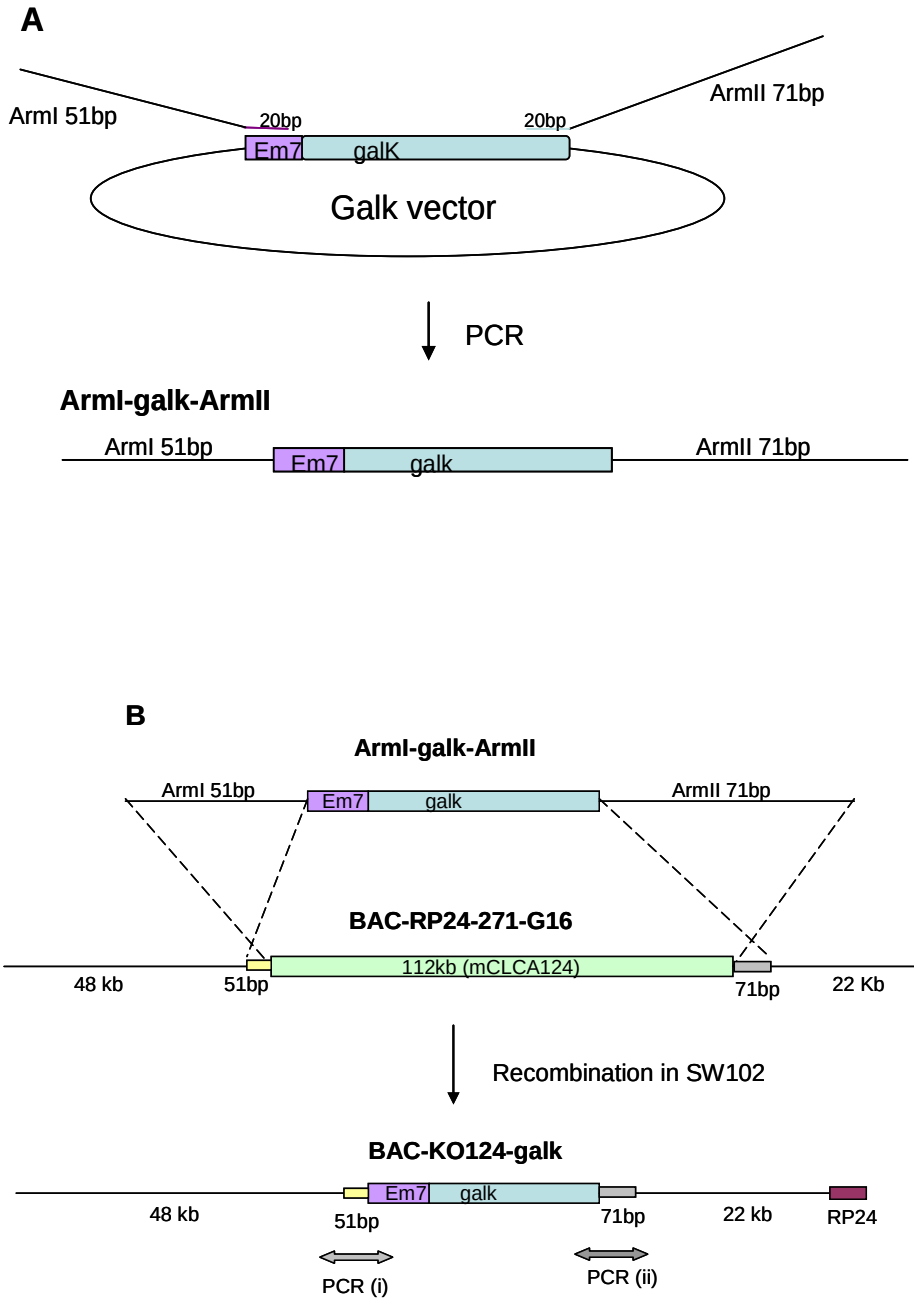
A
ArmI 51bp
20bp
20bp
ArmII 71bp
Em7
galK
Galk vector
PCR
ArmI-galk-ArmII
ArmI 51bp
Em7
galk
ArmII 71bp
B
ArmI-galk-ArmII
ArmI 51bp
Em7
galk
ArmII 71bp
BAC-RP24-271-G16
112kb (mCLCA124)
48 kb
51bp
71bp
22 Kb
Recombination in SW102
BAC-KO124-galk
Em7
galk
48 kb
51bp
71bp
22 kb
RP24
PCR (i)
PCR (ii)

4.3.4 Recombineering the targeting fragment and BAC in SW102 cells.

The SW102-RP24-271-G16 competent cells were made with CM selection and 3μl of 1.3 kb targeting fragment (ArmI-Galk-ArmII) was electroporated into the competent cells followed by plating on galk selection plates and colonies were observed after 3-4 days. Positive galk gene clones appeared bright pink on MacConkey Agar (Acumedia Manufactuers) plates. PCR products crossing the arms PCR(i): bef-armI-F (GGCACTAAACCATTAACTAAGT) and pgalk-R (GCGAACTTTACGGTCATCGCG) yielded a 393 bp product; PCR(ii): pgalk-F (GGTGCCTGCCGTACAGCAAGCT) and aft-armII-R (GAGAGTATACAGCACAGTTAA) yielded a 271 bp product; and the PCR products of the BAC ends (the same primers as listed in 4.3.1.) were generated and confirmed by sequencing (Figure 4.2 B)

4.3.5 Replacing galk gene with Neomycin gene.

Due to the further selection needed in ES cells, the galk gene in the BAC targeting construct was replaced by a Neomycin cassette. Two long oligos, (i) OligoA: ArmI (51 bp) plus 20 bp [before the first FRT site in PBS-neomycin/kanamycin (PBS-Neo/Kan) vector] (CTTCACAAAACTCCTTTTACAGGTATTATTGTTCTTACTTTACAGGTAAGA-GGATCTAGATAACTGATCAGC) and (ii) OligoB: ArmII (71bp) plus 20bp after second FRT site in PBS-Neo/Kan vector (CCGAGCAGCACCTGGATAGCTAGGGTGCTCAGTCGTCTGACTATCGCCAG CTACCCACAACACCCACCAA-CCATGGAGAAGTTACTATTC) were generated by IDT. The neomycin targeting fragment was made by PCR using OligoA and OligoB with PBS-Neo/Kan vector (self made) as a template. The PCR conditions

were: 94˚C 2 min, 94˚C 30 sec, 58˚C 30 sec, 72˚C 1 min 30 sec, repeat 5 cycles from step2, 94˚C 30 sec, 72 ˚C 1 min 30 sec, repeat 35 cycles from step 4, 72˚C for 10 min then hold at 4˚C. The neomycin targeting fragment (ArmI-Neo/kan-ArmII) PCR product was purified and sequenced. SW102-BAC-KO124-galk competent cells were made as described and 3µl of neomycin targeting fragment (ArmI-Neo/kan-ArmII) was electroporated into the competent cells. The cells were plated on Kan (25µl/ml)/CM(12.5µ/ml)/LB plates and incubated at 32˚C for 2-3 days. Six colonies were picked and checked by PCR with cross arm primers [PCR-a: (GGTCTACTATGTGACAGAATAG) / (CTCGTCTTGCAGTTCATTCAG) and generated 899 bp; PCR-b: (GCAGCGCATCGCCTTCTATCGC)/ (CATTATAAAGGTGCTGATACTGT) and yield 538 bp product] and with the ends primers. The PCR products were sequenced to confirm the BAC construct. For easy handling, the BAC-KO124-Neo construct plasmid DNA was electroporated into DH10 electro competent cells (Invitrogen) (Figure 4.3).

4.3.6 ES cell culture and handling.

E14Tg2A.4 feeder independent ES cells line (BayGenomics) used for this work was generated from 129P2/olaHsd strains with Pink-eyed chinchilla coat color (6). ES cells were grown in GMEM base media supplemented with 15% fetal calf serum (EmbryoMax, Chemicon), 1x L-glutamine (Gibco/Invitrogen), 1x NEAA (non essential amino acids) (Gibco/Invitrogene), 1x Na pyruvate (Gibco/Invitrogen), 1x β-mercaptoethanol (Gibco/Invitrogen), 1x Penicillin/Streptomycin (Gibco/Invitrogen) and 1000U/ml Leukemia Inhibitory Factor (LIF) (ESGRO, Millipore). The ES cell media was changed daily and the ES cells were split every other day to keep 60%-80% confluency. The 10 cm culture plates were coated with 0.1% gelatin (Chemicon) for 1 hour before replating the ES cells. Twenty-four hours after electroporation of the

Figure 4.3 Diagram depicting generation of BAC-KO124-neo/kan targeting vector for ES cells. A. The same homologous arms (ArmI/51bp and ArmII/71bp) plus a 20 bp sequence from PBS-Neo/kan vector were used were used to generate ArmI-Neo/kan-ARMII targeting fragment by PCR. B. ArmI-Neo/kan-ArmII targeting fragment was transfected into SW102-BAC-KO124-galk competent cells and resulted in SW102-BAC-KO124-Neo/kan. C. Two PCR products (PCR-a and PCR-b) crossing the arms plus two BAC ends PCR products were generated and sequenced to confirm the BAC sequence.

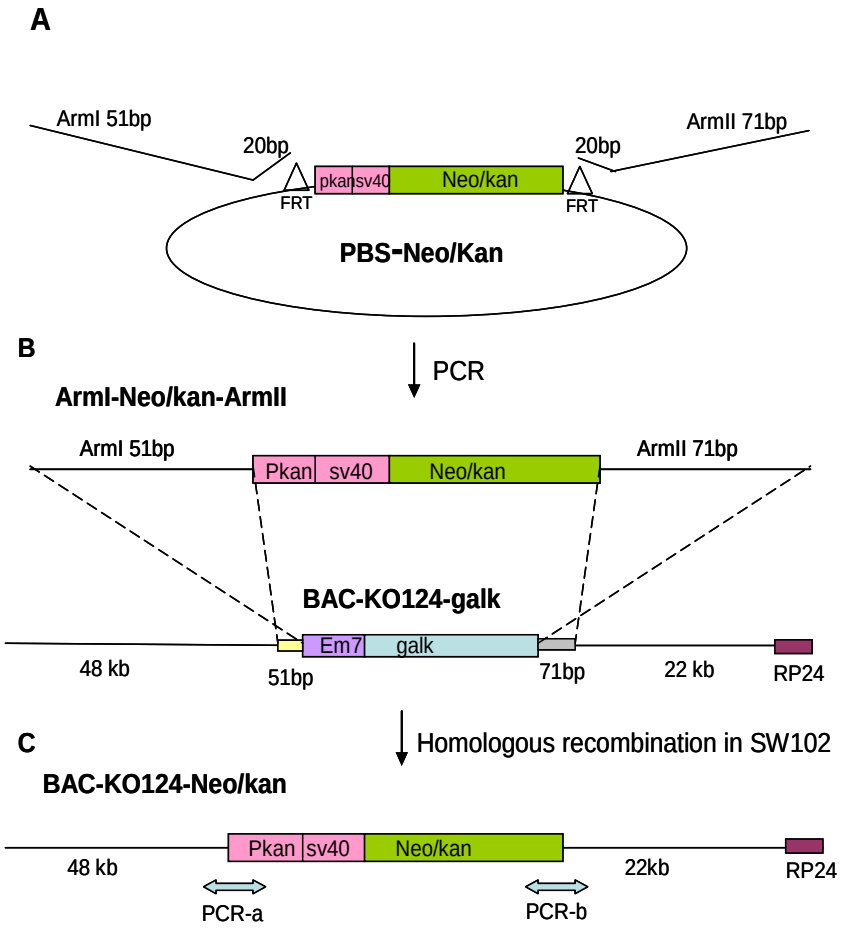
A
ArmI 51bp
20bp
ArmII 71bp
20bp
pkan
sv40
Neo/kan
FRT
FRT
PBS-Neo/Kan
B
PCR
ArmI-Neo/kan-ArmII
ArmI 51bp
Pkan
sv40
Neo/kan
ArmII 71bp
BAC-KO124-galk
Em7
galk
48 kb
51bp
71bp
22 kb
RP24
C
Homologous recombination in SW102
BAC-KO124-Neo/kan
Pkan
sv40
Neo/kan
48 kb
22kb
RP24
PCR-a
PCR-b

ES cells, G418 (200ng/ml) was added to the GMEM media for the neomycin positive selection.

4.3.7 ES cell targeting

ES cells ($2x10^7$) and linerized BAC-KO124-Neo targeting DNA fragment (24 μg) were mixed in 0.8 ml PBS solution in 0.4 cm gap Gene Pulser Cuvette (Bio-RAD) and the mixture was electroporated (3μF, 800V, 0.04 sec). After resting on ice for 30 minute, the ES cells were plated on 4 gelatin (10%) coaded plates with GMEM supplemented media and incubated at 37˚C, 5% CO_2. The G418 (200μg/ml in GMEM media) drug selection was started on the second day following electroporation and continued for 7-8 days. Three hundred and fifty colonies were picked at days 9-10 and transferred to 48-well gelatin coated plates. Half of the cells were frozen in liquid nitrogen with 2X frozen media (Chemicon) and half of the cells were harvest.

4.3.8 Homologous recombination positive clone detection.

DNA from ES cell clones was made according to the protocol in Gene Targeting book (1). The random insertion clones were excluded by one of the four BAC bone (vector) PCR products, 1) T7-BAC-end [RP24-T7 (TAATACGACTCACTATAGGGAGA) and G16R1 (GCTGTGTCCCCAAGACCAGCTA)], 699 bp; 2) Sp6-BAC-end [RP24-Sp6 (ATTTAGGTGACACTATAG) and G16-F1 (GTACTTCATAGCCTCAGTAATA)] 453 bp]; 3) BAC bone fragment-1 [RP24-12187(ATCCTGGTGTCCCTGTTG) and RP24-12691(CGGAAATCGTCGTGGTAT), 505 bp]; and 4) BAC bone fragment-2 [RP243229 (AATACAACGGCTATCACG) and RP24-3823 (AGCTTCTGGCTTTCTTTAC), 595 bp]. The clones without BAC bone PCR bands were checked by PCR to determine if they contained the Neomycin using the

following primer pairs: NeoGeneF2 (GCAGCGCATCGCCTTCTATCGC) and aft-A2-R (ACAGTATCAGCACCTTTATAATG), 443 bp product.

The clones without BAC bone but containing the Neomycin gene were then screened by real-time quantification PCR (qPCR) Relative Quantification (RQ) method. Three qPCR primers/probe sets (TaqMan probes) were made by ABI (Applied Biosystems) and used to screen positive clones: 1) ConKO124 (Forward primer-AGGTGCCATAGCAGATGAATGAAT, Reverse primer-CACATAAGTTACCTGTAGCTATTTCAGGAA; reporter-FAM probe CCCAACACAATTTCA); 2) KO124KO4 (Forward primer-GTGACTTTTAAGTGACCAGGACAAGA; Reverse primer-ATCATGAGTGTGCTCGAAGCT; reporter-FAM probe-ATGTGAGCCCAACTCC); and proKO124 (Forward primer-CGTTGGCCTTAGAAGAGTGTGA; Reverse prime-GCTCTGACTAGTTGAATGACCCTAA; reporter-FAM probe CCCCAGCCGGATTAT). In each reaction, 10 ng of sample DNA, 1X TaqMan universal PCR Master Mix (Applied Biosystems, manufactured by Roche) and 1X TaqMan probe (250 nM probe and 900 nM primers) were used. The was performed using the 7500 Real Time PCR System (Applied Biosystems) with the following cycling conditions: 50°C for 2 min, 95°C for 10 min, 95°C for 15 sec, 60°C for 1 min repeat 40 cycles from step 3. Every sample was run parallel with TaqMan Mouse β-actin (ACTB, Applied Biosystems) probe as an endogenous control to normalize variation in concentrations between samples to make the data comparable. RQ Study software included in the 7500 Real Time PCR System was used for the data analysis.

4.3.9 ES cell injection and mating strategy.

The positive clone 1C3 was injected into 3.5 days B6 blastocysts by Robert Munroe in Department of Biomedical Sciences, Cornell University using standard techniques (1) and resulted in 7 chimeric male founders. Three chimeric male mice were mated to C67Bl/6J females. To generate homozygous mCLCA1,2,4 triple knock-out mice, heterozygous (mCLCA1,2,$4^{+/-}$) males and females were mated and mCLCA1,2,$4^{-/-}$ mice were obtained.

4.3.10 Genotyping strategy to distinguish mCLCA4 offspring.

Four PCR products were used to distinguish mCLCA1,2,$4^{-/-}$, mCLCA1,2,$4^{+/-}$ and wildtype mCLCA1,2,$4^{+/+}$ mice. PCR products: i) Primers NeoGeneF2(c) and aft-A2-R(d) (538bp); ii) WT-genotypeF1(a) (GGTCTACTATGTGACAGAATAG) and Neo-VecR(b) (CCTCGTCTTGCAGTTCATTCAG), 899 bp; iii) WT-genotype-F2(f) (TGCTGTCCATGCTCAGGCAAAG) and aft-A2-R(d), 531 bp; and d) WT genotype-F1(a) and WT-genotype-R1(e) (GCTAATCAGACGAATCTGCCTG), 400 bp. The homozygous mice DNA will give PCR products “a/b” and “c/d” but no “a/e” and “f/d” products. The heterozygous mice DNA will give all 4 PCR products. The wild type mice DNA will give PCR product “a/e” and “f/d” but no products for “a/b” and “c/d”. (Figure 4.8).

4.3.11 Phenotypic evaluation of mCLCA1,2,4 knock-out mice

Body weights were measured at 3, 6 and 10 weeks of age. Initial histological evaluation of multiple organs was performed on two 6 week old mCLCA1,2,$4^{-/-}$ and wildtype littermates by Bendicht Pauli from Molecular Medicine Department at Cornell University.

4.4. Results

4.4.1. Generating BAC-KO124-Neo targeting construct by deleting 112kb fragment in BAC-RP24-271-G16

The BAC RP24-271-G16 was used for the triple gene knock-out construct. It contains 182 kb of mouse genomic sequence (including mCLCA1, mCLA2, mCLCA4 and EG622139 genes) and 10.6 kb RP24 vector. A 112 kb fragment was deleted from the mouse genome that included 74% (22.5 kb/30.4kb) of mCLCA1gene, all of mCLCA2 and all of mCLCA4 genes.

To take the advantage of the galk selection system I initially made a BAC-KO124-galk vector. Fifty one base pair sequence located before the 112 kb deletion region (ArmI) and 71 base pair sequence located after the 112 kb deletion region (ArmII) were used for the homologous recombination Arms for BAC recombineering (Figure 4. 2). Homologous recombination occurred between the BAC-RP24-271-G16 and ArmI-galK-ArmII targeting fragment in SW102 cells as evidenced by the fact that all the colonies that were picked from the galk plates (20/20) had the smaller size of insert fragment with NotI enzyme digestion and correct PCR products [PCR(i) and PCR(ii)] (Figures 4.2). The 112 kb sequence including three quarter of mCLCA1 gene, all of the mCLCA2 and all of the mCLCA4 was successfully excluded from BAC-RP24-271-G16 and named BAC-KO124-galk (Figure 4.2). These data demonstrate the efficiency of the galk system for generating targeting vectors.

Since ES cell do not contain a galk selection system, BAC-KO124-galk could not be used for ES cell targeting purpose. To make the ES cell targeting construct the galk promoter em7 and galk gene were replaced by the Psv40 promoter and Neomycin gene in BAC-KO124-galk BAC construct through one round of BAC recombineering, to produce targeting vector, named BAC-KO124-Neo (Figure 4.3).

4.4.2. ES cell targeting and detection of homologous recombination

After the 112 kb deletion, 48 kb (ArmA) and 22 kb (ArmB) of the genomic region remained in the BAC and were the homologous arms for recombination in the ES cells (Figure 4.3). To increase the likelihood of homologous recombination the BAC-KO124-Neo targeting vector DNA was prepared in large scale and linearized by the PI-SCEI restriction enzyme. The linearized BAC targeting fragment was electroporated into E14Tg2A ES cells and 350 clones were analyzed.

Due to the long homologous arms, traditional methods such as Southern Blot can not be used to distinguish homologously recombined clones from wild type or random insertion clones. I used two methods to determine which ES cells had homologous recombination occurring in one allele: regular PCR and qPCR. Initially, I used regular PCR and reasoned that if the linearized construct was randomly inserted into the genome, the BAC vector would be part of the insertion in the majority of cases. To take advantage of this idea, I used PCR products from the BAC vector to exclude random insertion clones (Figure 4.4). Fifty-six clones without BAC vector were detected by PCR products but contained the neomycin gene (the selection gene for G418 drug positive clones) PCR product (Figure 4.4).

Figure 4.5 shows the strategy used to confirm the PCR results in the 56 potential homologous recombined clones identified using regular PCR. Regular ES cell DNA was used as a calibrator in data analysis. The mCLCA4 knock-out construct was a 4.8 kb deletion and shared a 4.2 kb deletion window with mCLCA1,2,4 knock-out clones. mCLCA1,2,4$^{-/-}$and mCLCA1,2,4$^{+/-}$mice tail DNA and the injected knock-out mCLCA4 ES cell clone (1H8) were used as controls. (i) TaqMan Probe “Con” is ocated in the 4.8 kb ArmA region (non-deletion region) and every sample except the random insertion clones have the same Relative Quantification (RQ) value as ES cell

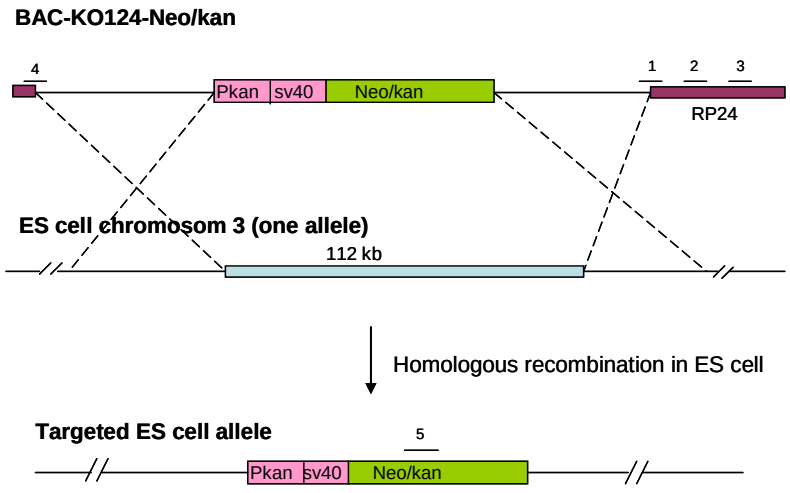

Figure 4.4 Homologous recombination between BAC-KO124-Neo/kan and one chromosome 3 allele in ES cells. When homologous recombination occurred a 112 kb genomic region was deleted from chromosome 3 (targeted ES cell allele). "1", "2", "3" and "4" show the PCR product positions from the BAC bone (RP24) and indicate that ES cell clones had random insertion. "5" is neomycin gene PCR product which indicated ES cell clones contained neomycin gene.

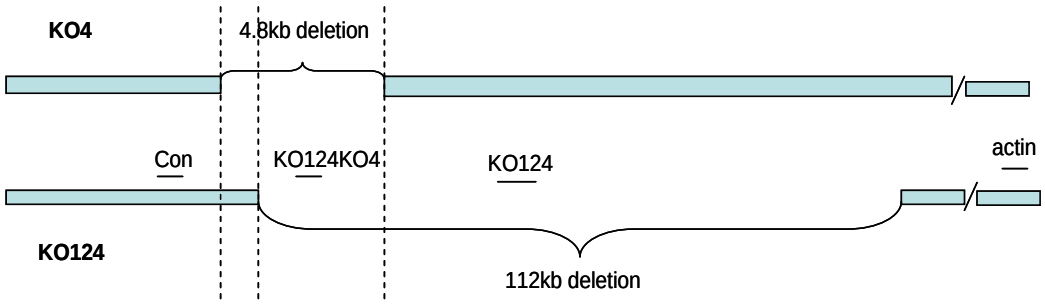

Figure 4.5 Diagram of the Real-time PCR strategy. Regular E14 ES cell DNA was used as a calibrator. mCLCA4 knock-out (KO4) ES cell clone (1H8) DNA and mCLCA4$^{+/-}$, mCLCA4$^{-/-}$ mice tail DNA were used as control to screen the homologous recombination ES cell clones of mCLCA1,2,4 knock-out. β-actin probe is the endogenous control to normalize the concentration variation of the samples. (i) The Con probe located in the non-deleted (ArmA) region and non-random insertion samples will show the same RQ value as ES cell DNA. Random insertion clones will show higher RQ value compared to ES cell DNA. (ii) KO124KO4 probe is located in the deleted window of mCLCA4 and mCLCA1,2,4 knock-out. mCLCA4$^{+/-}$ (KO4$^{+/-}$) tail DNA, 1H8 DNA and positive mCLCA1,2,4 ES cell clone DNA should show half of RQ value as ES cell DNA. mCLCA4$^{-/-}$ (KO4$^{-/-}$) tail DNA should show zero RQ value comparing with ES cell DNA. Random insertion clones will show the same RQ value as ES cell DNA. (iii) KO124 probe located in the mCLCA1,2,4 deletion region. Only mCLCA1,2,4 positive clones will have half of the RQ value as ES cell DNA. Others will show the same RQ value as ES cell DNA.

DNA. Random insertion samples had a higher RQ value than ES cell sample DNA (such as sample 41) (Figure 4.6 A). (ii) TaqMan Probe KO124KO4 is located in the shared deletion region and products from both knock-out mCLCA4 and knock-out mCLCA1,2,4 ES cell positive clone DNA should have half RQ value of the wildtype ES cell DNA. All other mCLCA1,2,4 ES cell non-positive clones had the same RQ values as wildtype ES cell (Figure 4.6). (iii) TaqMan probe KO124 is located in the 112 kb deletion but not in the mCLCA4 deletion region. In this case, mCLCA1,2,4$^{-/-}$ controls showed the same RQ value as wildtype ES cell sample. mCLCA1,2,4 homologous recombined clones showed half RQ value of wildtype and the other mCLCA1,2,4 clones showed the same RQ value as wildtype. Two clones, 1C3 and 2B, were determined to have undergone homologous recombination resulting in the removal of mCLCA1,2,4 (Figure 4.7). These data demonstrate the utility of using two PCR strategies to confirm homologous recombination in ES cells following BAC recombination.

4.4.3. Generating mCLCA 1,2,4 homozygous knock-out mice

One knock-out mCLCA1,2,4 ES cell clone (1C3) was injected into 3.5 days blastocysts of C57Bl/6 mice and seven nearly 100% chimeric male founder mice were obtained. Figure 4.8 shows the strategy to genotype the offspring by PCR and representative examples. Three founder males were mated to C56Bl/6J females generating normal size litters, 3-6 pups/litter. Six pairs of heterozygous mCLCA1,2,4 knock-out mice (mCLCA1,2,4$^{+/-}$) were mated and both male and female homozygous mCLCA1,2,4$^{-/-}$ mice were born. Figure 4.8 shows the PCR strategy genotype the offsprings and the mice tail genotype results.

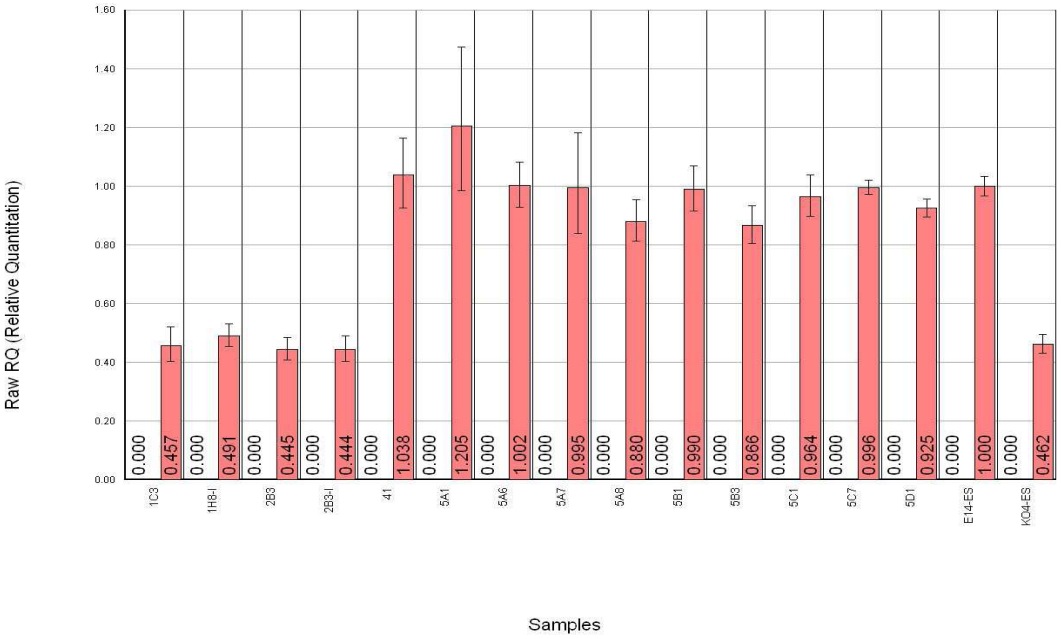

Figure 4.6 using KO124KO4 probe. Raw data from mCLCA1,2,4 ES cell clone screening. 1C3 and 2B3 are the clones with one deleted allele. KO4ES is the mCLCA4 knock-out ES cell clone (same as 1H8). "41" is the random insertion clone. E14 ES is the ES cell DNA sample as the calibrator. Clones, 5A1-5D1, are non-positive but without BAC bone clones.

Figure 4.7 qPCR results. A. Con probe, clone 41 have a higher PCR RQ value than ES cell DNA, suggesting random insertion, while all other clones had the same RQ value as ES cells. B. with KO124 probe, only two ES cell positive clones (1C3 and 2B3) showed half RQ value of ES cell DNA while others showed the same value as ES cell DNA. Note, the higher RQ value of 41, KO(+/-) probably due to the non-specific primer binding. C. With KO124KO4 probe, two mCLCA1,2,4 ES cell positive clones (1C3, 2B3), mCLCA4 ES cell positive clone (1H8), $mCLCA4^{+/-}$ [KO4(+/-)] tail DNA showed half RQ value of ES cell DNA while $mCLCA4^{-/-}$ [KO4(-/-)] tail DNA showed zero RQ value compared to the ES cell DNA (See Figure 4.5). The numbers under the bottom of each panel indicated the number of time the experiment repeated.

A

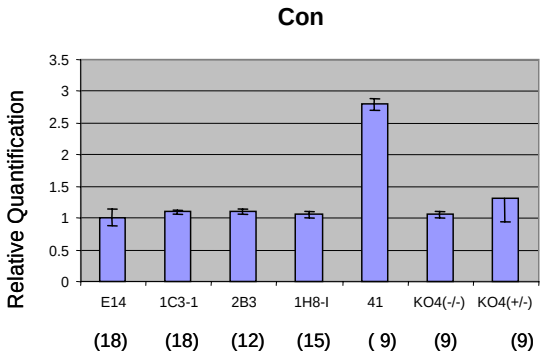
Con
Relative Quantification
3.5
3
2.5
2
1.5
1
0.5
0
E14
1C3-1
2B3
1H8-I
41
KO4(-/-)
KO4(+/-)
(18)
(18)
(12)
(15)
(9)
(9)
(9)

B

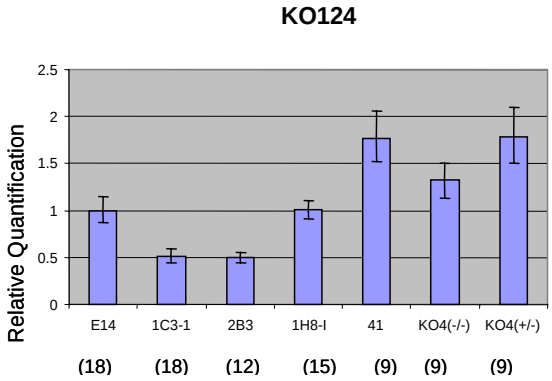
KO124
Relative Quantification
2.5
2
1.5
1
0.5
0
E14
1C3-1
2B3
1H8-I
41
KO4(-/-)
KO4(+/-)
(18)
(18)
(12)
(15)
(9)
(9)
(9)

C

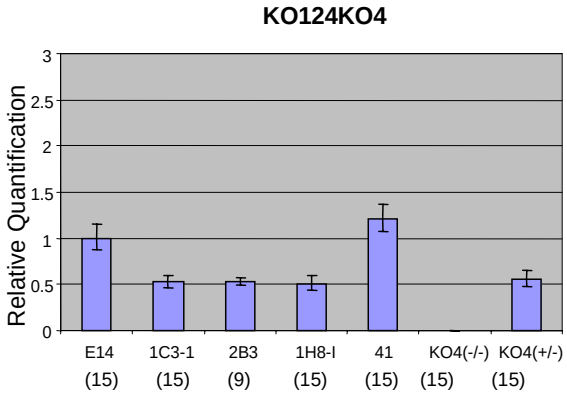
KO124KO4
Relative Quantification
3
2.5
2
1.5
1
0.5
0
E14
1C3-1
2B3
1H8-I
41
KO4(-/-)
KO4(+/-)
(15)
(15)
(9)
(15)
(15)
(15)
(15)

Figure 4.8 PCR strategy and results to genotype mCLCA1,2,4 mice. A. Location of four sets of primer to genotype offspring. B. Examples of PCR bands obtained from tail DNA of mCLCA1,2,4 knock-out mating offspring with genotyping primers in Panel A. mCLCA1,2,4$^{-/-}$ mice have 899 bp (a/b) and 538 bp (c/d) bands (left panel). mCLCA1,2,4$^{+/-}$ mice have all four bands (middle panel). mCLCA1,2,4$^{+/+}$ mice have two PCR products, 400 bp (a/e) and 531 bp (f/d) (right panel).

A

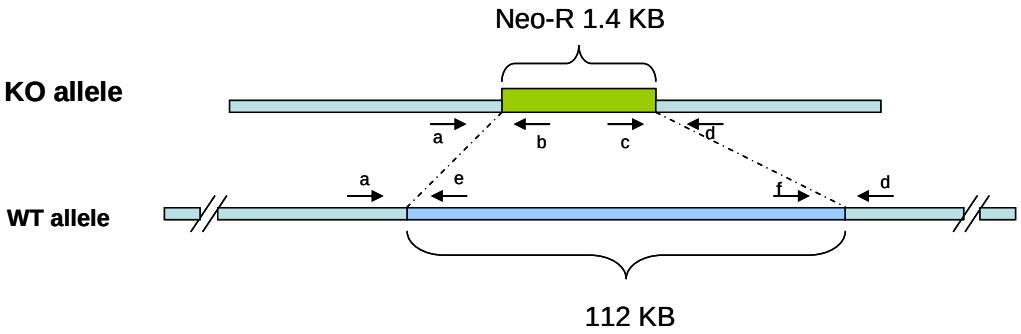

B

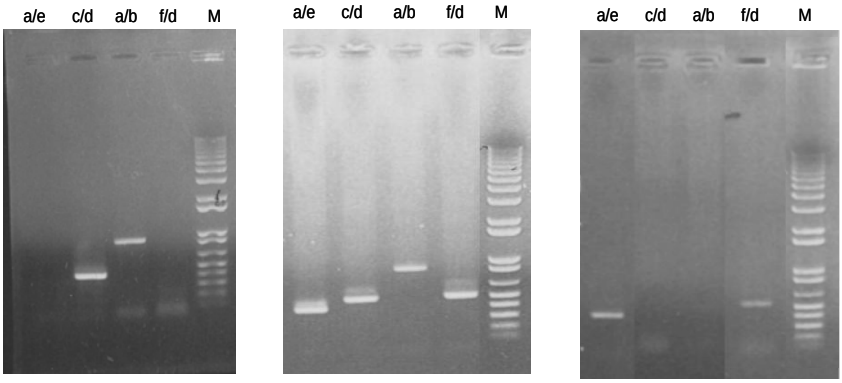

4.4.4 Characterization of mCLCA1,2,4$^{-/-}$ mice

mCLCA1,2,4$^{-/-}$ mice survive to at least 2 months of age. Table 4.1 shows weight taken at 3 different time points. Even though our mCLCA1,2,4$^{-/-}$ numbers do not allow us to perform statistical analysis it appears the female mice are smaller at 6 and 12 weeks of age compared to littermate mCLCA1,2,4$^{+/-}$ and mCLCA1,2,4$^{+/+}$. Organs were taken from two mCLCA1,2,4$^{-/-}$and two mCLCA1,2,4$^{+/+}$ littermate controls at 6 weeks of age. Hematoxylin and eosin staining of multiple tissues, such as brain, heart, liver, small and large intestine, ovary, bladder, thymus, lung, stomach, etc will be examined. I have observed postnatal day one mCLCA1,2,4$^{-/-}$ pup with eyes that appeared opaque compared to wildtype littermates (Figure 4.9 A). Histological evaluation of this pup showed hypopigment of the retainal epithelium (Figure 4.9 B). This potential phenotype will need to be confirmed in more mCLCA1,2,4$^{-/-}$ mice and their wildtype littermates.

4.5. Discussion

In this chapter I discussed two techniques that I developed and used successfully namely the deletion of a large region of genomic DNA through BAC recombineering and a PCR/qPCR strategy to screen ES cell clones. The BAC recombineering technique has become a very useful tool for various purposes, such as generating transgenic and knock-out constructs. Over the past several years I have played a key role in developing transgenic mouse BAC recombineering technologies in our laboratory by taking advantage of the full length gene promoter (5' flanking region of gene of interest in BAC) to drive reporter genes such as EGFP(3, 4). BAC recombineering technology offers several advantages to produce triple gene knock-out mice. First, BAC clones hold large fragments of genomic DNA. Second, mCLCA1, mCLCA2 and mCLCA4 cluster together on the same chromosome. Third, a large

Table 4.1 Evaluation of body weight in mCLCA1,2,4 knock-out offspring.

Two mCLCA1,2,4$^{-/-}$ female showed the weight lost in 6 weeks. * Note, only two animals obtained in this time and their weights were shown individulely.

	mCLCA1,2,4$^{+/+}$ weight (gm)		mCLCA1,2,4$^{+/-}$ weight (gm)		mCLCA1,2,4$^{-/-}$ weight (gm)	
Age(wks)/Sex(number)	F(8)	M(8)	F(15)	M(15)	*F(2)	M(3)
3	15 ± 2	16 ± 2	14.9 ± 2	16 ± 2	16 ; 12.5	13 ± 3
6	23 ± 3.5	25 ± 3	22 ± 2	24 ± 3	21.8; 18	25 ± 2
10	28 ± 3	34 ± 3	24 ± 4	32 ± 3	23 ; --	--

A **B**

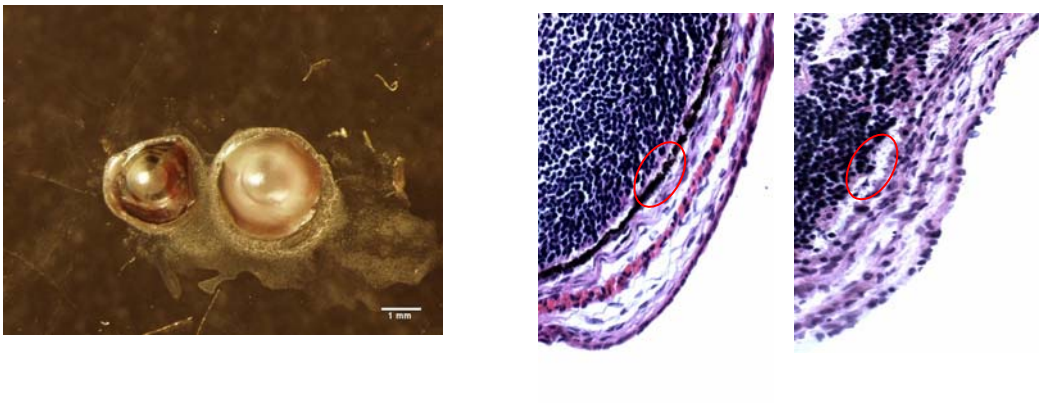

Figure 4.9 Evaluation of mCLCA1,2,4 eyes. A. Wide-field image of 1 day old pup eyes. mCLCA1,2,4$^{+/+}$ (left) and mCLCA1,2,4$^{-/-}$ (right). Note the opacity of the mCLCA1,2,4$^{-/-}$ eye compared to the mCLCA1,2,4$^{+/+}$ eye. B. Right is mCLCA1,2,4$^{-/-}$ pup eye and left is WT pup littermate (20X). The red oval area shows the retinal pigment epithelium cells.

deletion can be accomplished by BAC recombineering. Unfortunately, the high percentage of identity shared between mCLCA gene family made it very difficult to find unique sequences for the homologous arms that were used for BAC recombineering. In this study I successfully deleted 112 kb specific region from a BAC and the construct still contained enough genomic DNA for the homologous arms.

Due to the large homologous arms, traditional colony screening methods such as Southern blotting could not be used to detect whether recombination had occurred. I used two methods to screen for homologously recombined positive clones: regular PCR and qPCR (5). In the majority of cases, ES clones with random insertion of the linearized BAC construct were excluded by detecting the BAC bone (vector) using multiple sets of primers to the BAC bone. Once clones were excluded due to random insertion the remaining clones were then screened for the neomycin gene to further confirm the clones. The second step involved a qPCR strategy to quantitatively detect the difference between two wildtype alleles versus one wildtype allele and one knock-out allele with specific TaqMan probes within and outside the deleted region. The combination of these two PCR strategies resulted in the identification of 2 mCLCA1,2,4 knock-out ES clones—1C3 and 2B3.

The real-time PCR system uses fluorescent-based PCR chemistry to provide quantitative detection of DNA sequence with real-time analysis. The PCR product of the region of interst is quantitatively detected by a fluorescent labeled probe. There are two types of quantitative real-time PCR: absolute and relative. Relative quantification (RQ) type suited my purpose and was used for this study. It determines the change of targeted nucleic acid sequence of samples (ES cell clones) relative to the same sequence in the calibrator sample (unmodified E14 ES cell DNA). RQ provides accurate comparison between the samples and the calibrator and good results can be obtained (Figure 4.7).

The finished targeting construct of knock-out mCLCA1,2,4 (BAC-KO124-Neo) for ES cell is 80.6 kb. It contains 48 kb and 22 kb homology arms separated by neomycin gene and contains the BAC vector. In general, large deletions in the genome need large homologous arms in ES cell during the recombination process, but the ratio between the length of the deletion and the length of the arms remains unknown. Using a linearized targeting construct turned out to be a critical step as after screening over 250 non-linearized targeting clones not one homologous recombined clone was found when circular targeting DNA was used. Once the DNA was linearized, I obtained two mCLCA1,2,4 knock-out clones after screening the first 100 targeted clones. Thus, linearizing DNA is a critical step for homologous recombination to occur in ES cells.

The E14Tg2A ES cell line was advantageous for this study compared to the R1 feeder dependent ES cell line used for the mCLCA4 knock-out mice (Chapter 3). E14Tg2A ES cells are a feeder independent cell line which decreases cost and time associated with feeder cells used for R1 ES cells. It has a fast growth rate and is capable of germ line transmission.

In conclusion, this chapter details the galk and neomycin selection systems combined with BAC recombineering techniques to produce a large deletion of genomic DNA. ES cell clones screening strategy used both regular PCR and qPCR. mCLCA1,2,4 triple gene knock-out homozygote mice have been obtained, demonstrating the utility of this new method to produce null mice. mCLCA1,2,4$^{-/-}$ mice are not embryonic lethal and survive until at least 12 weeks. Further studies are ongoing to evaluate the gross phenotype and behavior of these animals.

REFERENCE

1. **Joyner A.** *Gene Targeting*, 2000.

2. **Robichaud A, Tuck SA, Kargman S, Tam J, Wong E, Abramovitz M, Mortimer JR, Burston HE, Masson P, Hirota J, Slipetz D, Kennedy B, O'Neill G, and Xanthoudakis S.** Gob-5 is not essential for mucus overproduction in preclinical murine models of allergic asthma. *Am J Respir Cell Mol Biol* 33: 303-314, 2005.

3. **Tallini YN, Greene KS, Craven M, Spealman A, Breitbach M, Smith J, Fisher PJ, Steffey M, Hesse M, Doran RM, Woods A, Singh B, Yen A, Fleischmann BK, and Kotlikoff MI.** c-kit expression identifies cardiovascular precursors in the neonatal heart. *Proc Natl Acad Sci U S A* 106: 1808-1813, 2009.

4. **Tallini YN, Shui B, Greene KS, Deng KY, Doran R, Fisher PJ, Zipfel W, and Kotlikoff MI.** BAC transgenic mice express enhanced green fluorescent protein in central and peripheral cholinergic neurons. *Physiol Genomics* 27: 391-397, 2006.

5. **Valenzuela DM, Murphy AJ, Frendewey D, Gale NW, Economides AN, Auerbach W, Poueymirou WT, Adams NC, Rojas J, Yasenchak J, Chernomorsky R, Boucher M, Elsasser AL, Esau L, Zheng J, Griffiths JA, Wang X, Su H, Xue Y, Dominguez MG, Noguera I, Torres R, Macdonald LE, Stewart AF, DeChiara TM, and Yancopoulos GD.** High-throughput engineering of the mouse genome coupled with high-resolution expression analysis. *Nat Biotechnol* 21: 652-659, 2003.

6. **Ward CM, Stern P, Willington MA, and Flenniken AM.** Efficient germline transmission of mouse embryonic stem cells grown in synthetic serum in the absence of a fibroblast feeder layer. *Lab Invest* 82: 1765-1767, 2002.

7. **Warming S, Costantino N, Court DL, Jenkins NA, and Copeland NG.** Simple and highly efficient BAC recombineering using galK selection. *Nucleic Acids Res* 33: e36, 2005.

CHAPTER 5

SUMMARY AND FUTURE RESEARCH DIRECTION

5.1. Summary

Chloride channel, calcium activated gene family members exist in more than 30 species (18). Originally, it was proposed that CLCAs were the integral channel protein, but later studies have proved this to be incorrect [(9, 11, 17, 22), chapter 2]. All the members of this family have a similar structure but they are expressed in different tissues (4, 7, 10, 12, 13, 18, 20). The proteins are cleaved and secreted out of the cell and associate with the plasma membrane [(11, 17), chapter 2]. Many studies have been focused on the role CLCAs play in the pathophysiology of human diseases. Some CLCAs functions may be related to asthma, such as hCLCA1 and mCLCA3 (14, 19); some of them are involved in CF, such as hCLCA1, hCLCA4 and mCLCA3 (6, 15, 21), and others (hCLCA2, mCLCA1 and mCLCA2) may play a role in tumor suppression, cancer and cell adhesion (1-3, 5, 16, 23-25). However, molecular level function of this group of genes remains unknown.

I started this study to understand the function of one murine CLCA member, mCLCA4. The mCLCA4 gene is located on mouse chromosome 3, clustering with seven other family members (5 genes were cloned and 2 gene were predicted). It is highly expressed in smooth muscle cells. Transient transfection studies indicated that mCLCA4 may be related to a chloride channel (8). mCLCA4 gene spans 26 kb with a 2.7 kb mRNA transcript that codes for a 909 aa peptide (8). mCLCA4 protein contains a N-terminal hydrolase domain, a VWA domain and a Fib3 domain (Figure 1.3).

In Chapter 2, I described the cellular processing and regulatory sequences underlying mCLCA4 proteins. After glycosylation the 125 kDa protein product was cleaved to 90 kDa NH_2- and 30 kDa COOH-terminal fragments, and both fragments were secreted into the cell media and associated with the cell membrane. The full-length 125-kDa protein was only found in the ER. I discovered specific luminal

diarginine retention and dileucine forward trafficking signals in the CLCA4 sequence that regulate export from the ER and proteolytic processing (Chapter 2).

To study the function of mCLCA4 *in vivo,* I generated a mouse lacking mCLCA4 gene expression. These animals displayed no gross phenotype and bred normally. Specific challenge experiments are being undertaken by collaborators (Michael Holtzman et al. at Washington University) to examine the effect of airway challenge on mClCa4 null mice. My hypothesis for why mCLCA4 null mice have no overt phenotype is that mCLCA1 and/or mCLCA2 compensate for loss of mCLCA4 (Chapter 3).

To further understand the role of the mCLCA4 gene and its highly homologous family members, I generated mCLCA1, mCLCA2, mCLCA4 triple knock-out mice. I developed a novel method to delete a large fragment of DNA from the mouse genome based on BAC recombineering techniques and successfully used it to delete three linked genes. I also developed a novel PCR and qPCR based ES cell clone screening method. The triple gene knock-out null mice survive to at least six months of age, but the homozygous with homozygous mating has not obtained offspring yet. It is too soon to conclude whether the male or female animal is sterile or it is just take time to get the progenys. Phenotype studies had been started with few mice and are continuing with more (Chapter 4).

5.2 Future direction and studies

5.2.1 mCLCA1,2,4 triple gene knock-out mice phenotype study

Currently, preliminary studies are underway to determine whether any phenotype exists in mCLCA1,2,4$^{-/-}$ mice. A few interesting potential phenotypes have been observed. First, it appears that adult female mCLCA1,2,4$^{-/-}$ mice may be underweight compared to wildtype littermate controls. Second, some null animals may

have hypopigmentation of the eye. Third, the homozygous male and female mating has not produced the offspring as yet, suggesting that one or both sexes may be sterile. However, these observations need to be confirmed by increasing the number of animals in the study. I am collaborating with Bendicht Pauli in Molecular Medicine Department, Cornell University, to determine the phenotypes of mCLCA1,2,4$^{-/-}$ mice.

5.2.2. mCLCA1,2,4$^{-/-}$ Physiological Function: Predictions

Based on the literature, CLCAs play roles in asthma (hCLCA1 and mCLCA3)(14, 19), and in cancer (hCLCA4, mCLCA1 and mCLCA2)(1-3, 5, 23-25). mCLCA4 is expressed at high levels in airway smooth muscle (8) and it may be involved in airway disease. Future study should investigate whether mCLCA4, mCLCA1 and /or mCLCA2 play roles in asthma or cancer suppression and, if so, through what pathway it acts. These questions may be answered using mCLCA4 knock-out mice and mCLCA1,2,4 triple gene knock-out mice. It will also be of interest to determine what domain(s) in the protein structures are the key domain(s) for the function. Specific challenge studies for asthma (19) and cancer in the two lines of knock-out mice I have gnearated will help elucidate the roles of these genes in these two diseases. For asthma challenge studies, I will continue collaboration with Michael Holtzman et al. at Washington University to determine if these three genes contribute to asthma susceptibily in accordance with his animal model.

CLCA proteins are the calcium activated chloride channel regulators. Although the mechanism of regulation is not clear, CLCA proteins will still become the useful biomarkers and therapeutic targeting molecules for asthma, cancer and chloride currents related diseases.

5.2.3. Generating additional CLCA knock-out mice

Eight mCLCA genes cluster together on mouse chromosome 3. They have with similar protein structure but divers tissue/organ expression patterns. This fact suggested that mCLCA genes play different roles in different tissues but that other family members may compensate if the function of one is lost. This group of genes may function as a team and compensate for each other when the function of one is lost. To understand the *in vivo* functions of all eight genes, deletion of the whole family from mouse genome may necessary. However, deletion of a large specific region (total ~340 kb) from mouse genome is not yet possible with current technology. It is possible, nonetheless, to delete more members from the mouse genome based on the technique I developed and used in my study, as described below.

Since the BAC recombineering technique was successfully used for this study, we can now generate a mouse with additional CLCA members deleted from the genome and discover the function of these genes in murine life. For example, a BAC containing mCLCA6, AI747448 (mCLCa7) and EG622139 (mCLCA8) genes could be chosen and these three genes deleted using the galk selection system with two genomic regions across the deletion area remaining called ArmC-Neo-ArmD (Figure 5.1A). To take advantage of the mCLCA1,2,4 BAC knock-out construct (ArmA-Neo-ArmB) with three genes deleted, ArmD of BAC-ArmC-Neo-ArmD construct would be replaced by ArmB through gap repair. The Neomycin gene of BAC-ArmC-Neo-ArmB would be replaced by a puromycin gene for further 1C3 ES cell (the ES cell line with mCLCA1,2,4 knock-out) selection since this ES cell already contains a neomycin gene, named BAC-ArmC-Puromycin-ArmB (Figure 5.1B-D). ES cell 1C3 (mCLCA1,2,4, knock-out clone) could used for the ES cell source for targeting. This line of knock-out mice will be very useful for further understanding the molecular function of this group of genes.

5.2.4. CLCA family and its future

The CLCA family has drawn the attention of researchers for many years and in many ways. The family members have been excluded as chloride channel integral proteins, but they still play roles in regulating chloride currents. The function of some of the members is related to asthma and cystic fibrosis diseases, while others are tumor suppressors. It is still unknown, however, how these proteins function at the molecular level and the roles they play in disease. The answers will be taken a few steps further with my contribution of mCLCA4 knock-out and mCLCA1,2,4 knock-out mice.

Figure 5.1 Diagram depicting strategy to make mCLCA1,2,4,6,7,8 knock-out mice. A. Choose a BAC that contains mCLCA6, mCLCA7 and mCLCA8 and a free region crossing the genes. B-C. Use BAC recombineering/gap repair to replace ArmD in BAC-KO378-Neo construct with ArmB in BAC-KO124-Neo construct after deletion of three genes with galk selection and replacing galk gene with neomycin gene. D. With one round of BAC recombineering, Neomycin gene will be replaced by the puromycin gene for further ES cell selection.

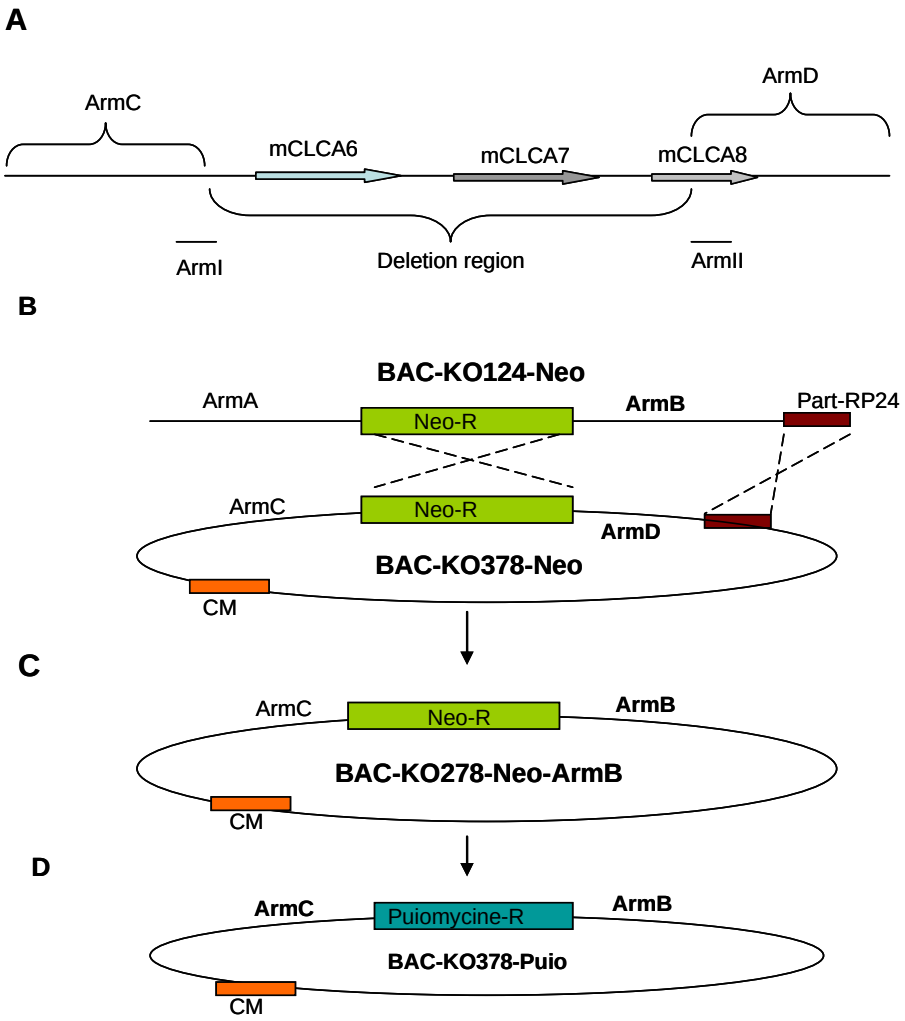
A
ArmC
ArmD
mCLCA6
mCLCA7
mCLCA8
ArmI
Deletion region
ArmII
B
BAC-KO124-Neo
ArmA
Neo-R
ArmB
Part-RP24
ArmC
Neo-R
ArmD
BAC-KO378-Neo
CM
C
ArmC
Neo-R
ArmB
BAC-KO278-Neo-ArmB
CM
D
ArmC
Puiomycine-R
ArmB
BAC-KO378-Puio
CM

REFERENCE

1. **Abdel-Ghany M, Cheng HC, Elble RC, Lin H, DiBiasio J, and Pauli BU.** The interacting binding domains of the beta(4) integrin and calcium-activated chloride channels (CLCAs) in metastasis. *J Biol Chem* 278: 49406-49416, 2003.

2. **Abdel-Ghany M, Cheng HC, Elble RC, and Pauli BU.** The breast cancer beta 4 integrin and endothelial human CLCA2 mediate lung metastasis. *J Biol Chem* 276: 25438-25446, 2001.

3. **Abdel-Ghany M, Cheng HC, Elble RC, and Pauli BU.** Focal adhesion kinase activated by beta(4) integrin ligation to mCLCA1 mediates early metastatic growth. *J Biol Chem* 277: 34391-34400, 2002.

4. **Agnel M, Vermat T, and Culouscou JM.** Identification of three novel members of the calcium-dependent chloride channel (CaCC) family predominantly expressed in the digestive tract and trachea. *FEBS Lett* 455: 295-301, 1999.

5. **Balakrishnan A, von Neuhoff N, Rudolph C, Kamphues K, Schraders M, Groenen P, van Krieken JH, Callet-Bauchu E, Schlegelberger B, and Steinemann D.** Quantitative microsatellite analysis to delineate the commonly deleted region 1p22.3 in mantle cell lymphomas. *Genes Chromosomes Cancer* 45: 883-892, 2006.

6. **Brouillard F, Bensalem N, Hinzpeter A, Tondelier D, Trudel S, Gruber AD, Ollero M, and Edelman A.** Blue native/SDS-PAGE analysis reveals reduced expression of the mClCA3 protein in cystic fibrosis knock-out mice. *Mol Cell Proteomics* 4: 1762-1775, 2005.

7. **Danahay H, Atherton H, Jones G, Bridges RJ, and Poll CT.** Interleukin-13 induces a hypersecretory ion transport phenotype in human bronchial epithelial cells. *Am J Physiol Lung Cell Mol Physiol* 282: L226-236, 2002.

8. **Elble RC, Ji G, Nehrke K, DeBiasio J, Kingsley PD, Kotlikoff MI, and Pauli BU.** Molecular and functional characterization of a murine calcium-activated chloride channel expressed in smooth muscle. *J Biol Chem* 277: 18586-18591, 2002.

9. **Elble RC, Walia V, Cheng HC, Connon CJ, Mundhenk L, Gruber AD, and Pauli BU.** The putative chloride channel hCLCA2 has a single C-terminal transmembrane segment. *J Biol Chem* 281: 29448-29454, 2006.

10. **Elble RC, Widom J, Gruber AD, Abdel-Ghany M, Levine R, Goodwin A, Cheng HC, and Pauli BU.** Cloning and characterization of lung-endothelial cell adhesion molecule-1 suggest it is an endothelial chloride channel. *J Biol Chem* 272: 27853-27861, 1997.

11. **Gibson A, Lewis AP, Affleck K, Aitken AJ, Meldrum E, and Thompson N.** hCLCA1 and mCLCA3 are secreted non-integral membrane proteins and therefore are not ion channels. *J Biol Chem* 280: 27205-27212, 2005.

12. **Gruber AD, Elble RC, Ji HL, Schreur KD, Fuller CM, and Pauli BU.** Genomic cloning, molecular characterization, and functional analysis of human CLCA1, the first human member of the family of Ca2+-activated Cl- channel proteins. *Genomics* 54: 200-214, 1998.

13. **Gruber AD and Pauli BU.** Molecular cloning and biochemical characterization of a truncated, secreted member of the human family of Ca2+-activated Cl- channels. *Biochim Biophys Acta* 1444: 418-423, 1999.

14. **Kamada F, Suzuki Y, Shao C, Tamari M, Hasegawa K, Hirota T, Shimizu M, Takahashi N, Mao XQ, Doi S, Fujiwara H, Miyatake A, Fujita K, Chiba Y, Aoki Y, Kure S, Tamura G, Shirakawa T, and Matsubara Y.** Association of the hCLCA1 gene with childhood and adult asthma. *Genes Immun* 5: 540-547, 2004.

15. **Leverkoehne I and Gruber AD.** The murine mCLCA3 (alias gob-5) protein is located in the mucin granule membranes of intestinal, respiratory, and uterine goblet cells. *J Histochem Cytochem* 50: 829-838, 2002.

16. **Li X, Cowell JK, and Sossey-Alaoui K.** CLCA2 tumour suppressor gene in 1p31 is epigenetically regulated in breast cancer. *Oncogene* 23: 1474-1480, 2004.

17. **Mundhenk L, Alfalah M, Elble RC, Pauli BU, Naim HY, and Gruber AD.** Both cleavage products of the mCLCA3 protein are secreted soluble proteins. *J Biol Chem* 281: 30072-30080, 2006.

18. **Patel AC, Brett TJ, and Holtzman MJ.** The Role of CLCA Proteins in Inflammatory Airway Disease. *Annu Rev Physiol*, 2008.

19. **Patel AC, Morton JD, Kim EY, Alevy Y, Swanson S, Tucker J, Huang G, Agapov E, Phillips TE, Fuentes ME, Iglesias A, Aud D, Allard JD, Dabbagh K, Peltz G, and Holtzman MJ.** Genetic segregation of airway disease traits despite redundancy of calcium-activated chloride channel family members. *Physiol Genomics* 25: 502-513, 2006.

20. **Pawlowski K, Lepisto M, Meinander N, Sivars U, Varga M, and Wieslander E.** Novel conserved hydrolase domain in the CLCA family of alleged calcium-activated chloride channels. *Proteins* 63: 424-439, 2006.

21. **Ritzka M, Stanke F, Jansen S, Gruber AD, Pusch L, Woelfl S, Veeze HJ, Halley DJ, and Tummler B.** The CLCA gene locus as a modulator of the gastrointestinal basic defect in cystic fibrosis. *Hum Genet* 115: 483-491, 2004.

22. **Whittaker CA and Hynes RO.** Distribution and evolution of von Willebrand/integrin A domains: widely dispersed domains with roles in cell adhesion and elsewhere. *Mol Biol Cell* 13: 3369-3387, 2002.

23. **Zhu D, Cheng CF, and Pauli BU.** Blocking of lung endothelial cell adhesion molecule-1 (Lu-ECAM-1) inhibits murine melanoma lung metastasis. *J Clin Invest* 89: 1718-1724, 1992.

24. **Zhu D and Pauli BU.** Correlation between the lung distribution patterns of Lu-ECAM-1 and melanoma experimental metastases. *Int J Cancer* 53: 628-633, 1993.

25. **Zhu DZ, Cheng CF, and Pauli BU.** Mediation of lung metastasis of murine melanomas by a lung-specific endothelial cell adhesion molecule. *Proc Natl Acad Sci U S A* 88: 9568-9572, 1991.